



Escola de Camins
Escola Tècnica Superior d'Enginyeria de Camins, Canals i Ports
UPC BARCELONATECH

Effects of cultivation conditions on polyhydroxybutyrate production in cyanobacterial cultures

Treball realitzat per:

Ana Álvarez González

Dirigit per:

Rubén Díez Montero

Estel Rueda Hernández

Màster en:

Enginyeria Ambiental

Barcelona, 20 de junio de 2021

Departament Enginyeria Civil i Ambiental

TREBALL FINAL DE MÀSTER

Index

List of abbreviations	4
List of figures	6
List of tables.....	11
Abstract	13
Resumen.....	14
1. Introduction	15
1.1 Plastic.....	15
1.2 Polyhydroxybutyrate (PHB)	16
1.3 Cyanobacteria.....	18
1.4 Metabolism of PHB	19
Metabolic pathways related to PHB metabolism.....	22
1.5 PHB production by cyanobacteria	24
2. Objectives	28
3. Material and methods	29
3.1 Media and reagents	29
3.2 Cyanobacteria cultures	29
3.3 Experiments	30
First experiment: inorganic carbon (IC) effect	32
Second experiment: additions of nitrogen and phosphorus effect	33
Third experiment: salinity effect.....	33
3.4 Analytical methods	34
3.5 RT-q-PCR analysis	38
4. Designing, developing and implementing RT-q-PCR protocols.....	40

4.1. Introduction.....	40
4.2 Optimization of the nucleic acid extraction	43
4.3 Optimization of the DNase treatment	44
4.4 Optimization of the RT-q-PCR	45
4.5 Conclusions.....	52
5. Results and discussion	53
5.1 Experiment 1: influence of inorganic carbon availability on PHB production.....	53
5.2 Experiment 2: effect of intermittent additions of N and P on PHB production.....	62
5.3 Experiment 3: influence of salinity in the culture media on PHB production.....	67
6. Conclusion	75
7. Future perspectives	76
8. References	80
Annex I.....	91
A. RNA extraction from Bacterial Cells	91
B. DNase on-column treatment.....	91
C. Reverse transcription.....	92
D. q-PCR.....	93
Annex II	94
A. RNA extraction	94
B. Reverse transcription protocol for specific-target.....	96
Annex III.....	97

List of abbreviations

%dcw: percentage dry cell weight

3PG: 3-phosphoglycerate

Acetyl-CoA: Acetyl Coenzyme A

ATP: adenosine triphosphate

DNA: deoxyribonucleic acid

DO: dissolved oxygen

IC: inorganic carbon

mRNA: messenger ribonucleic acid

NADH: nicotinamide adenine dinucleotide

NADPH: nicotinamide adenine dinucleotide phosphate

ORP: Open Race Ponds

PBR: photobioreactor

PHA: polyhydroxyalkanoates

PhaA: PHA specific β -ketothiolase

PhaB: Acetoacetyl-CoA reductase

PhaC: Pha synthase

PhaEC: PHB synthase

PHB: polyhydroxybutyrate

q-PCR: quantitative polymerase chain reaction

RNA: ribonucleic acid

rRNA: ribosomal ribonucleic acid

RT: reverse transcription

RT-q-PCR: reverse transcription quantitative polymerase chain reaction

TCA cycle: tricarboxylic acid cycle

USD: United States dollar

UV: ultraviolet

VSS: volatile suspended solids

List of figures

Figure 1. Structure of poly(3-hydroxybutyrate).....	17
Figure 2. Schematic representation of PHA inclusion, obtained from Sudesh et al. (2000).	20
Figure 3. Metabolic pathway of PHB synthesis in <i>Synechocystis</i> PCC 6803 (Price et al., 2020).	20
Figure 4. Molecular organization of genes encoding PHA synthases of type III, which are composed of two different subunits, obtained from Rehm and Steinbüchel (1999).	21
Figure 5. Cyclic metabolic nature of P(3HB) biosynthesis and degradation in bacteria. PhaA, β - ketothiolase; PhaB, NADPH-dependent acetoacetyl-CoA reductase; PhaC, PHA synthase; PhaZ, PHA depolymerase; 1, dimer hydrolase; 2, (R)-3-hydroxybutyrate dehydrogenase; 3, acetoacetyl- CoA synthetase; 4, NADH-dependent acetoacetyl-CoA reductase, obtained from Sudesh et al. (2000).	23
Figure 6. Picture of the photobioreactor.	30
Figure 7. Scheme of the different phases during the production of PHB.	32
Figure 8. First experiment diagram.....	32
Figure 9. Second experiment diagram.	33
Figure 10. Third experiment diagram.	34
Figure 11. Diagram of the analytical measures that were carried out during the experiments.....	38
Figure 12. Schematic representation of the steps involved in the RT-q-PCR.	43
Figure 13. Evolution of volatile suspended solids concentration during experiment 1. The vertical line indicates the start of the accumulation phase (day 11). The growth phase values are calculated as the average of the values of the four PBR replicates and the standard deviation is indicated with error bars.	54
Figure 14. Evolution of nitrogen and phosphorus concentration during experiment 1. The vertical line indicates the start of the accumulation phase (day 11). The growth phase values are calculated as the average of the values of the four PBR replicates and the standard deviation is indicated with error bars.	55
Figure 15. Chlorosis effect. Picture of cultures with different concentration of nutrients. Cultures 1 and 2 had enough nutrients, so the culture has green intense color. Culture 3 has run out of nitrogen, so the culture has turned the color into green-yellow. Culture 4 was starting the chlorosis process, so the green color is starting to turn into yellow.....	56

Figure 16. Evolution of glycogen content during experiment 1. The vertical line indicates the start of the accumulation phase. The growth phase values are calculated as the average of the values of the four PBR replicates and the standard deviation is indicated with error bars.	57
Figure 17. Evolution of PHB content during experiment 1. The vertical line indicates the start of the accumulation phase. The growth phase values are calculated as the average of the values of the four PBR replicates and the standard deviation is indicated with error bars.	59
Figure 18. Evolution of volatile suspended solids concentration in experiment 2. The vertical line indicates the start of the accumulation phase (day 28). The growth phase values are calculated as the average of the values of the four PBR replicates and the standard deviation is indicated with error bars. ↑ indicates the different additions: P↑ (additions of phosphorus), N↑↑ (high frequency additions of nitrogen), N ↑ (low frequency additions of nitrogen).	63
Figure 19. Evolution of nitrogen and phosphorus concentration during experiment 2. The vertical line indicates the start of the accumulation phase (day 28). The growth phase values are calculated as the average of the values of the four PBR replicates and the standard deviation is indicated with error bars. ↑ indicates the different additions: P↑ (additions of phosphorus), N↑↑ (high frequency additions of nitrogen), N ↑ (low frequency additions of nitrogen).	64
Figure 20. Evolution of glycogen content during experiment 2. The vertical line indicates the start of the accumulation phase. The growth phase values are calculated as the average of the values of the four PBR replicates and the standard deviation is indicated with error bars. ↑ indicates the different additions: P↑ (additions of phosphorus), N↑↑ (high frequency additions of nitrogen), N ↑ (low frequency additions of nitrogen).....	65
Figure 21. Evolution of PHB content during experiment 2. The vertical line indicates the start of the accumulation phase. The growth phase values are calculated as the average of the values of the four PBR replicates and the standard deviation is indicated with error bars. ↑ indicates the different additions: P↑ (additions of phosphorus), N↑↑ (high frequency additions of nitrogen), N ↑ (low frequency additions of nitrogen).	66
Figure 22. Evolution of volatile suspended solids concentration in experiment 3. The vertical line indicates the start of the accumulation phase (day 12). The growth phase values are calculated as the average of the values of the four PBR replicates and the standard deviation is indicated with error bars.	68

Figure 23. Evolution of nitrogen and phosphorus concentration during experiment 3. The vertical line indicates the start of the accumulation phase (day 12). The growth phase values are calculated as the average of the values of the four PBR replicates and the standard deviation is indicated with error bars.	70
Figure 24. Evolution of glycogen content during experiment 3. The vertical line indicates the start of the accumulation phase. In this case, glycogen was not measured during the growth phase...	71
Figure 25. Evolution of PHB content during experiment 3. The vertical line indicates the start of the accumulation phase. The growth phase values are calculated as the average of the values of the four PBR replicates and the standard deviation is indicated with error bars.	72
Figure 26. Highly simplified biosynthetic pathways for glycogen conversion to polyhydroxybutyrate (PHB) in cyanobacteria, including the biosynthetic pathway of glucosylglycerol.	74
Figure 27. Results of q-PCR (using primers of bacterial general 16S). Orange curve represents the positive control. Blue curve represents the sample using the on-column modified treatment. Red curve represents de negative control. Green curve represents the sample using the treatment in dissolution.	97
Figure 28. Results of q-PCR (using primers of general 16S specific of <i>Synechocystis</i>). Results of RT-q-PCR using primers from 16S rRNA from <i>Synechocystis</i> . Blue curve represents de positive control. Red curve represents the negative control. Grey, orange and green represent the samples.	98
Figure 29. Results of q-PCR targeting different genes. RT was performed using random primers. First, <i>fbp</i> gene: grey curve represents the positive control. Second, <i>glgX</i> gene: light yellow curve represents the positive curve. Third, <i>rnpA</i> gene: pink curve represents the positive curve. Blue curve represents sample 1 when targeted with <i>glgX</i> gene. The rest of samples and the negative control are not detected.	99
Figure 30. Results of RT-q-PCR using primers from <i>rnpA</i> gene <i>Synechocystis</i> , after the second extraction. Blue curve represents de positive control. Red curve represents the negative control. Green curve represents the frozen sample. The inoculum sample is not detected.	100
Figure 31. Results of q-PCR (using primers of bacterial general 16S), after the second extraction. Pink curve represents the positive control. Yellow curve represents de negative control. Grey curve represents the sample from the inoculum. The red curve represents the frozen sample.	101

Figure 32. Results of q-PCR (using primers of 16S rRNA from <i>Synechocystis</i>), after the second extraction. Brown curve represents the positive control. Green curve represents the negative control. Orange curve represents the sample from the inoculum. The grey curve represents the frozen sample.	102
Figure 33. Results of RT-q-PCR using primers from <i>rnpA</i> gene <i>Synechocystis</i> . Orange curve represents the positive control. Blue curve represents the negative control. Maroon curve represents the inoculum sample. Green curve represents the frozen sample. 2 μ L of sample were added instead of 1 μ L.	103
Figure 34. Results of RT-q-PCR using primers from <i>rnpA</i> gene <i>Synechocystis</i> . Grey curve represents the positive control. Purple curve represents the negative control. Yellow curve represents the inoculum sample. Yellow curve represents the frozen sample. 3 μ L of sample were added instead of 1 μ L. 500 nM primers were used instead of 300 nM.	104
Figure 35. Results of RT-q-PCR using primers from <i>fbp</i> gene <i>Synechocystis</i> . Orange curve represents the positive control. Red curve represents the negative control. Green curve represents the inoculum sample. Blue curve represents the frozen sample.	105
Figure 36. RT-q-PCR results, targeting <i>fbp</i> gene from <i>Synechocystis</i> , using the gene-specific RT approach. Orange curve represents the positive control. Red curve represents the negative control. Green curve represents N1, (negative control from RT, including the mixture of primers and the enzyme, without RNA sample).	106
Figure 37. Results of RT-q-PCR using a mixture of primers during the RT. q-PCR has targeted 16S rRNA gene. Orange curve represents the positive control. Red curve represents the negative control. Blue curve represents the inoculum sample. Green curve represents the frozen sample.	107
Figure 38. Results of RT-q-PCR using a mixture of primers during the RT. q-PCR has targeted <i>fbp</i> gene. Grey curve represents the positive control. Blue curve represents the negative control. Yellow curve represents the inoculum sample. Light yellow curve represents the frozen sample.	108
Figure 39. Results of RT-q-PCR using a mixture of primers during the RT. q-PCR has targeted <i>gltA</i> . Maroon curve represents the positive control. Red curve represents the negative control. Blue curve represents the inoculum sample. Purple curve represents the frozen sample.	109

Figure 40. Results of RT-q-PCR using a mixture of primers during the RT. q-PCR has targeted rnpA. Maroon curve represents de positive control. Grey curve represents the negative control. Orange curve represents de inoculum sample. Purple curve represents the frozen sample. 110

Figure 41. RT-q-PCR results, targeting 16S rRNA from Synechocystis, using the mixture of primers. Green curve represents the positive control. Orange curve represents the negative control. Purple curve represents N1, (negative control from RT, including the mixture of primers and the enzyme, without RNA sample). Grey curve represents N2 (negative control from RT, including the mixture of primers and RNA sample, without the enzyme). 111

Figure 42. q-PCR results, targeting fbp gene, after applying 10 mM random primers in the RT. Orange curve represents the positive. Red curve represents the negative. Light orange represents the sample from the inoculum. Grey curve represents the frozen sample. 112

List of tables

Table 1. Classification of the enzymes involved in PHA metabolism, according to Steinbüchel et al. (2011).	22
Table 2. Initial concentrations of nitrogen and phosphorus in each experiment.	31
Table 3. Experimental conditions for salinity effect.....	34
Table 4. Schedule of the analytical analysis performed. Electrical conductivity* was only measured in the third experiment.....	36
Table 5. Description of the genes studied with the name of the protein that encoded, the microorganism, the pathway, the enzyme classification (EC) and the reference.	39
Table 6. Results of the quantification of the samples after the extraction step was performed....	44
Table 7. Results of q-PCR after applying different DNase treatments. The q-PCR targeted the bacterial 16S rRNA gene. The results are obtained from figure 26.....	45
Table 8. Results of q-PCR after performing RT step, using random primers. The q-PCR targeted the 16S-rRNA gene from Synechocystis. The three samples are triplicates.	46
Table 9. Results of q-PCR after performing RT step, using random primers. The q-PCR targeted the fbp, glgX and rnpA gene from Synechocystis. The three samples are triplicates.	46
Table 10. Results of q-PCR after performing RT step, using random primers. The q-PCR targeted the bacterial 16S rRNA, and 16S rRNA and rnpA gene from Synechocystis.....	47
Table 11. Original conditions of the q-PCR and two different modifications, regarding the primers concentration and the volume of sample.	48
Table 12. Results of q-PCR after performing RT step, using random primers. The q-PCR targeted the rnpA gene from Synechocystis. Modified conditions 1 refers to 2 μ L of sample and 300 nM of primers. Modified conditions 2 refers to 3 μ L of sample and 500 nM of primers.	48
Table 13. Results of q-PCR after performing RT step, using specific primers for fbp gene. The concentration of the primers was 1.67 μ M.	49
Table 14. q-PCR results of performing gene specific RT, targeting fbp gene, with two different negatives: N1 includes the primers and RT enzyme; N2 includes the primers and RNA sample, but no RT enzyme.	49
Table 15. Results of q-PCR after performing RT step, using a mixture of genes from Synechocystis (16S rRNA, fbp, gltA, rnpA). The concentration of the primers was 1.67 μ M.....	50

Table 16. Results of q-PCR after performing RT step, using a mixture of genes from <i>Synechocystis</i> (16S rRNA, fbp, gltA, rnpA). The concentration of the primers was 1.67 μ M. The targeted gene during q-PCR was 16S rRNA. N1 refers to the negative control without sample, but including the mixture of primers and the RT. N2 refers to the negative control without the RT, but adding the sample and the mixture of genes.....	51
Table 17. Results of q-PCR after performing RT step, using random primers. The q-PCR targeted the fbp gene from <i>Synechocystis</i> . The concentration of the random primers was raised 10 times in comparison to the initial conditions (manufacturer's instructions).	52
Table 18. Classification of microorganisms according to their relationship to salt.....	69
Table 19. Standard cycling mode.....	93
Table 20. Dissociation curve conditions (melt curve stage).	93

Abstract

Bioplastics, such as polyhydroxybutyrate (PHB), are expected to revolutionize the traditional plastic market, which has a fossil fuel origin and give rise to huge pollution at the environment. PHB can be produced by microorganisms and therefore can be biodegraded. In order to make the process sustainable and low-cost, the best solution consists in using photoautotrophic microorganisms, which uses inorganic carbon, such as carbon dioxide, and sunlight as carbon and energy sources, respectively. Among these microorganisms, we find cyanobacteria, specifically *Synechocystis*. However, when they are submitted to the autotrophic mode, they present low PHB productivities. In previous studies the maximum production of PHB was 5.9% of the dry cell weight (dcw) with the studied strain of *Synechocystis*.

In this project, different environmental conditions for the growth of cyanobacteria have been studied in relation to PHB production. The following main results have been obtained: PHB reaches a maximum of 14.4%_{dcw} with a high concentration of inorganic carbon in the culture media (2000 mg/L of bicarbonate) and deprivation of nitrogen and phosphorus; intermittent additions of nitrogen and phosphorus during the accumulation phase reduced the PHB production; this biosynthesis might be related to salinity and the results might indicate that a high electrical conductivity (13 mS/cm) due to salt (5.8 g/L NaCl) and a low concentration of inorganic carbon (100 mg/L bicarbonate) could increase PHB production. Moreover, in the studied conditions, it is observed the interconversion of glycogen to PHB. What is more, it seems that the initial concentration of nutrients in the growth phase could have an effect over PHB production during the accumulation phase.

On the other hand, it has been observed that the reverse-transcription quantitative polymerase chain reaction (RT-q-PCR) protocols given by manufactures for molecular biology analysis did not allow for the isolation of mRNA. Therefore, it is proposed a RT-q-PCR protocol to assess the gene expression of several genes involved in PHB metabolism and other related routes. This molecular analysis will give an insight into the behavior of this microorganism in relation to PHB biosynthesis.

Resumen

Se espera que los bioplásticos, como el polihidroxibutirato (PHB), revolucionen el mercado tradicional del plástico, que tiene un origen en los combustibles fósiles y suponen una importante contaminación para el medio ambiente. El PHB puede ser producido por microorganismos y por lo tanto puede ser biodegradado. Con el fin de hacer el proceso sostenible y de bajo costo, la mejor solución consiste en el uso de microorganismos fotoautotróficos, que utilizan carbono inorgánico, como dióxido de carbono, y la luz solar como fuentes de carbono y energía, respectivamente. Entre estos microorganismos, encontramos cianobacterias, específicamente *Synechocystis*. Sin embargo, cuando se utilizan en modo autotrófico, presentan bajas productividades de PHB. En trabajos anteriores, la producción máxima de PHB fue del 5.9% del peso seco celular (dcw) con la cepa seleccionada para este estudio.

En este proyecto, se han estudiado diferentes condiciones ambientales de crecimiento de cianobacterias en relación con la producción de PHB y se han obtenido los siguientes principales resultados: la cantidad de PHB alcanza un máximo del 14.34%_{dcw} con una alta concentración de carbono inorgánico en el medio de cultivo (2000 mg/L de bicarbonato) en ausencia de nitrógeno y fósforo; adiciones intermitentes de nitrógeno y fósforo durante la fase de acumulación redujeron la producción de PHB; esta biosíntesis podría estar relacionada con la salinidad y los resultados podrían indicar que una alta conductividad eléctrica (13 mS/cm) debido a la sal (NaCl) y una baja concentración de carbono inorgánico (100 mg/L bicarbonato) podría aumentar la producción de PHB. Asimismo, en las condiciones estudiadas, se observa la interconversión de glucógeno a PHB. Además, parece que la concentración inicial de nutrientes en la fase de crecimiento podría tener un efecto sobre la producción de PHB durante la fase de acumulación.

Por otra parte, se ha observado que los protocolos de reacción en cadena de la polimerasa con transcriptasa inversa (RT-q-PCR) proporcionados por los fabricantes no permitían el aislamiento del ARNm. Por lo tanto, se ha propuesto un protocolo RT-q-PCR para evaluar la expresión génica de varios genes involucrados en el metabolismo de PHB y otras rutas relacionadas. Este análisis molecular ayudará a comprender el comportamiento de este microorganismo en relación con la biosíntesis PHB.

1. Introduction

1.1 Plastic

Plastics were first used in the early 20th century, although they were not spread worldwide until II World War (Geyer et al., 2017). This is mainly due to their cheap manufacture process which makes them used on large scale (Rhodes, 2018). It is estimated that, in the year 2015, 381 million of tonnes of plastic were produced in the world (Geyer et al., 2017). China has become the greatest producer of plastic waste, with 59.08 million tonnes in 2010. It is followed by the United States, with 37.83 million tonnes in the same year (Jambeck et al., 2015).

Plastics are formed by polymer backbones, which consist in the repetition of a unit, named monomer. The monomer is usually composed of carbon, but it can have other atoms, like oxygen or nitrogen, or even silicon or sulphur (Rhodes, 2018). The molecular composition of the monomer defines the physical and chemical properties of the plastic and also classifies it in different types: polyethylene, polypropylene, polyacrylics, etc. (Rhodes, 2018).

The most common used material to produce plastic are propylene and ethylene, which are obtained from fossil fuels, making them not biodegradable (Geyer et al., 2017). Some characteristics, like stability and durability, make plastics really difficult to decompose (Rhodes, 2018). As a consequence, plastics are accumulated in landfills or directly in the environment. Plastics can be also recycled, although the percentage of recycled plastic is still very low (Geyer et al., 2017). However, there has been a change in plastic final destination since 1980, where the total amount of plastic was discarded: in the year 2015, it is estimated that 9% of total plastic waste has been recycled, 12% incinerated and 79% discarded (Geyer et al., 2017).

The contamination has been so extended, that plastics have been found in every ecosystem, like ocean basins and freshwater surfaces (Geyer et al., 2017). There is a notable contamination with big pieces of plastic, such as plastic bags or six pack rings, which can be lethal for living beings. Nevertheless, there is another important issue about microplastics, plastics with small size particles, which can be ingested by animals and negatively affect them (Rhodes, 2018). Plastic pollution is not only found in aquatic ecosystems, but also in the soil due to the landfill of wastewater sludge and agricultural plastic mulch, where is progressively gaining more attention (Fuller and Gautam, 2016). In the same way as the aquatic organisms, the terrestrial ones can ingest plastics, which have negative effects on their bodies (Chae and An, 2018).

Whereas in 2015, 60-99 million tonnes of mismanaged plastic were estimated, in 2050 this number is expected to increase up to 155-265 million tonnes, with the current business model (Lebreton and Andrady, 2019). With this future scenario, it is clear that solutions are needed. Bioplastics are gaining more and more attraction and importance, as they can be responsible for driving further change in this market.

1.2 Polyhydroxybutyrate (PHB)

Bioplastics market has grown four times between 2007 and 2011. In 2011, 1.1 million tons of bioplastic were produced (Sreedevi et al., 2014) in comparison to 325 million tons of global plastic (Geyer et al., 2017). In 2017, bioplastics market was valued in 17\$ billion USD and they supposed 1% of the plastic market (Price et al., 2020). Bioplastics produced from starch and polylactic-acid-based plastics are the most produced in the global market whereas polyhydroxyalkanoates (PHAs) bioplastics are still in an early stage (Sreedevi et al., 2014). Regarding production, North America produces the highest amount of bioplastics, followed by Europe (Khazir and Shetty, 2014). However, PHAs produced by microorganisms are expected to become one the most important bioplastics in the future (Sreedevi et al., 2014).

Polyhydroxyalkanoates (PHAs) are macromolecules produced by many microorganisms as a carbon storage. These compounds have similar properties to conventional plastics, like polypropylene (Byrom, 1987). However, as they are biologically produced, they can be naturally degraded, becoming this their main advantage (Jendrossek et al., 1996). Moreover, they can be also recycled (Madison and Huisman, 1999). PHAs can be classified according to the length of their chain, which means the number of carbon atoms (Kavitha et al., 2018): short chain length (scl-PHA) are composed of 3-5 carbon atoms, medium chain length (mcl-PHA) are composed of 6-14 carbon atoms and long chain length (lcl-PHA) are composed of more than 15 carbon atoms. Some chemical and physical properties will depend on the number of carbon atoms (Kavitha et al., 2018).

Polyhydroxybutyrate (PHB) is the most common type of PHA and has gained commercial interest in recent years. They are storage compounds and they were first discovered in 1920 by Maurice Lemoigne (Padovani et al., 2016). They are composed of 3-hydroxybutyrate monomers (Figure 1) and they are classified as short chain length (scl-PHA) (Madison and Huisman, 1999). PHB become highly crystalline when extracted with organic solvents (Doi, 1995) and they have a

melting point around 170°C (Madison and Huisman, 1999). They have really interesting properties, like biodegradability. This means that natural microorganisms have the required enzymes to degrade them, ranging from months (anaerobic sewage) to years (in seawater) (Byrom, 1987). What is more, they have a renewable origin, instead of fossil fuels (Madison and Huisman, 1999). According to Sreedevi et al. (2014), commercial PHB is only produced by *Alcaligenes eutrophus* due to its efficiency and its cost is currently 16 times the price of polypropylene.

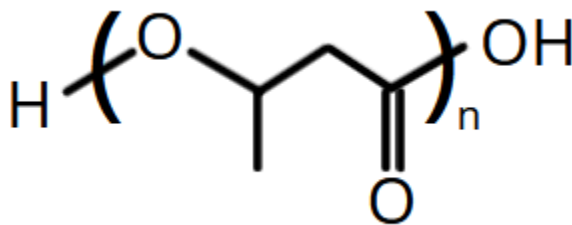


Figure 1. Structure of poly(3-hydroxybutyrate).

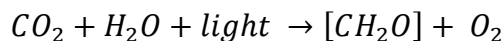
PHB has a wide range of applications, from medical to agricultural industries. Some examples of applications are (Sreedevi et al., 2014): medical field (sutures, tissue engineering, drug delivery), industrial application (food packaging, plastic bottles), agricultural field (carriers of pesticides, herbicides). Although the economic analysis shows that they are not yet feasible on large scale production, they are really suitable in applications which involve low-volume high-cost items (Keshavarz and Roy, 2010).

PHB has been traditionally produced by heterotrophic bacteria which need large amounts of organic carbon sources which are highly costly. The use of photoautotrophic microorganisms, like cyanobacteria, could be one solution. These microorganisms use energy from sun light and CO₂, making the PHB production more sustainable (Troschl et al., 2017). Although cyanobacteria have lower nutrient requirements than heterotrophic bacteria, the efficiency of the process must be higher in order to be competitive, in comparison to petroleum-plastics (Costa et al., 2018). Furthermore, the use of cyanobacteria avoids problems related to competition with arable lands, as they can be grown in non-agricultural sites and do not require organic carbon from vegetal origin (Rueda et al., 2020).

1.3 Cyanobacteria

Cyanobacteria are aerobic prokaryotic microorganisms. They mainly obtain energy by performing photosynthesis, so they produce oxygen and they uptake carbon dioxide and light (Chorus, 1999). They also need inorganic nutrients like nitrogen, phosphorus, some trace metals and micronutrients (Stal, 1992). Their habitats are marine environments, salty or fresh water, with global distribution. Many fresh-water species are capable to survive in water with high concentrations of salt, indicating that they are halotolerant (Chorus, 1999). Their optimum growing temperature is usually higher than eukaryotic algae and they are abundant at higher pH values (Whitton and Potts, 2012).

From the morphology point of view, cyanobacteria can be classified into unicellular, colonial and multicellular filamentous forms (Chorus, 1999). They are prokaryotic: do not have sub-cellular organelles, do not have an organized nucleus with membrane and they possess a wall structure composed of a peptidoglycan layer (Chorus, 1999). As photosynthetic organisms, they have chlorophyll, specifically chlorophyll a, which gives the green colour (Whitton and Potts, 2012). However, they can also produce other colour pigments, like carotenoids (beta-carotene) or phycocyanin, that usually mask the green colour (Chorus, 1999).



The above equation is the most general form of representing photosynthesis, where $[CH_2O]$ represents a general carbohydrate. In most plants, algae and cyanobacteria, water (H_2O) is the electron donor, and as consequence, it is produced oxygen (Mathews et al., 2013). Cyanobacteria is a photosynthetic microorganism that have two photosystems (PSI and PSII). Both photosystems contain chlorophyll a in the reaction centre (Stal, 2012).

During photosynthesis, the reactions that take place can be classified into light and dark reactions (Markou et al., 2012). The light reactions involve the absorption of light to transform the water into oxygen, with the consequent release of protons and electrons. These protons and electrons are then used to form NADPH and ATP, molecules that give the needed energy to the metabolism (Markou et al., 2012). The dark reactions involve the fixation of CO_2 . Carbon dioxide is used to carboxylate the ribulose 1,5-biphosphate into two molecules of 3-phosphoglycerate, which are then used to form carbohydrates (Taiz and Zeiger, 2010).

In the last years, important information regarding cyanobacteria has been revealed. This has led to opening a big range of biotechnology applications, for example, as bioactive compounds producers. Their metabolites include antibacterial, antifungal, antiviral, anticancer, antiplasmodial, algicide and immunosuppressive agents (Abed et al., 2009). Moreover, it is known that some species have the ability to accumulate PHAs, which can be used to produce bioplastics. Cyanobacteria have been also studied to clean-up wastewaters, especially if they are contaminated with oil-derived compounds (Abed and Köster, 2005).

1.4 Metabolism of PHB

Cyanobacteria have evolved along history, with the consequent adaptation to different environments. These environments can vary the amount of available nutrients, so cyanobacteria, as a way of adaptation, have acquired the ability to produce storage compounds, such as PHB. With these storage compounds, they are able to survive during long periods of time in conditions where nutrients are lacking (Price et al., 2020).

Scientists have studied the role of PHB during the last decades, but there is no clue about its real physiology function. Koch et al. (2020) studied the possible functions PHB might have over *Synechocystis* by submitting a strain incapable of producing PHB and a strain which produces PHB under different abiotic factors, such as temperature, light, variations in the dark/light cycles, salt and carbon availability. The results showed that the two different strains present no differences regarding the cells growth under the stressful factors. However, it has to be taken into account that the experiments were carried out using agar plates. The results might be different if the experiments were performed in liquid cultures.

The enzymes involved in both, biosynthesis and degradation of PHA, are located in the surface of the PHA inclusions (Sudesh et al., 2000). In this sense, the analysis of PHB inclusions revealed that they are composed of 98% poly- β -hydroxybutyrate, 2% protein and small amounts of lipids (Griebel et al., 1968). In fact, the inclusions (Figure 2) have been described as a hydrophobic core of amorphous PHA that is embedded in a phospholipid monolayer, which presents catabolic and non-catabolic proteins (Sudesh et al., 2000).

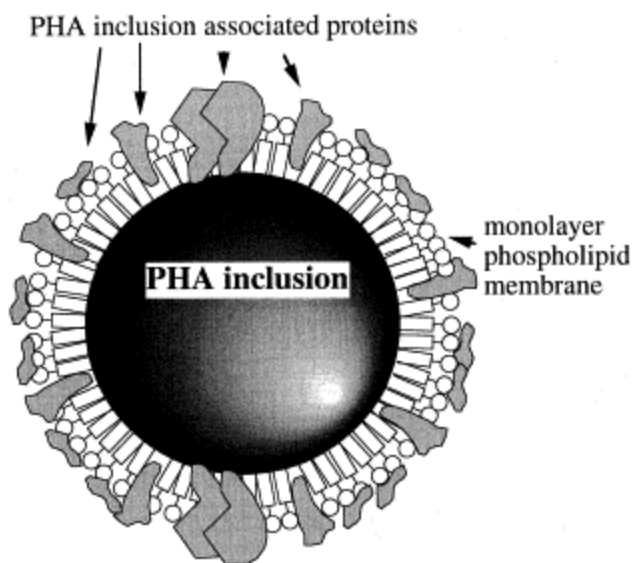


Figure 2. Schematic representation of PHA inclusion, obtained from Sudesh et al. (2000).

The metabolism through which atmospheric CO_2 is converted into PHB involves the Calvin cycle. It is performed the glycolysis to pyruvate and then to Acetyl coenzyme A (Acetyl-CoA). There are needed three known enzymes to transform the Acetyl-CoA into PHB (Figure 3). First, PHA specific β -ketothiolase (PhaA) combines two Acetyl-CoA molecules into Acetoacetyl-CoA. Second, this compound is reduced to hydroxybutyryl-CoA by the enzyme Acetoacetyl-CoA reductase (PhaB), NADPH dependent. Finally, the PHB synthase (PhaEC) adds hydroxybutyryl-CoA fatty acid monomer to a growing PHB molecule through ester bonds (Balaji et al., 2013).

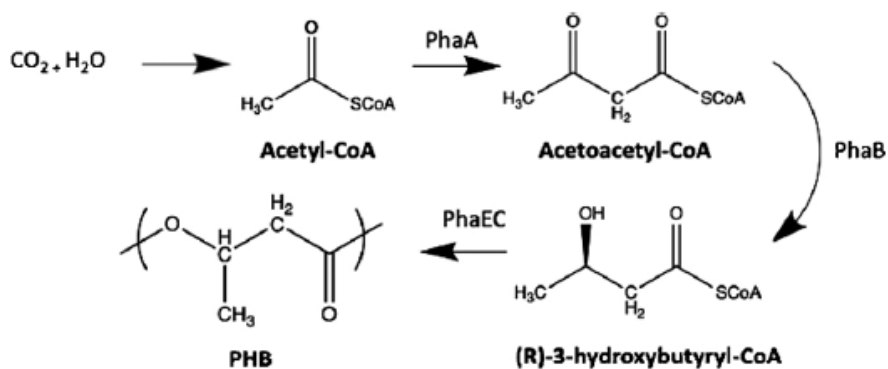


Figure 3. Metabolic pathway of PHB synthesis in *Synechocystis* PCC 6803 (Price et al., 2020).

Pha synthase (PhaC), the polymerizing enzyme, has been described as the protein responsible of the final type of PHA (Sudesh et al., 2000). Depending on the substrate specificity and the structure, Pha synthase can be classified into three different groups (Steinbüchel et al., 1992). First type, which is clearly represented by PHA synthase of *R. eutropha*, produces short-chain-length (SCL) HA monomers (Sudesh et al., 2000). Second type, which is represented by two PHA synthases of *P. oleovorans*, produces larger monomers (6-14 carbon atoms), medium-chain-length (MCL) HA. Third type has a main difference with respect the other two types. The enzymes classified as third type, present two subunits: C-subunit (40 kDa) and E-subunit (40kDa). The two subunits are necessary so that the enzyme catalyzes its corresponding enzymatic activity (Sudesh et al., 2000).

In *Synechocystis*, PHA synthase is classified as third type (Hein et al., 1998). Genome studies revealed that *phaC* and *phaE* are directly linked in the genomes and constitute most probably single operons whereas the rest of the genes encoding enzymes involved in PHB metabolism definitely do not map close to the *phaEC* locus (Rehm and Steinbüchel, 1999). Figure 4 represents the organization of several pha genes in different microorganism. It is clear that *Synechocystis* presents a distinct organization. The substrate of this type of enzyme is not well established, although it seems to be short-chain-length (Sudesh et al., 2000).

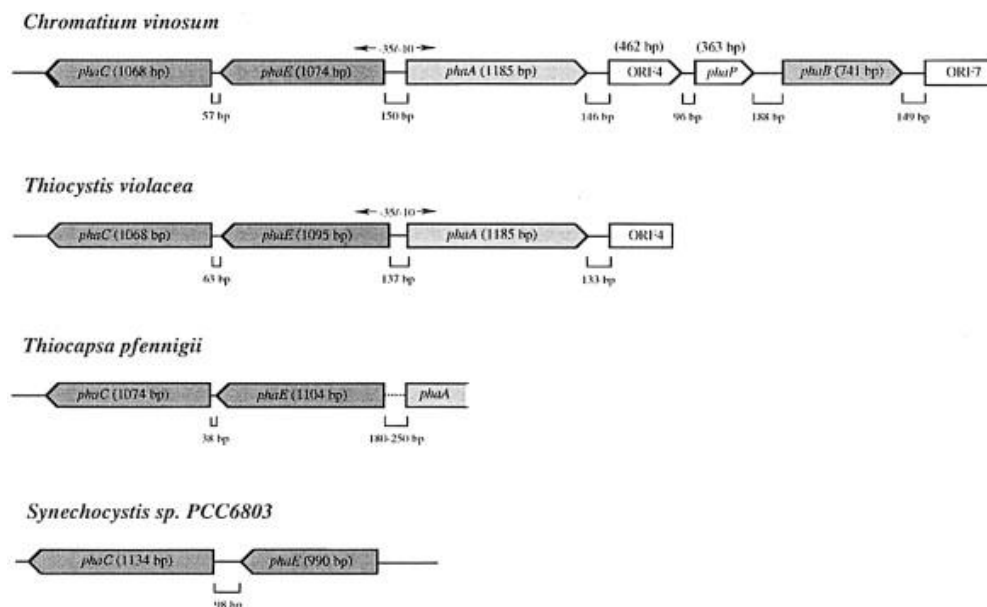


Figure 4. Molecular organization of genes encoding PHA synthases of type III, which are composed of two different subunits, obtained from Rehm and Steinbüchel (1999).

Apart of the above mentioned enzymes, it is also important to mention the PHA depolymerases, which break the bonds and has to be able to recover the carbon stored. However, the PHA depolymerase has not been described as well as the synthase (Sudesh et al., 2000).

Regarding proteins associated to PHA metabolism, it is also worth mentioning the phasins. Phasins constitute an important fraction of the total cellular protein and are supposed to form a protein layer over PHA inclusions, providing a link between the hydrophilic cytoplasm and the hydrophobic PHA core (Steinbüchel et al., 2011). All in all, the whole enzymatic system involved in PHB metabolism can be classified as shown in Table 1.

Table 1. Classification of the enzymes involved in PHA metabolism, according to Steinbüchel et al. (2011).

Class I	PHA synthases	Link the components
Class II	PHA depolymerases	Break the bonds
Class III	Phasins	Stabilization of the inclusions
Class IV	Rest of proteins associated to PHA inclusions	

Metabolic pathways related to PHB metabolism

Microorganisms are capable of producing PHAs from a wide range of carbon sources (Sudesh et al., 2000). Therefore, there are more than one metabolic pathway involved in their production, as it is represented in Figure 5. Cyclic metabolic nature of P(3HB) biosynthesis and degradation in bacteria. PhaA, β -ketothiolase; PhaB, NADPH-dependent acetoacetyl-CoA reductase; PhaC, PHA synthase; PhaZ, PHA depolymerase; 1, dimer hydrolase; 2, (R)-3-hydroxybutyrate dehydrogenase; 3, acetoacetyl-CoA synthetase; 4, NADH-dependent acetoacetyl-CoA reductase, obtained from Sudesh et al. (2000).

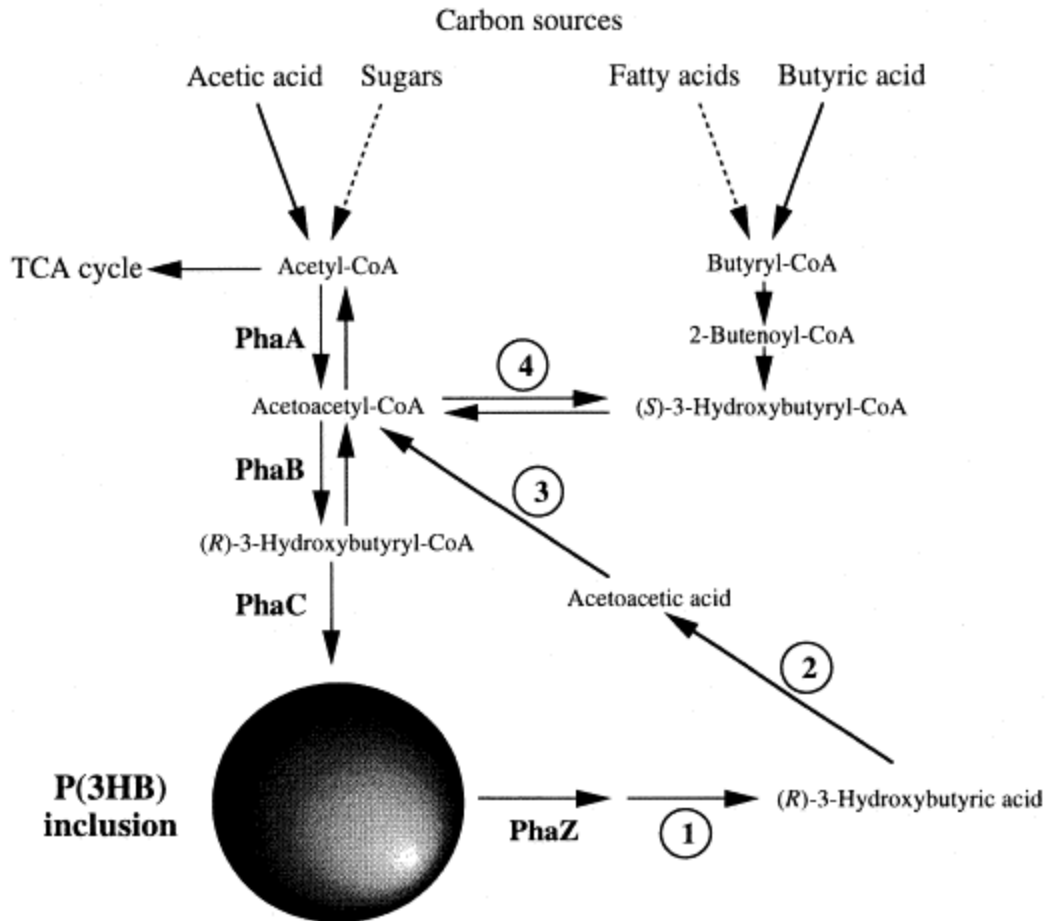


Figure 5. Cyclic metabolic nature of P(3HB) biosynthesis and degradation in bacteria. PhaA, β -ketothiolase; PhaB, NADPH-dependent acetoacetyl-CoA reductase; PhaC, PHA synthase; PhaZ, PHA depolymerase; 1, dimer hydrolase; 2, (R)-3-hydroxybutyrate dehydrogenase; 3, acetoacetyl-CoA synthetase; 4, NADH-dependent acetoacetyl-CoA reductase, obtained from Sudesh et al. (2000).

Acetyl-CoA is the main molecule involved in PHB production. Through the central metabolism, it can be produced from carbon fixation, catabolism of glycogen or glucose (Mills et al., 2020). Carbon is fixed from CO_2 through the Calvin-Benson-Bassham cycle (Price et al., 2020). It is the most common used metabolism pathway in plants, algae and cyanobacteria. CO_2 is then reduced into organic molecules, concretely glycerate-3-P (Shinde et al., 2020). This organic compound is transformed into Acetyl-CoA, which can be finally transformed into polyhydroxybutyrate (Mills et al., 2020).

Glycogen catabolism is catalysed by GlgX and GlgP and is transformed into glucose-1-P. Glucose can be degraded by three metabolic pathways: glycolysis (the Embden–Meyerhof–Parnas (EMP) pathway), the oxidative pentose phosphate pathway and the Entner-Doudoroff (ED) pathway (Mills et al., 2020). All these reactions finally form molecules of Acetyl-CoA, which can be used

to form polyhydroxybutyrate. There are other metabolic pathways related to Acetyl-CoA production: β -oxidation of fatty acids and *de novo* fatty acid biosynthesis pathway, from sugars (Sudesh et al., 2000).

On the other hand, glycogen is synthesized from ADP-Glucose, which is the major limiting step in its synthesis (Ball and Morell, 2003). The glycogen biosynthetic pathway and the PHB biosynthetic pathway compete for the same intermediate, 3-phosphoglycerate (3PG). Thus, a part of the 3PG produced during CO₂ fixation, is consumed during the formation of glycogen, reducing PHB productivity (Singh et al., 2017). Moreover, glycogen allows the cells to survive under nutrient deprivation conditions (Preiss, 1984). Therefore, it makes sense to jointly study glycogen and PHB synthesis.

However, Acetyl-CoA can be consumed through the tricarboxylic acid cycle. This pathway plays an important role in all organisms. It involves the reactions to oxidase Acetyl-CoA to CO₂, with the consequent production of energy molecules, as NADPH. In cyanobacteria, there is a main difference in comparison to other microorganisms: they do not have the enzyme α -ketoglutarate dehydrogenase, which converts α -ketoglutarate to succinyl-CoA. *Synechocystis* presents, instead, two different enzymes that catalyze the transformation of α -ketoglutarate to succinate (Mills et al., 2020).

1.5 PHB production by cyanobacteria

Not all species of cyanobacteria are capable of producing PHB. Many studies revealed negligible percentages of PHB by dry cell weight (at below 1%_{dcw}), although some authors obtained percentage up to 40%_{dcw} by using heterotrophic production instead of autotrophic (Price et al., 2020). The study by Kaewbai-ngam et al. (2016) reported around 20-25%_{dcw} of PHB using non-genetically modified strains of cyanobacteria. Genetic engineering can provide strains with high productivity values, making the PHB production process more feasible. For example, Kamravamanesh et al. (2018) produced randomly mutants of *Synechocystis* by applying ultraviolet (UV) light. One of the strains showed percentages of PHB around 37%_{dcw}, 2.5-fold higher PHB productivity than the wild type.

PHB production can vary depending on the environmental conditions. Kaewbai-ngam et al. (2016) studied the PHB production under different nutrient limitations, including nitrogen, phosphorus, potassium and their combinations. The results showed first that PHB production was strain

specific. Moreover, the highest percentage of PHB accumulation was observed in nitrogen deprivation conditions. Other nutrient conditions, like phosphorus or/and potassium deprivation, also showed an increase in PHB production. The change response in PHB accumulation was also strain specific. Arias et al. (2020) summarized the different PHB percentage by dry mass in different cyanobacteria strains and the methodology to obtain such results. Nutrients limitation is the most common approach and has allowed percentages around 10-50%_{dcw} using organic carbon source. However, it seems more attractive the use of inorganic carbon source, to reduce production costs. Using a microbial consortium, formed mainly by cyanobacteria from wastewater, with inorganic carbon source, under nitrogen or phosphate limitation, PHB percentages were 5.4%_{dcw} and 5.9%_{dcw}, respectively (Arias et al., 2018).

The different behaviour of cyanobacteria depending on the environmental conditions has a molecular explanation: the biosynthesis of PHB can be regulated at the enzymatic level (Steinbüchel and Schlegel, 1991). For example, it is known that the enzyme PhaA is regulated by free Coenzyme A (Haywood et al., 1988). When the culture medium is not nutrient-limited, the concentration of Coenzyme A is pretty high. Then, the enzyme PhaA is inhibited and there is no PHB production. On the contrary, if there are nitrogen-limited conditions, the concentration of Coenzyme A decreases, so PhaA will be functionable and PHB will be produced (Steinbüchel and Schlegel, 1991).

Industrial production of PHB using cyanobacteria is still really costly. It is principally due to the cost related to biomass cultivation and harvesting. These costs make the process not commercialised yet. First, the needed bioreactors (Open Race Ponds, ORP and photobioreactors, PBR) are more expensive, while building and operating, than obtaining biomass from terrestrial crop sources (Price et al., 2020). Second, terrestrial crops are easier to harvest because they are much concentrated than microalgae (Fasaei et al., 2018). Third, photoautotrophic PHB production is still really low in comparison with the heterotrophic one, so they have a low volumetric productivity (Price et al., 2020). Moreover, cyanobacteria, as photoautotrophic microorganisms, need large amounts of surface as they need light to grow. In conclusion, cyanobacteria will need a surface hundreds of thousands times larger than heterotrophic cultures. Finally, low productivity raise the price of the downstream processes as the amount of waste is bigger than the desirable product (Price et al., 2020).

The economic disadvantages need to be overcome in order to produce bioplastics from cyanobacteria and take advantage of their environmental benefits (Price et al., 2020). The use of wastewater as the nutrient source for the production of bioplastics could be one solution. The use of algal communities to treat wastewater has been studied since 1965. It is an economical and environmentally friendly process, due to the fact that it is a photosynthetic process and the biomass can be reused (Lee et al., 2015). They have also showed higher efficiency rates than activated sludge within nutrient assimilation (Arias et al., 2020). Thus, cyanobacteria could be used in wastewater treatments with two main benefits: firstly, reducing the pollutants in water and, secondly, obtaining desirable products, like PHB.

One of the advantages of cyanobacteria is that these microorganisms can grow in three different modes: photoautotrophic, mixotrophic and heterotrophic. In the photoautotrophic mode, carbon dioxide is used as the carbon source and light as the energy source. In the heterotrophic mode, both carbon and energy source are obtained from organic compounds. Lastly, in the mixotrophic mode, in the presence of light both organic and inorganic compounds are used (Singh et al., 2017). In the heterotrophic production, approximately 50% of the cost is due to the substrate supply (Price et al., 2020). A suitable solution is to employ carbon dioxide as the carbon source, which might be the residue of a nearby industry.

With the above information, the study and analysis of PHB production by cyanobacteria seems to be crucial to improve the productivity. In the present study, a strain of cyanobacteria (*Synechocystis*) has been grown following the most used methodology to enhance PHB production, nutrients limitation approach. Different factors have been analysed: initial inorganic carbon concentration, different additions of nitrogen and phosphorus, and salinity in the culture medium. Then, glycogen and PHB content have been monitored in order to get a better understanding of their metabolism and state which are the conditions that get the highest PHB production. Moreover, reverse-transcription quantitative polymerase chain reaction (RT-q-PCR) protocols have been implemented in order to assess the gene expression of several genes involved in PHB metabolism.

This document is organised in sections: section 1 includes the introduction, section 2 includes the main objective and the sub-objectives of the different experiments, section 3 includes all materials and methodologies used, section 4 includes the design and implementation of reverse transcription

quantitative polymerase chain reaction (RT-q-PCR), with the specific results of that part. Then, section 5 includes the results and discussion of the experiments about PHB production by *Synechocystis*, section 6 includes the conclusion and finally, section 7 includes ideas for continuing the investigation.

2. Objectives

The general objective of this study is to enhance the production of polyhydroxybutyrate (bioplastic) by *Synechocystis*. The strain used in this study was previously isolated from wastewater and produced 5.9%_{dcw} of PHB. To increase the productivity, three experiments were carried out with different environmental conditions. In this sense, it has been studied the effect of inorganic carbon, of several additions of nitrogen and phosphorus, and of salinity over PHB biosynthesis. Moreover, it is also important to study the gene expression regarding PHB metabolism and other routes related to this compound. RT-q-PCR is the best tool to assess the gene expression. However, as it is the first time this molecular technology is used in this laboratory, the first step consisted in designing, developing and implementing RT-q-PCR protocols.

This project has the following specific objectives:

- Maintenance of cyanobacterial cultures at different laboratory-scale reactors.
- Implementation of RT-q-PCR protocols to study the gene expression.
- Maintenance and operation of laboratory-scale photobioreactors (3L).
- Evaluation of the effect of culture conditions on PHB accumulation: to assess the effect of the amount of inorganic carbon in the media on PHB production and accumulation, to assess the effect of intermittent additions of nutrients on PHB production and accumulation, to assess the effect of the salinity in the culture media on PHB production and accumulation.

3. Material and methods

3.1 Media and reagents

Cyanobacterial cultures were prepared using BG-11 medium, which consisted of: 1500 mg/L NaNO_3 , 31.4 mg/L K_2HPO_4 , 36 mg/L MgSO_4 , 36.7 mg/L $\text{CaCl}_2 \cdot 2\text{H}_2\text{O}$, 20 mg/L Na_2CO_3 , 1 mg/L NaMgEDTA , 5.6 mg/L citric acid, 6 mg/L Ferric ammonium citrate and 120 mg/L NaHCO_3 . Cyanobacterial colonies were maintained in plates with solid medium which consisted of BG-11 supplemented with 1% bacteriological agar. However, the initial concentration of nitrogen and phosphorus varied in each experiment (Table 2).

The reagents for the modified BG-11 used in the reactors (K_2HPO_4 , NaNO_3 , NaHCO_3 , $\text{CaCl}_2 \cdot 2\text{H}_2\text{O}$, NaOH , Na_2EDTA , NaHCO_3) and the reagents needed for NO_3^- , NO_2^- , NH_3 and P analysis were obtained from Panreac (Barcelona, Spain). $\text{MgSO}_4 \cdot 7\text{H}_2\text{O}$, $\text{C}_6\text{H}_8\text{FeNO}_7$ (ammonium ferric citrate), $\text{C}_6\text{H}_8\text{O}_7$ (citric acid), HCl , chloroform (CHCl_3) and D-glucose were obtained from Scharlau (Barcelona, Spain). Reagents needed for PHB measures, H_2SO_4 and MeOH , were obtained from Panreac (Barcelona, Spain) and Scharlau (Barcelona, Spain), respectively. PHB-PHV (86:14% wt, CAS 80181-31-3) copolymer standard was obtained from Sigma-Aldrich (St. Louis, US).

3.2 Cyanobacteria cultures

The experiments were performed using four 2.5 L closed photobioreactors (PBR). These polymethacrylate PBRs were of cylindrical shape, with a total volume of 3L (Figure 6). The mixing in the PBRs was continuous, and it was magnetic (with a magnetic stirrer, VELP scientifica, Usmate, Italy). Temperature was set at 30°C (± 2) and they were illuminated with warm white LED stripes rolled up around each reactor ($102 \mu\text{mol PAR} \cdot \text{m}^2/\text{s}$) and 14W cool-white LED lights with a regimen of 15:9h light:dark. Using a pH probe (HI1001, HANNA instruments, Italy), pH was monitored in-line. An automatic pH controller (HI 8711, HANNA instruments, Italy) kept pH at 8 by controlling the injection of CO_2 . BG-11 medium and all the materials were sterilized by using the autoclave (Wisd laboratory instruments, Italy) (121°C , 40 minutes) or using NaHClO (70 % v/v). PBRs were also connected to CO_2 bottles and they have valves to maintain atmospheric pressure. They all have $0.2 \mu\text{m}$ filters, to avoid contamination.

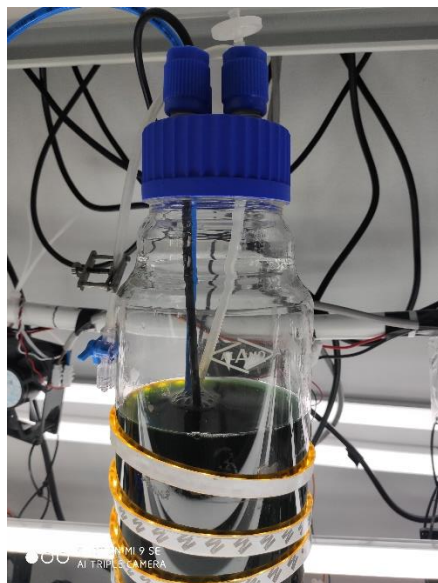


Figure 6. Picture of the photobioreactor.

Once the medium and materials were sterilized, PBRs were inoculated working in a laminar flow chamber to avoid contaminations. The laminar flow chamber has been always disinfected with ultraviolet light and ethanol (70 % v/v). The initial cyanobacterial cultures were obtained from wastewater, as described by Rueda et al. (2020). In this study, PBRs were inoculated with *Synechocystis*, which are maintained in 1 L Erlenmeyer flask. Samples were taken every working day, using a vacuum system connected to the PBR, to control the process during the whole experiment. The vacuum system has 0.2 μm filters, to avoid contamination. Samples were weekly observed with the microscope (Nikon, eclipse E200) in order to see if there were any contamination.

3.3 Experiments

Continuing the results previously obtained by Rueda et al. (2020), it was applied the two-steps cultivation approach for each experiment (Figure 7). It consisted of an initial phase, in which biomass grows in a medium containing all the nutrients and then, a limitation/accumulation phase, in which they are cultivated without nitrogen and phosphorus in the media (Kamravamanesh et al., 2018). Then, different conditions have been analysed in order to enhance PHB production. These conditions are: the concentration of inorganic carbon, the positive or negative effect of intermittent

additions of nitrogen and phosphorus during the accumulation phase, and the concentration of salt (NaCl). The two phases were performed as described in the followings:

- Growth phase: 3L PBRs contain the nutrients in high concentrations to allow the growth of the biomass without limitations. This phase can last between 10 and 30 days, until nitrogen and phosphorus are depleted. The initial concentrations of nitrogen and phosphorus are shown in Table 2.

Table 2. Initial concentrations of nitrogen and phosphorus in each experiment.

	Experiment 1	Experiment 2	Experiment 3
Nitrogen (mg/L)	43	37	51
Phosphorus (mg/L)	7	8	2

- Accumulation phase: this phase starts when nitrogen and phosphorus are depleted in the culture media. Three experiments were carried out with different conditions in the accumulation phase. First, the effect of the inorganic carbon (IC) content has been analysed. At this aim, the IC content in the four PBRs was progressively increased from 0 to 2000 *mg/L*. Second, the effect of nitrogen and phosphorus additions has been analyzed. Third, the effect of salinity in the media has been also analyzed. For this purpose, the salinity content in the four PBRs was progressively increased by adding NaCl and bicarbonate, from an initial electrical conductivity of 12 *mS/cm* to 48 *mS/cm*.

The three experiments performed to assess the effect of these operational conditions are described in the followings.

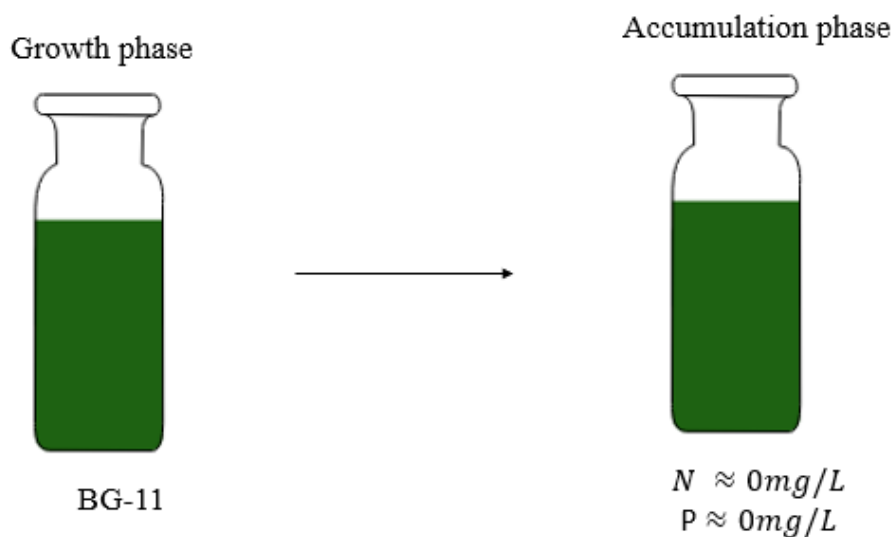


Figure 7. Scheme of the different phases during the production of PHB.

First experiment: inorganic carbon (IC) effect

The four PBRs were inoculated with *Synechocystis* at a concentration of 1065.78 mg/L of volatile suspended solids (VSS). The initial growth phase lasted 10 days. After the growth phase, the content of all reactors was mixed and equal volumes were transferred into the 4 PBRs for the accumulation phase. The experimental conditions (Figure 8) for each PBR during the accumulation phase were the followings: (PBR1) $IC = 0 \text{ mg/L}$, (PBR2) $IC = 30 - 50 \text{ mg/L}$ (maintained with a daily addition of $10 \text{ g/L } HCO_3^-$), (PBR3) $IC = 120 - 130 \text{ mg/L}$ (maintained with CO_2), (PBR4) $IC = 2000 \text{ mg/L}$ (maintained with CO_2). The accumulation phase lasted 26 days.

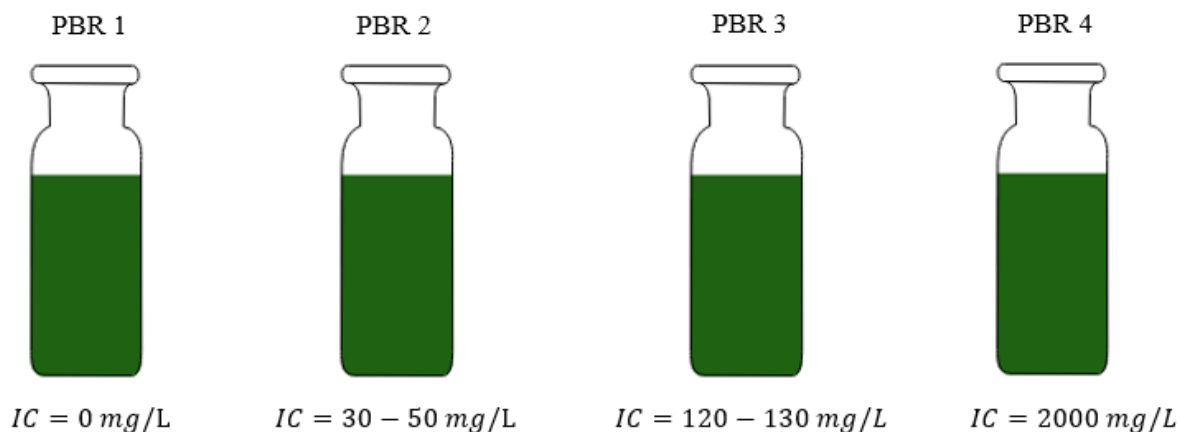


Figure 8. First experiment diagram.

Second experiment: additions of nitrogen and phosphorus effect

For this experiment, the four PBRs were inoculated with an initial concentration of 1347.30 mg/L of VSS. The initial growth phase lasted 27 days. After that, all reactors were mixed and equal volumes were transferred into the 4 PBRs. The accumulation phase started with an addition of 2000 mg/L of bicarbonate. The experimental conditions (Figure 9) for each PBR during the accumulation phase were the followings: (PBR1) no additions, as control, (PBR2) addition of phosphorus (day 31), (PBR3) addition of nitrogen (days 29,31,34,36,38,41,43) when phosphorus was finished, (PBR4) two additions of nitrogen (days 34, 41). The accumulation phase lasted 15 days.

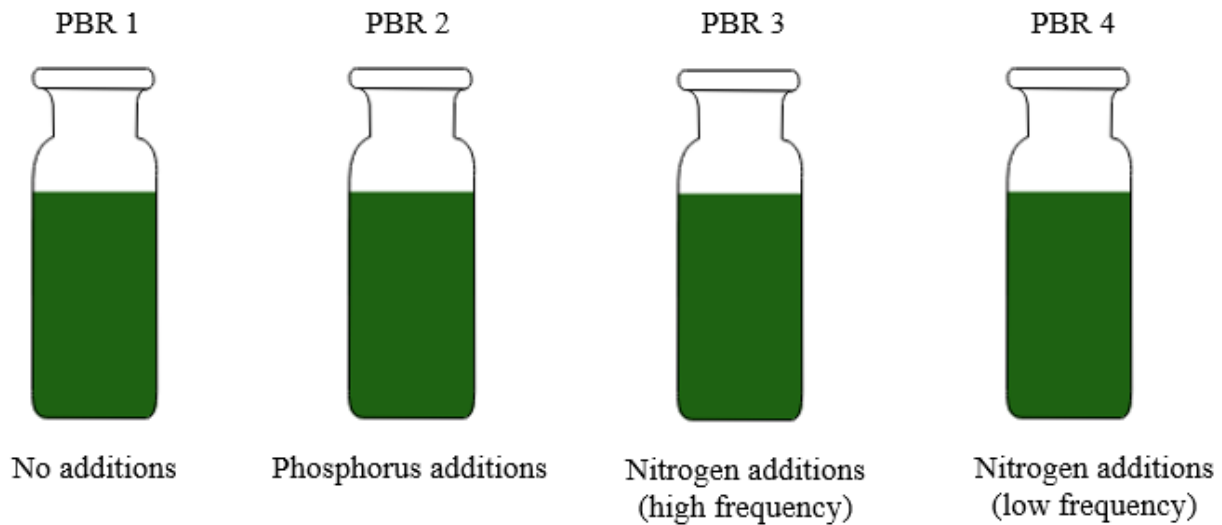


Figure 9. Second experiment diagram.

Third experiment: salinity effect

For his experiment, the four PBRs were inoculated with an initial concentration of 723.36 mg/L of VSS. The initial growth phase lasted 27 days. After that, all reactors were mixed and equal volumes were transferred into the 4 PBRs. Different additions of IC and NaCl were performed to achieve different salinity and electrical conductivity in the PBRs at the beginning of the accumulation phase, which lasted 15 days. The experimental conditions (Figure 10) for each PBR were the followings, Table 3:

Table 3. Experimental conditions for salinity effect.

	IC (mg/L)	NaCl (g/L)	Electrical conductivity (mS/cm)
PBR 1	2000	0	12
PBR2	100	5.80	13
PBR3	2000	8.04	24
PBR4	2000	30.77	48

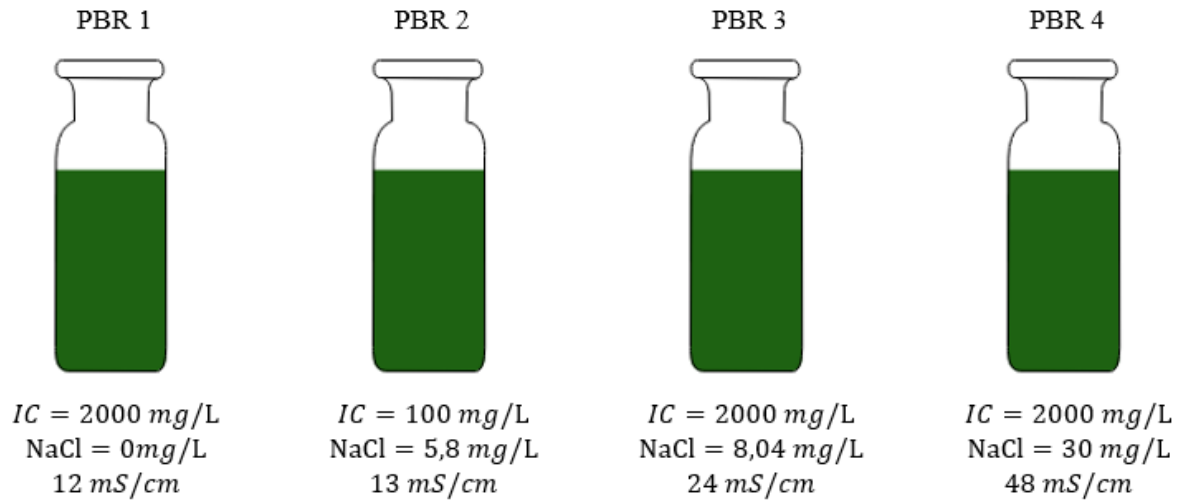


Figure 10. Third experiment diagram.

3.4 Analytical methods

Different analytical measures were performed every working day to analyse culture growth and the concentration of nutrients in the medium. In this sense, there were measured: turbidity, dissolved oxygen (DO), alkalinity, total and volatile suspended solids, nitrogen and phosphorus content as principal nutrients and carbohydrates and PHB content.

Turbidity indicates the presence of suspended solids in a water sample. It is measured with nephelometers and they measure the light scattered at an angle of 90° from the incident light beam. The unit is Nephelometric Turbidity Unit (NTU). The higher the amount of suspended solids (microbiological contamination), the higher the turbidity. Due to this reason, together with the

easiness of measuring turbidity, it is usually used to assess water quality. Dissolved oxygen is the amount of oxygen that is present in the samples and it is available for the microorganisms. It is measured with a dissolved oxygen meter. Alkalinity can be defined as the capacity of acid neutralizing and it measured as *mg/L of CaCO₃*.

The different solids, organic or inorganic, are classified according to their size and method of elimination of these particles in water. Total solids (TS) refer to the total amount of solid substances present in a water sample. They can also be suspended solids (SS): those that are larger than 0.45 μm and are therefore retained by a filter with this pore size or dissolved (filterable) solids (DS): those that pass through a filter with a pore size of 2 μm . On the other hand, within each type, volatile solids (VS) are distinguished, of an organic nature that are volatilized in the muffle at 550°C and fixed solids (FS), of an inorganic nature that correspond to inert substances and therefore not degradable by biological action. The latter are not volatilized at 550°C. Bacterial cells are classified as volatile suspended solids (VSS).

Turbidity (HI93703, HANNA Instruments) and dissolved oxygen (HI94142, HANNA Instruments) were measured every working day. Alkalinity (MD 600 photometer, Lovibond) was measured one day per week. Total suspended solids (TSS) and volatile suspended solids (VSS) were measured three days per week following the gravimetric methods 2540C and 2540 D described in the Standard Methods for the Examination of Water and Wastewater (APHA et al., 2012). Electrical conductivity (Conductimeter GLP 31, Crison, Spain) was daily measured in experiment 3.

Nitrate (N-NO₃) was measured following the spectrophotometric method (4500-NO₂⁻ for nitrites and 4500-NO₃⁻ for nitrates) described in (Clesceri et al., 1999). It was measured every working day during growth phase. During the accumulation phase, in experiment 1, it was measured once a week; in experiment 2, it was measured once a week in PBR 1 and PBR2, daily in PBR3 and three times per week in PBR4; in experiment 3, it was measured every working day until they were finished. Phosphate (P-PO₄) was measured following the spectrophotometric method (4500-PE and 4500-P) described in (Clesceri et al., 1999). It was measured every working day during growth phase. During the accumulation phase, in experiment 1, it was measured once a week; in experiment 2, it was measured once a week in PBR 1, daily in PBR3 and three times per week in PBR2 and PBR4; in experiment 3, it was measured three times per week.

PHB was measured once a week during growth phase and two days per week during the accumulation phase. Glycogen was measured once a week during growth phase and daily during the accumulation phase. Figure 11 shows a summary of all the analytical measures and Table 4 shows the schedule that was followed during the experiments.

Table 4. Schedule of the analytical analysis performed. Electrical conductivity* was only measured in the third experiment.

Growth phase				
Monday	Tuesday	Wednesday	Thursday	Friday
DO	DO	DO	DO	DO
Turbidity	Turbidity	Turbidity	Turbidity	Turbidity
Alkalinity	Conductivity*	Conductivity*	Conductivity*	Conductivity*
Conductivity*	Nitrate	TSS/VSS	Nitrate	TSS/VSS
TSS/VSS	Phosphate	Nitrate	Phosphate	Nitrate
Nitrate	PHB	Phosphate		Phosphate
Phosphate	Glycogen			
Accumulation phase				
DO	DO	DO	DO	DO
Turbidity	Turbidity	Turbidity	Turbidity	Turbidity
Alkalinity	Conductivity*	Conductivity*	Conductivity*	Conductivity*
Conductivity*	PHB	TSS/VSS	PHB	TSS/VSS
TSS/VSS	Glycogen	Glycogen	Glycogen	Glycogen
Glycogen				
First experiment				
Nitrate				
Phosphate				
Second experiment				
Nitrate	Nitrate (PBR3)	Nitrate	Nitrate (PBR3)	Nitrate
Phosphate	Phosphate	(PBR3/PBR4)	Phosphate	(PBR3/PBR4)
	(PBR3)	Phosphate	(PBR3)	Phosphate
		(PBR3/PBR4)		(PBR3/PBR4)

Third experiment				
Nitrate Phosphate	Nitrate	Nitrate Phosphate	Nitrate	Nitrate Phosphate

Description of PHB extraction and quantification method

It was taken 50 mL of sample from each photobioreactor. The samples were centrifuged (Centrifuge 5424 R, Sigma-Aldrich) at a centrifugal force of 18407 rcf during 20 minutes. Then, the supernatant was removed and the final precipitate was transferred into 1 mL Eppendorf tubes. These tubes were frozen at -80°C overnight in ultra-freezer (Arctiko, Denmark) and then freeze-dried for a period of 24 hours in a freeze dryer (Scanvac, Denmark) at the following conditions of temperature and pressure: -110 °C, 0.049 hPa.

The freeze-dried samples were submitted to PHB extraction. First, it was measured between 3 and 3.5 mg of lyophilized biomass for each sample. Then, it was added 1 mL of CHCl₃ (chloroform) mixed with benzoic acid as internal standard and 1 mL of MeOH acidified with H₂SO₄ (20% v/v). Next, the tubes were incubated at 100°C in a dry-heat thermo-block (Selecta, Spain). After 5 hours, the reaction was stopped by submerging the tubes in an ice-bath for 20 minutes and it was added 1 mL of distilled water to each tube. The samples were then vortexed for one minute and a half, so there were formed two clearly separated phases: one organic (which contains the PHB) and one aqueous. Finally, with the help of a Pasteur pipette it was obtained the organic phase and transferred it to vials with molecular sieves. These molecules were used to remove the water molecules that could be remained. The PHB content was measured using gas chromatography (GC) (7820A, Agilent Technologies, USA).

As the same way as the sample, a calibration curve with six points was prepared using the co-polymer of PHB-PHV.

Description of carbohydrates quantification method

Glycogen was measured by using the carbohydrate method (DuBois et al., 1956). It was measured both, the total and soluble glycogen. For the total, it was used samples directly obtained from the photobioreactor. For the soluble one, samples were first filtered. Both samples were then treated in the same way. First, 2 mL of HCl (1N) were added to the samples and then, they were incubated

at 100°C in a dry-heat thermo-block (Selecta, Spain). After 2 hours, the samples were cooled down at room temperature. Finally, it was added 0.5 mL of phenol (5% w/v) and 2.5 mL of H₂SO₄ (conc.). Samples were thoroughly mixed and after 10 minutes at room temperature, they were submerged in a bath at 35°C for 15 minutes. The carbohydrates are measured spectrophotometrically, at 492 nm, with a spectrophotometer (Spectronic Genesys 8, Spectronic instrument, UK). It has to be taken into account that this method measures all the carbohydrates in the sample, not only glycogen.

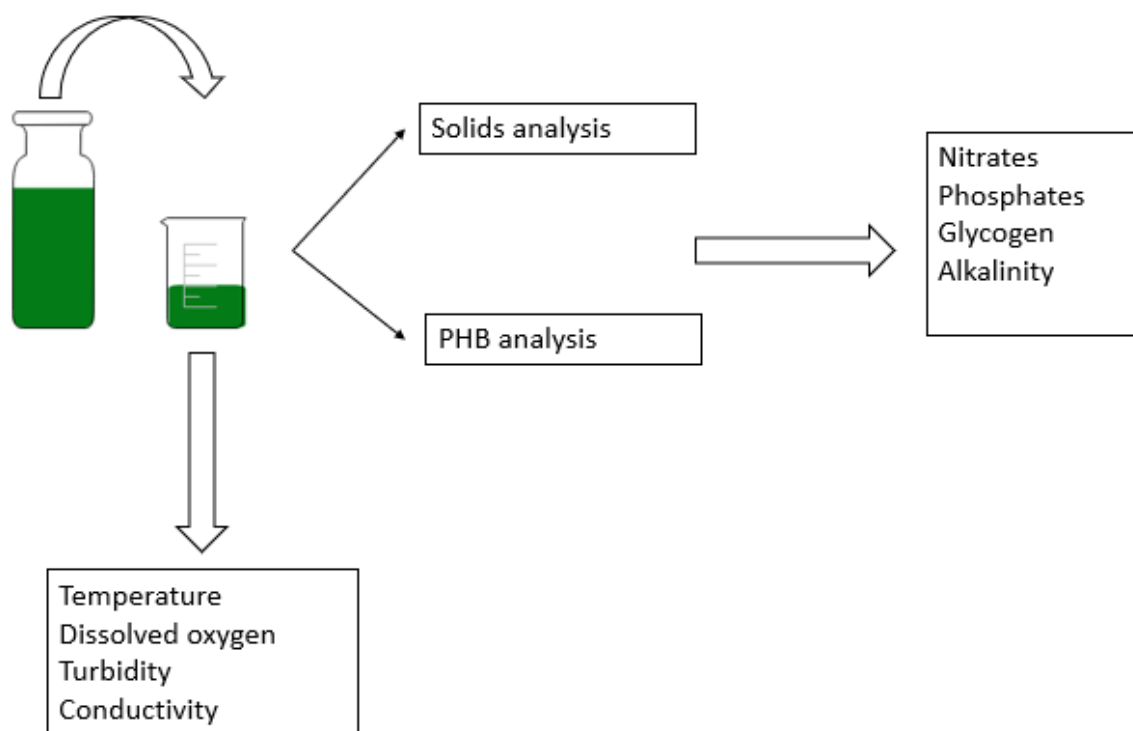


Figure 11. Diagram of the analytical measures that were carried out during the experiments.

3.5 RT-q-PCR analysis

1.5 mL of sample were transferred from the photobioreactors to RNase-free Eppendorf tube, working in the Laminar Flow Chamber. The Eppendorf tubes must be on ice to avoid the degradation of RNA. Then, samples were centrifuged at 18407 rcf for 5 minutes. The supernatant was discharged and the pellets are stored at -80°C (ARCTIKO).

RNA extraction was performed with PureLink Mini Kit (Ambion by Life Technologies, ThermoFisher Scientific, USA) according to the manufacturer's recommendation (protocol is

added in Annex II). DNA digestion was performed on a column containing RNase-free DNase (On-column DNAase I Digestion Set, Sigma, Austria) and following the manufacturer's recommendation (Annex II). The RNA was reverse transcribed using the RevertAid™ Reverse Transcriptase kit (ThermoFisher Scientific, USA) and the provided random hexamer primers, following the manufacturer's instructions (Annex II). q-PCR was performed, using Luna Universal qPCR Master Mix (New England Biolabs, USA), 300 nM primers in the system and 5µL PowerUp™ SYBR™ Green Master Mix (appliedbiosystems). The thermal cycling conditions are described in Annex I, according to the manufacturer's instructions. The genes studied are described in Table 5.

Table 5. Description of the genes studied with the name of the protein that encoded, the microorganism, the pathway, the enzyme classification (EC) and the reference.

Gene	Protein	Microorganism	Pathway	EC	Reference
fbp	Fructose-1,6-bisphosphatase class 1	<i>Synechocystis</i> sp. (strain PCC 6803)	Calvin cycle	3.1.3.11	(Mokrasch et al., 1956)
glgX	Glycogen operon protein GlgX	<i>Synechocystis</i> sp. (strain PCC 6803)	Glycogen catabolic process		(Davies, G., Henrissat, B., 1995)
rnpA	Ribonuclease P protein component	<i>Synechocystis</i> sp. (strain PCC 6803)	tRNA processing	3.1.26.5	(Pascual and Vioque, 1999)
gltA	Citrate synthase	<i>Synechocystis</i> sp. (strain PCC 6803)	Tricarboxylic acid cycle	2.3.3.16	(Karpusas et al., 1990)

4. Designing, developing and implementing RT-q-PCR protocols

4.1. Introduction

One of the objectives of this study was to design, develop and implement the reverse-transcription polymerase chain reaction (RT-q-PCR) protocols, since this is the first time that this molecular tool has been used in this laboratory for analyzing gene expression of cyanobacteria. The objectives, methods, results and conclusions of this part of the study are presented in this section 4 of the document.

As it was previously described, PHB production by cyanobacteria is high variable depending on different factors. In order to industrially produce this biomaterial, it is needed to thoroughly study the metabolism of the cells and understand in detail their behaviour. For this purpose, a reliable analysis of the genetic expression seems to be crucial (Pinto et al., 2009). As a consequence of the environmental conditions, the metabolism of the cells is altered. This change is due to variations in the transcriptional rates, but also through the processing of the mRNA precursor, the efficiency of nucleocytoplasmic transport and the degradation of mRNA inside the cell (Farrel, 2010).

There are different molecular methods, but quantitative reverse-transcription polymerase chain reaction (RT-q-PCR) has become the most used technology to quantify mRNA for gene expression (Jahn et al., 2008). This type of molecular techniques depends on the quality of the extracted RNA and the degree of the genomic DNA contamination (Pinto et al., 2009). Moreover, mRNA is very sensitive to degradation with RNases, process that can occur during improper handling (Jahn et al., 2008).

Quantitative real-time PCR (q-PCR) involves multiple amplification cycles that include the following steps: DNA denaturation, annealing of oligonucleotide primers targeting specific sequences, extension of a complementary strand to each primer by a DNA polymerase (which is exponentially increased with each PCR cycle), detection of a fluorescence reporter that indicates the DNA amplification (Smith and Osborn, 2009).

Reverse transcription (RT) is the process through which a complementary DNA (cDNA) is obtained from RNA (Nelson and Cox, 2015). It is a process quite variable and frequently unreproducible due to several factors: the state of the cells; the quality of the RNA (which is high unstable); the abundance of the template (Miranda and Steward, 2017). The enzyme that catalyses

the reaction is the reverse transcriptase and three reactions are involved: synthesis of complementary DNA from RNA, degradation of the RNA and synthesis of DNA from the complementary DNA (Nelson and Cox, 2015). To start the reaction, the reverse transcriptase needs a short chain of DNA oligonucleotides, called primer (Nelson and Cox, 2015). Depending on the type of primers, the reverse transcription can be initiated in three different ways:

- A. Random primers: they prime multiple points along the transcripts, so they produce several cDNA per original target (Bustin and Nolan, 2004). Therefore, it is a nonspecific method.
- B. Oligo-dT primers: it is more precise than random primers, as they do not transcribe ribosomal RNA, only the mRNA that contains a polyA tail (Bustin and Nolan, 2004).
- C. Target-specific primers: it synthesizes the most specific cDNA, but it requires a reverse transcription for each target (Bustin and Nolan, 2004).

RT-q-PCR is used as a powerful tool to analyse gene expression, by detecting and quantifying RNA (in terms of rRNA or mRNA transcripts) in environmental samples (Smith and Osborn, 2009). However, these studies are highly complex due to the lability of RNA, which has a potentially short half-life (Grunberg-Manago, 1999). Moreover, it is well known that environmental samples might present PCR inhibitor, negatively affecting the q-PCR (Stults et al., 2001). What is more, RNA samples must be free from DNA contamination, that would interfere with the final results and must be studied by triplicates ($n=3$), in order to generate statistical data (Smith and Osborn, 2009).

However, cyanobacteria present several properties that makes the RNA extraction a challenging step (Pinto et al., 2009). To start with, the fact that many strains release mucilaginous polysaccharides. These compounds complicate the cell lysis and also interfere with most nucleic acid purification protocols (Pinto et al., 2009). Cyanobacteria also produce endo- and exonucleases and photosynthetic pigments that can inhibit the enzymes during reverse transcription and PCR (Tillett and Neilan, 2000). In this sense, to study the genetic expression in cyanobacteria, RNA extraction is the first step and it seems to be the most crucial.

There have been developed different techniques to isolate nucleic acids from cyanobacteria cells, which are usually complex and laborious: mechanical cell breakage, enzyme digestions, multiple organic solvent extractions, grinding under liquid nitrogen or dry ice, hot phenol or caesium chloride ultracentrifugation (Tillett and Neilan, 2000). In cyanobacteria, one of most common

strategy is to combine the guanidinium thiocyanate-phenol-chloroform extraction commercially available as TRIzol (from Invitrogen) or TRI Reagent (from Molecular Research Center) with bead beating, which allows to physically lysate the cells (Pinto et al., 2009).

RNA extraction starts with cellular lysis. This step is typically performed using lysis buffers, which can be classified into two main groups: consisting of agents that break cell membrane and inactivate the RNase activity or buffers that solubilize the membrane but maintain intact the cellular organelles (Farrel, 2010). TRIzol, which is a mixture of guanidinium thiocyanate and phenol, is classified as the first type buffers and is one of the most effective lysis buffers (Pinto et al., 2009). These buffers can lysate the cells rapidly and completely while inactivate the RNase activity. They obtain very high-quality RNA samples due to its characteristic of protein denaturants. The effectiveness can be raised by adding beta-mercaptoethanol, which breaks intramolecular protein disulfide bonds. It is also used in combination with phenol, which allows the separation of the aqueous and the organic phases (Farrel, 2010). Cell lysis can be also enzymatically performed. This last method involves enzymes such as lysozyme, lysostaphin, zymolase, cellulase, protease or glycanase. Lysozyme is used for bacterial cell lysis, is available commercially and can be used for large scale (Shehadul Islam et al., 2017).

However, it is more and more common the use of commercial kits that isolate RNA with a higher productivity. These kits minimize or eliminate the use of hazardous reagents, such as phenol or chloroform. Instead, they are based in the use of silica columns (Farrel, 2010). These columns consist of silica filters (glass microfibers) that fits inside a 1.5 mL microcentrifuge tube. The sample passes through the filter and, in the presence of a high-salt and chaotropic environment, RNA binds to silica. Then, RNA is obtained after a series of washes under very low salt conditions (Farrel, 2010).

Apart from the above techniques, cells that have a strong wall are lysate by vortexing the samples in the presence of glass beads. This technique breaks the cell structure in a non-enzymatic manner (Farrel, 2010). The BeadBeater technique is used when chemical lysis is inefficient. It is a mechanical lysis in which small beads lysate rapidly the cells by the collisions of the beads with the cells (Farrel, 2010).

In this context, RT-q-PCR protocols has been designed, developed and implemented as it is the first time this molecular tool has been used in this laboratory. First, the protocols have been

performed following the manufacturer's instructions. Then, different modifications have been performed in order to improve the method and obtain the best results. The RT-q-PCR analysis is divided into four steps (Figure 12): nucleic acid extraction, treatment with DNase, RT (reverse transcription) and q-PCR. After the purification of the RNA with the DNase treatment, a q-PCR is performed in order to check that there is no DNA that could interfere with the final results. Although q-PCR is mostly used to obtain quantitative results, in this work only qualitative results are obtained in order to determine which protocols produce the highest quality results. The results of the optimization of each step of the RT-q-PCR are presented in the following subsections.

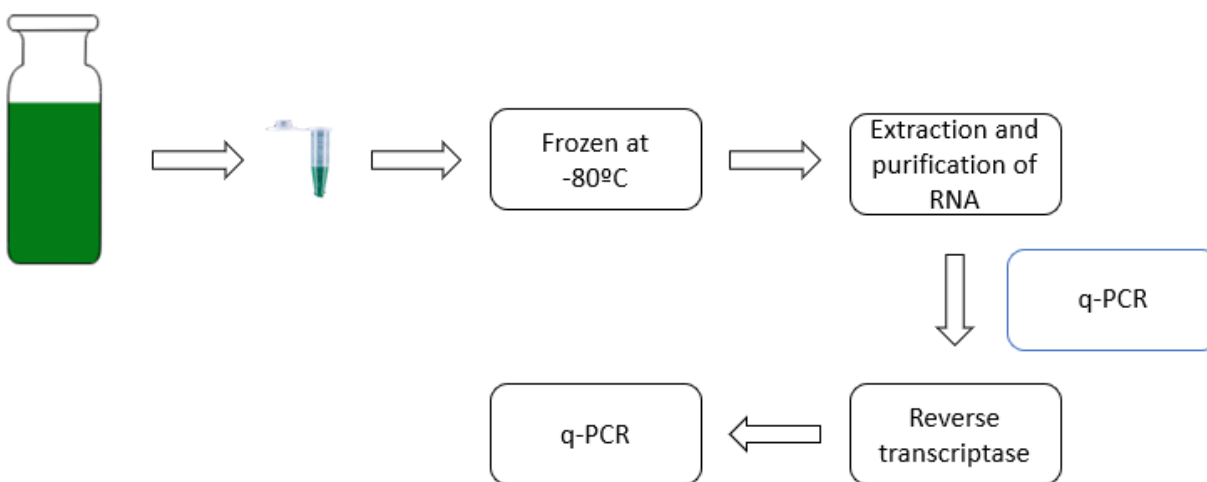


Figure 12. Schematic representation of the steps involved in the RT-q-PCR.

4.2 Optimization of the nucleic acid extraction

The extraction was performed using the PureLink RNA Mini Kit (Ambion by Life Technologies, ThermoFisher Scientific, USA) according to the manufacturer's recommendation. However, it was observed that the filter of the column was saturated when the samples were added. This was probably due to the presence of polysaccharides and to inefficient cell lysis. To overcome this problem, two strategies were applied: adding a step of bead beating (MP biomedical, LLC, USA) and adding a step with TRIzol reagent (Ambion by life technologies, ThermoFisher Scientific, USA) and bead beating (MP biomedical, LLC, USA). With both methods, the column was no longer saturated.

After using the PureLink RNA Mini Kit, samples were quantified in order to determine which strategy allows the highest content of nucleic acid. The results are shown in Table 6. TRIzol

reagent, combined with bead beating, did not supposed any advantage in comparison to only bead beating. Both strategies improved the nucleic acid yield in comparison to the commercial kit. These results are consistent with the experimental observations of the column.

Table 6. Results of the quantification of the samples after the extraction step was performed.

	Nucleic acid (ng/ μ L)
PureLink RNA Mini Kit	1.7
PureLink RNA Mini Kit + bead beating	4.1
PureLink RNA Mini Kit + bead beating + TRIZOL	4

The following extractions were performed combining only the PureLink RNA Mini Kit with bead beating, as TRIZOL is a toxic compound which must be used working in a fume hood and did not supposed any improvement.

4.3 Optimization of the DNase treatment

The extraction can isolate both DNA and RNA. Since the objective is to analyse the expression of mRNA, the DNA must be digested by applying a treatment with a DNase. DNA digestion was performed on a column containing RNase-free DNase (On-column DNAase I Digestion Set, Sigma, Austria) and following the manufacturer's recommendation. To check the efficiency of the treatment, a q-PCR was performed, using Luna Universal qPCR Master Mix (New England Biolabs, USA), 300 nM primers in the system and targeting highly conserved regions of the bacterial 16S rRNA gene.

The first results indicate that the treatment was inefficient, so the first strategy to improve the efficiency consisted in performing the treatment in dissolution (not on-column). This treatment was also performed by following the manufacturer's recommendation. In this case, the results showed that the DNA was efficiently digested. This protocol presents two main differences respective the on-column treatment protocol: the time of incubation with the enzyme is higher (30 minutes instead of 15) and the temperature is also higher (37°C instead of room temperature). Therefore, the original protocol of the on-column treatment was modified with these two

parameters in order to see if the efficiency was improved (the incubation time with the enzyme was raised to 30 minutes and the temperature was raised to 37°C). The results (Table 7) indicate that this treatment was also inefficient. The on-column treatment showed the presence of DNA while the sample with the treatment in dissolution was amplified below the negative control, indicating that there was no presence of DNA. For more details the reader is referred to Anex III (Figure 27).

Table 7. Results of q-PCR after applying different DNase treatments. The q-PCR targeted the bacterial 16S rRNA gene. The results are obtained from Figure 27.

DNase treatment	Result
On-Column (37°C and 30 minutes)	Positive
In dissolution	Negative
Positive control	Positive
Negative control	Negative

4.4 Optimization of the RT-q-PCR

The RNA was reverse transcribed using the RevertAid™ Reverse Transcriptase kit (ThermoFisher Scientific, USA) and the provided random hexamer primers, following the manufacturer's instructions. Then, the q-PCR was performed. The RT-q-PCR steps were performed after it was checked that there was no DNA in the samples.

First, primers from ribosomal DNA (16S rRNA gene) specific of *Synechocystis* were used. The results (Figure 28,

Table 8) indicate that all the samples were positive which means that the samples contained cDNA (as result of the reverse transcriptase) and it corresponded to a fragment of the 16S rRNA gene from *Synechocystis*.

At this point, it can be summarized that rRNA can be extracted from *Synechocystis* samples using the PureLink Mini Kit combined with bead beating, applying the DNase treatment in dissolution, performing the reverse transcription using RevertAid™ kit (with random primers) and identifying the results with the q-PCR (using SYBRN as the fluorescence reporter and 16S rRNA primers).

Table 8. Results of q-PCR after performing RT step, using random primers. The q-PCR targeted the 16S-rRNA gene from *Synechocystis*. The three samples are triplicates.

Samples	q-PCR result
Positive control	Positive
Sample 1	Positive
Sample 2	Positive
Sample 3	Positive
Negative control	Negative

As the reverse transcription was performed using random primers, the presence of cDNA from mRNA was searched. Therefore, the samples of the previous RT (Sample 1, 2 and 3) were used in a q-PCR, targeting specific genes of *Synechocystis* (*fbp*, *glgX* *rnpA*). The results (Table 9, Figure 29) indicate that all samples were negative, which means that the cDNA from mRNA was not amplified.

Table 9. Results of q-PCR after performing RT step, using random primers. The q-PCR targeted the *fbp*, *glgX* and *rnpA* gene from *Synechocystis*. The three samples are triplicates.

	Targeting <i>fbp</i> gene	Targeting <i>glgX</i> gene	Targeting <i>rnpA</i> gene
Positive control	Positive	Positive	Positive
Sample 1	Negative	Negative	Negative
Sample 2	Negative	Negative	Negative
Sample 3	Negative	Negative	Negative
Negative control	Negative	Negative	Negative

By applying the same conditions of RT-q-PCR, the results in Table 8 and Table 9, show that only cDNA from rRNA was detected. This was probably due to the lower amount of mRNA in comparison to rRNA (Bustin et al., 2005). In this sense, two hypotheses were suggested: first, the samples had not much biomass, so the mRNA transcribed was below the detecting limit of the q-PCR; second, the mRNA had been degraded when freezing the samples (they were stored at -80°C).

From this point, the different experimental designs were intended to observe the amplification of cDNA from mRNA.

Therefore, the whole process was repeated with different samples: one from a fresh inoculum and other from a sample, that was stored at -80°C, with more biomass than the previous one (0.88 g/L VSS instead of 0.37 g/L VSS). The sample from the inoculum was obtained as the following: 1.5 mL of the inoculum were transferred into an Eppendorf tube (in the laminar flow chamber) and it was centrifuged (5 minutes, 18407 rcf). The supernatant was discharged and the pellet was directly used for the extraction step. The two samples were treated in the same way: the extraction was performed combining it with bead beating, the RNA purification was carried out with DNase I treatment (without using the column) and the reverse transcription was performed using random primers.

Table 10. Results of q-PCR after performing RT step, using random primers. The q-PCR targeted the bacterial 16S rRNA, and 16S rRNA and rnpA gene from Synechocystis.

	Bacterial 16S rRNA	Synechocystis 16S rRNA	rnpA gene
Positive control	Positive	Positive	Positive
Inoculum sample	Positive	Positive	Negative
Frozen sample	Positive	Positive	Negative
Negative control	Negative	Negative	Negative

The results showed in Table 10 (Figure 30, Figure 31 and Figure 32) reveal that both samples, the one obtained from the fresh inoculum and the frozen sample, amplified the fragment from rRNA gene, both the general from bacteria and from *Synechocystis*. However, the same results regarding mRNA were obtained as the previous experiment. There was no amplification of cDNA from mRNA. It can be concluded from these results that the mRNA might not be lost when the samples are stored at -80°C and the quantity of biomass used was not enough to detect the mRNA.

In order to try to detect the mRNA, the conditions of the q-PCR were modified, summarized in Table 11. The primers used were concentrated inside the recommended range (300-800 nM). The volume of sample was doubled and triplicated, up to a final volume of 10 µL.

Table 11. Original conditions of the q-PCR and two different modifications, regarding the primers concentration and the volume of sample.

	Original conditions	Modified conditions 1	Modified conditions 2
Primers concentration	300 nM	300 nM	500 nM
Volume of sample (μ L)	1	2	3

Table 12. Results of q-PCR after performing RT step, using random primers. The q-PCR targeted the *rnpA* gene from *Synechocystis*. Modified conditions 1 refers to 2 μ L of sample and 300 nM of primers. Modified conditions 2 refers to 3 μ L of sample and 500 nM of primers.

RnpA gene		
	Modified conditions 1	Modified conditions 2
Positive control	Positive	Positive
Inoculum sample	Negative	Negative
Frozen sample	Negative	Negative
Negative control	Negative	Negative

The results showed in Table 12 (Figure 33 and Figure 34) indicate that the mRNA remained undetectable despite modifying the conditions of the q-PCR. Adding more sample or raising the concentration of the primers did not help detecting the low quantity of mRNA.

It is well known that, when the cDNA is transcribed from RNA using the random primers approach, the majority of the cDNA is from ribosomal RNA (Bustin et al., 2005). Therefore, the mRNA could not be correctly transcribed and, consequently, not amplified. Then, target-specific primers approach is suggested. This approach results in the most specific cDNA (Lekanne Deprez et al., 2002). However, it is not the best method when lots of genes will be studied because it requires reverse transcription for each gene (Bustin et al., 2005). Bustin and Nolan (2004) found that the best results were obtained when using target-specific primers.

Up to this point, the reverse transcription was performed using the provided random primers. Therefore, it will be performed a gene-specific reverse transcription with primers for *fbp* gene from *Synechocystis*. The concentration of the primers was 1.67 μ M, following manufacturer's instructions.

Table 13. Results of q-PCR after performing RT step, using specific primers for *fbp* gene. The concentration of the primers was 1.67 μ M.

Gene-specific RT (<i>fbp</i> gene)	
Positive control	Positive
Inoculum sample	Positive
Frozen sample	Positive
Negative control	Negative

The results of the gene-specific RT are shown in Table 13 (Figure 35). It is shown that, finally, DNA from mRNA was detected when applying the specific-targeted approach in reverse transcription. This result agrees with the previous results of (Bustin and Nolan, 2004). It is also shown that samples can be stored at -80°C, mRNA is not degraded.

Finally, it is performed the gene-specific RT, targeting *fbp* gene, with a negative sample in order to see if the primers could be given fluorescence signal in the follow q-PCR. In this case, the results will be a false positive. The negative N1 included the primers and the reverse transcriptase, but not RNA sample.

Table 14. q-PCR results of performing gene specific RT, targeting *fbp* gene, with two different negatives: N1 includes the primers and RT enzyme; N2 includes the primers and RNA sample, but no RT enzyme.

Fbp gene	
q-PCR Negative	Negative
N1	Negative
q-PCR Positive	Positive

The results shown in Table 14 (Figure 36) revealed that the gene-specific RT, targeting *fbp* gene, did not show any fluorescence signal, so this approach can be used in RT-q-PCR for amplifying mRNA.

Taking into account these results, it was decided to do a mixture of several primers from different genes. This mixture was used in the reverse transcription and then, the different genes were targeted with the q-PCR. The studied genes (from *Synechocystis*) are: 16S rRNA, rnpA, fbp and gltA. In the mixture, each primer will be added to a final concentration of 1.67 μ M.

Table 15. Results of q-PCR after performing RT step, using a mixture of genes from Synechocystis (16S rRNA, fbp, gltA, rnpA). The concentration of the primers was 1.67 μ M.

	16S rRNA	fbp	gltA	rnpA
Positive control	Positive	Positive	Positive	Positive
Inoculum sample	Positive	Positive	Positive	Positive
Frozen sample	Positive	Positive	Positive	Positive
Negative control	Negative	Negative	Negative	Negative

The results of using a mixture of primers for several genes are shown in Table 15 (Figure 37, Figure 38, Figure 39 and Figure 40). All the samples amplified DNA from both, ribosomal and messenger RNA.

Nevertheless, the above-mentioned results could not be realistic, as the mixture of primers could be giving a positive result without the presence of cDNA from mRNA. To investigate this hypothesis, two different negative controls were performed: first, a negative control (N1) with the mixture of primers and the reverse transcriptase, but without the samples from the extraction; second, a negative control (N2) with the mixture of primers and the samples from the extraction, but without reverse transcriptase.

The results shown in Table 16 (Figure 41) indicate that the mixture of primers was amplified in the q-PCR, suggesting that the results in Table 15 are not correct, they are false positives. The mixture of primers cannot be used to perform the RT-q-PCR.

Table 16. Results of q-PCR after performing RT step, using a mixture of genes from *Synechocystis* (16S rRNA, *fbp*, *gltA*, *mnpA*). The concentration of the primers was 1.67 μ M. The targeted gene during q-PCR was 16S rRNA. N1 refers to the negative control without sample, but including the mixture of primers and the RT. N2 refers to the negative control without the RT, but adding the sample and the mixture of genes.

16S rRNA	
Positive control	Positive
N1	Positive
N2	Negative
Negative control	Negative

TRIzol reagent is expected to avoid the degradation of the mRNA, preserving high RNA quality and quantity (Mohammad Najafi, 2014). So, it was performed a nucleic acid extraction using the PureLink mini kit combined with bead beating and TRIzol, following the manufacture's instruction (Annex II). The DNase treatment was applied in dissolution. A q-PCR was performed to check that there was no DNA remaining. Then, the reverse transcription was performed with random primer.

Also, another strategy to raise the quantity of mRNA consists in raising the concentration of random primers in the reverse transcription step. This was a strategy followed by Miranda and Steward (2017). These authors found that the best results were obtained after raising the concentration of the random primers by at least two orders of magnitude in comparison with the manufacturer's instructions. Therefore, the concentration of random primers was raised 10x, with both samples: one using TRIzol in the extraction step and another without TRIzol.

However, as the results in Table 17 (Figure 42) show, this strategy was ineffective, as the q-PCR was incapable of detecting any DNA from mRNA. In this case, TRIzol did not help to the detection of cDNA from mRNA and neither did raising the concentration of the random primers.

Table 17. Results of q-PCR after performing RT step, using random primers. The q-PCR targeted the *fbp* gene from *Synechocystis*. The concentration of the random primers was raised 10 times in comparison to the initial conditions (manufacturer's instructions).

Concentration random primers (10X)	
Positive control	Positive
TRIzol sample	Negative
Free-TRIzol sample	Negative
Negative control	Negative

4.5 Conclusions

The conclusions from the specific experiments for the design, development and implementation of RT-q-PCR are:

- The PureLink Mini Kit could not be used with *Synechocystis* samples without combining it with other lysis methods, such as bead beating or TRIzol reagent.
- TRIzol reagent did not suppose any advantage in comparison to bead beating in terms of RNA quantity and in stability of mRNA. Glass beads method is easier to use, does not generate toxic residues and it is not hazardous.
- The DNase treatment was inefficient when using it on-column, both with the conditions of the manufacture's protocol and the modified conditions. It was efficient when applying it in dissolution.
- RevertAid™ Reverse Transcriptase kit, using random primers, only transcribed rRNA in enough quantity to be detected by q-PCR.
- Raising the concentration of random primers (10X) was not enough to transcribe mRNA in enough quantity to be detected by q-PCR.
- The cDNA from mRNA was only detected when applying the reverse transcription with target-specific primers (1.67 μ M).
- Modifications of the protocol of q-PCR (more volume of sample and raising the concentration of the primers) did not help to detect the presence of cDNA from mRNA.

5. Results and discussion

This project seeks the optimization of the culture conditions of a strain of *Synechocystis*, isolated from wastewater, in order to increase the production of polyhydroxybutyrate. This strain was previously reported to produce a maximum PHB content of 5 %_{dcw} (Rueda et al., 2020), following the feast-famine strategy: first, a phase in which the microorganisms were provided with all nutrients and then, a phase in which there was deprivation of nitrogen and phosphorus. Finally, bicarbonate was added as a source of inorganic carbon in order to boost PHB content. The results of that study suggested that the final PHB content might be influenced by the amount of dissolved inorganic carbon.

Thus, the first experiment of the present study analyses the influence of inorganic carbon over the production of PHB and glycogen in *Synechocystis* in order to find out if PHB production is raised by supplementing the medium with inorganic carbon. The second experiment analyses if different additions of nitrogen or phosphorus in a medium already lacking nitrogen and phosphorus allow to obtain higher PHB content than the control (nitrogen and phosphorus deprivation), with no additions. Moreover, the additions will analyze whether, once the maximum value has been reached, it can be maintained over time or, on the contrary, as in the case of the control, the PHB content decreases. The results obtained in first experiment could be due to the extra content of carbon or due to the raise in the electrical conductivity of the medium. In order to analyze this hypothesis and clarify this issue, the third experiment study the effect of the salinity over PHB metabolism. The results of all these three experiments are presented and discussed in the following subsections.

5.1 Experiment 1: influence of inorganic carbon availability on PHB production

Figure 13 shows the evolution of biomass concentration, represented as the volatile suspended solids (VSS) during the whole experiment. Biomass grew rapidly during the growth phase (from 0.1 gVSS/L to 0.4 gVSS/L), where there were all nutrients. Then, the maximum of biomass was reached at the start of the accumulation phase and then it decreased as a consequence of the lacking nutrients. The maximum value of biomass reached was 0.9 gVSS/L in PBR4 (2000 mg/L bicarbonate). Then, PBR3 (120-130 mg/L bicarbonate) reached a maximum of biomass of 0.6 gVSS/L. The bioreactors that present a higher concentration of inorganic carbon (IC) show a higher concentration of biomass. Thus, it seems that there is a positive relationship between the IC

content and the biomass content. On the contrary, Kamravamanesh et al. (2017) showed that a high concentration of CO₂ reduced the biomass concentration. Eberly and Ely (2012) indicated that biomass growth was similar under different CO₂ concentrations. This result might indicate that the regulatory mechanisms involved are strain-dependent.

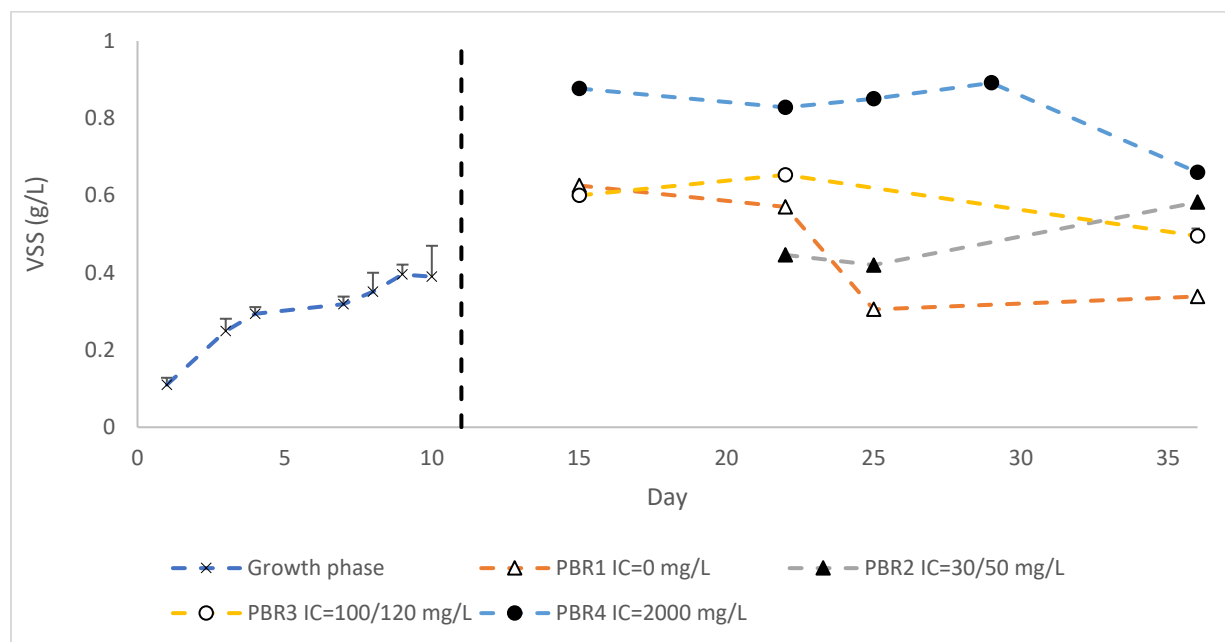


Figure 13. Evolution of volatile suspended solids concentration during experiment 1. The vertical line indicates the start of the accumulation phase (day 11). The growth phase values are calculated as the average of the values of the four PBR replicates and the standard deviation is indicated with error bars.

The microscopic observation of the samples revealed the presence of protozoa in the bioreactors. These microorganisms engulf the *Synechocystis* cells. This is a common contamination, which is difficult to control and there are only a few approaches to kill protozoa that are effective (Ma et al., 2017).

Figure 14 shows the evolution of nitrate and phosphate concentration in the whole experiment. The nitrate content decreased from the start of the experiment to a final value of zero in the accumulation phase, as it was the objective. Although it was expected the same behaviour for the phosphate, the drop is slower and values near zero were reached only at the end of the experiment.

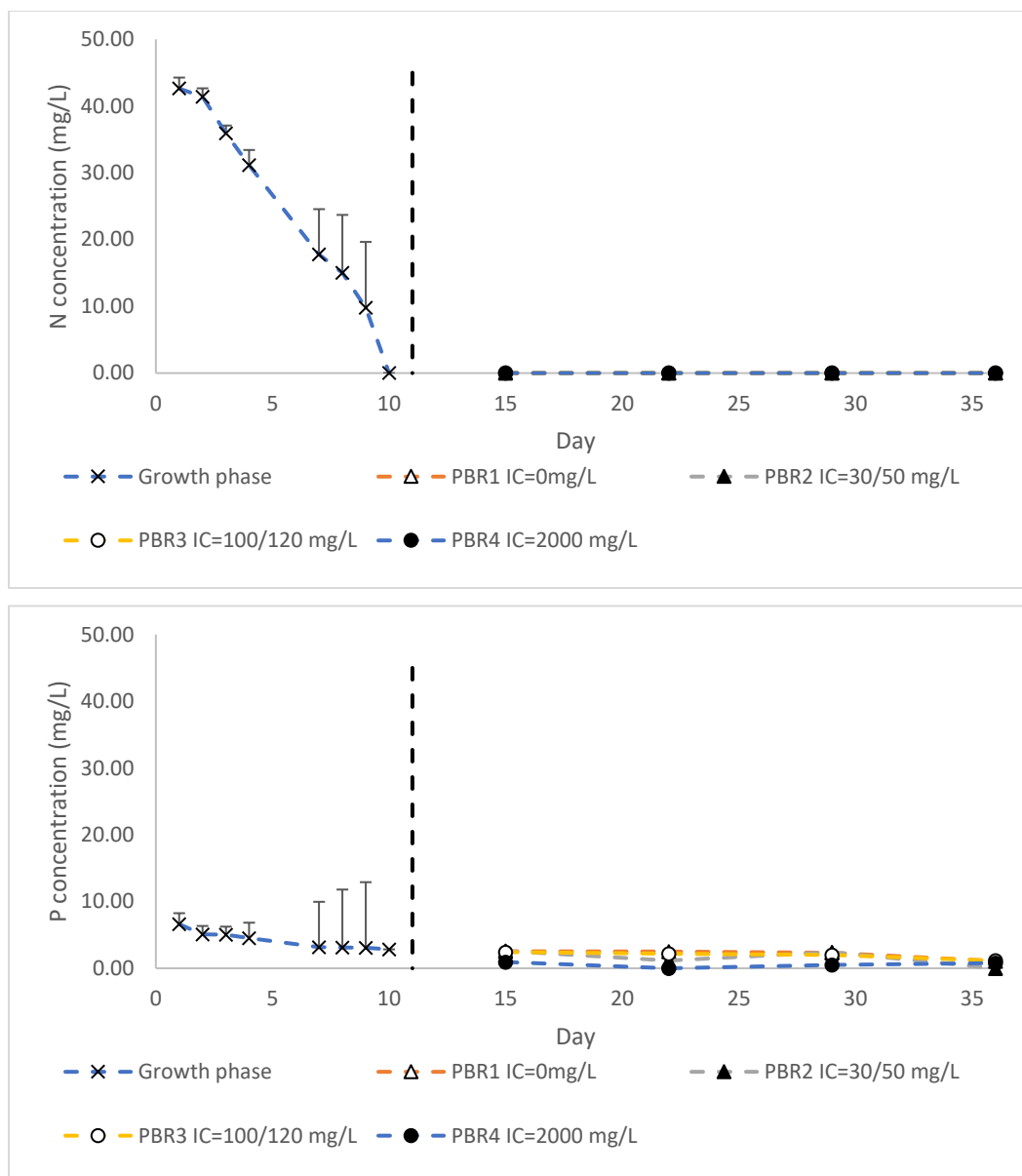


Figure 14. Evolution of nitrogen and phosphorus concentration during experiment 1. The vertical line indicates the start of the accumulation phase (day 11). The growth phase values are calculated as the average of the values of the four PBR replicates and the standard deviation is indicated with error bars.

When nitrogen is the limiting nutrient, the cultures turn the colour; from intense green to light green and even brown/orange. This a process known as chlorosis (Allen and Smith, 1969). Cyanobacteria bleaches as a result of growing in a medium with nitrogen deprivation. This process does not involve the loss of cell viability (Sauer et al., 2001). This effect is shown in Figure 15, where cultures of preliminary experiments had different concentrations of nitrogen (do not misunderstand, these samples do not correspond to PBRs 1 to 4). Cultures 1 and 2 presented a green intense color, indicating that the culture had a high concentration of nitrogen. Culture 3

presented a yellow color, indicating the chlorosis process. Culture 4 was starting to turn the color into yellow.



Figure 15. Chlorosis effect. Picture of cultures with different concentration of nutrients. Cultures 1 and 2 had enough nutrients, so the culture has green intense color. Culture 3 has run out of nitrogen, so the culture has turned the color into green-yellow. Culture 4 was starting the chlorosis process, so the green color is starting to turn into yellow.

Figure 16 shows the evolution of glycogen content. First, it is shown the average content of glycogen in the four photobioreactors. At the start of the experiment, the initial content of glycogen was 11%. It is clear that there was an increase in the glycogen content during the accumulation phase, mostly in PBR4 (up to 82 %). Then, it decreased and had the same behavior as the rest of the conditions, where there are no differences regarding glycogen. So, it seems that a high concentration of inorganic carbon (2000 mg/L) enhances glycogen metabolism in the studied strain of *Synechocystis*. The highest concentration of inorganic carbon produced the highest content of glycogen. This result is consistent with the previous results of Rueda et al. (2020), where it was suggested that glycogen was consumed in first place when there were deficits in carbon source. Therefore, in all other bioreactors in which the carbon concentration in the medium was lower, glycogen was not stored, suggesting that it was consumed in order to provide the precursors for other metabolic reactions.

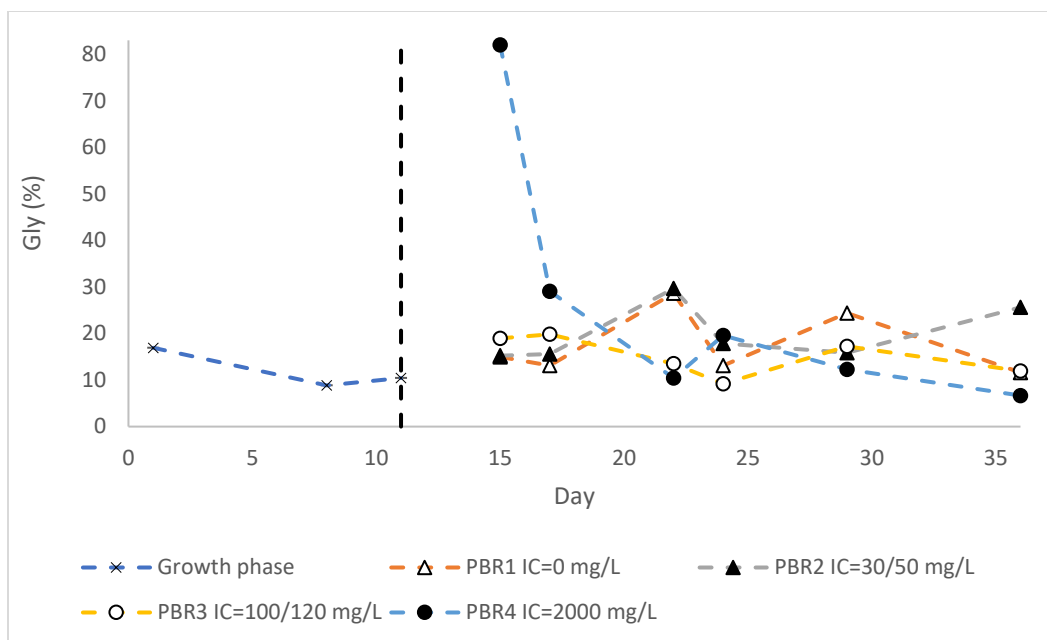


Figure 16. Evolution of glycogen content during experiment 1. The vertical line indicates the start of the accumulation phase. The growth phase values are calculated as the average of the values of the four PBR replicates and the standard deviation is indicated with error bars.

The synthesis of glycogen starts with the formation of ADP-Glucose from glucose-1-phosphate and ATP, catalysed by glucose-1-phosphate adenylyltransferase, AGPase (Gründel et al., 2012). Then, the ADP-Glucose is transferred to the non-reducing end of a linear α -1,4-glucane primer and finally the α -1,6-glycosidic branches are introduced into the polymer (Preiss and Romeo, 1994). The enzyme AGPase is allosterically activated by 3-phosphoglycerate, the product of the CO₂ fixation through Calvin-Benson-Bassham cycle (Gründel et al., 2012). Through this regulation, cyanobacteria is capable of storing polysaccharides by CO₂ fixation (Ball and Morell, 2003). In this sense, the hypothesis previously reported seems more feasible: the more inorganic carbon in the medium, the more 3-phosphoglycerate is produced through rubisco activity, the AGPase is activated and glycogen is produced.

On the contrary, Eberly and Ely (2012) showed that there was no relationship between glycogen synthesis and the concentration of inorganic carbon in the medium. It has to be taken into account that in their study, it was used a thermophilic strain (*Thermosynechococcus elongatus*) which might have a completely different regulatory mechanism. In fact, it is known that the isoenzymes regarding glycogen synthesis vary between cyanobacterial species (Gründel et al., 2012). This could explain why Eberly and Ely (2012) presented contrary results in comparison with the results in this work.

Cyanobacteria synthesize glycogen as the main storage compound. This carbohydrate allows them to grow under different environmental conditions, providing them with the needed energy to perform the metabolic reactions and allows the cells to survive under adverse conditions (Markou et al., 2012). Interestingly, glycogen metabolism could be related to the maintenance of the redox homeostasis and to the response to changes in photosynthetic activity because it could produce all precursor required in other metabolic pathways (Gründel et al., 2012). Mutants defective in glycogen synthesis are not capable of cell division and of the chlorotic response, resulting in the loss of viability whereas mutants defective in PHB synthesis were barely affected in its viability (Taroncher-Oldenburg and Stephanopoulos, 2000). These results were also reported by Velmurugan and Incharoensakdi (2018). Glycogen is therefore reported to play a more decisive role in comparison to PHB.

The above explanation about the role of glycogen could explain the results shown in Figure 13, regarding the evolution of VSS concentration. After the growth phase, the cells are submitted to nitrogen deprivation, which can cause a decrease in cell survival. However, the maximum content of biomass (in terms of VSS) was obtained in PBR 4, which is also the reactor with the maximum content of glycogen. This result was also obtained by Velmurugan and Incharoensakdi (2018). This might indicate a clear relationship between the biomass growth and the glycogen content, which could be helping the cells to cope with the stressful conditions.

Figure 17 shows the evolution of PHB content during the experiment. First, it is represented the growth phase, where all nutrients were available. These values are calculated as the average of the four photobioreactors (PBRs) and it is also represented the standard deviation. In the growth phase, PHB content was very low, with values of 1 %_{dcw}. So, unlike glycogen, PHB is not produced when there is no limitation of nutrients. Then, the accumulation phase started. It is clear that PHB content raises in all conditions, although PBR4 reached the highest content (14.3%_{dcw}). PBR4 started with the highest content of inorganic carbon. It is followed by PBR3, which has a maximum PHB content of 11.3%_{dcw}. The content of IC in PBR3 was higher than PBR2. This result suggests that there is a positive correlation between IC concentration and PHB production.

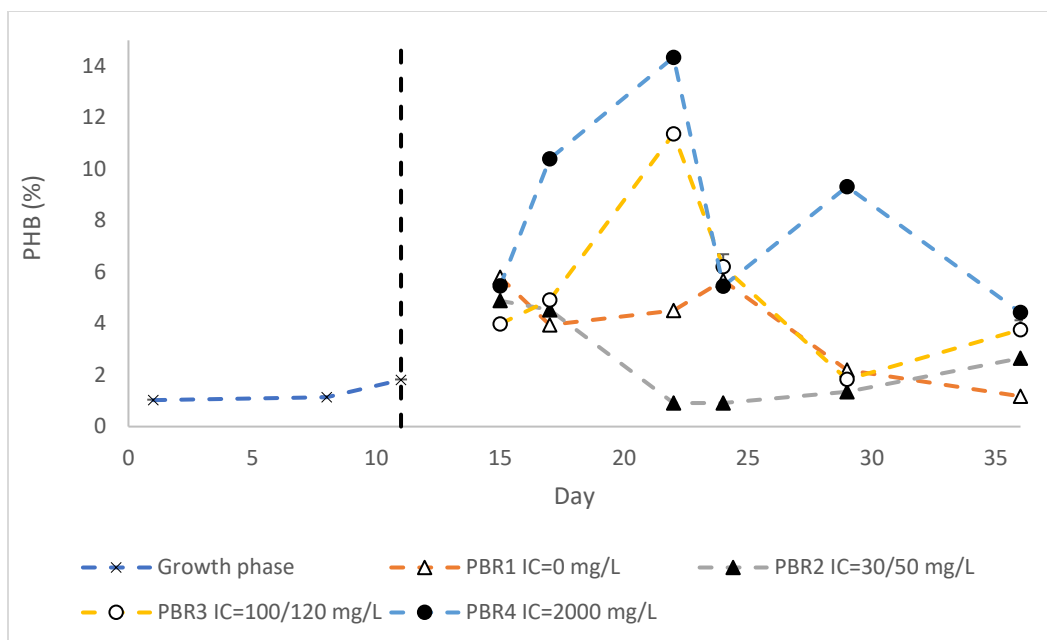


Figure 17. Evolution of PHB content during experiment 1. The vertical line indicates the start of the accumulation phase. The growth phase values are calculated as the average of the values of the four PBR replicates and the standard deviation is indicated with error bars.

The maximum content of PHB was 14 %_{dcw} with a high concentration of inorganic carbon. This value has increased 2.8 times the value of 5.9%_{dcw} obtained in previous studies (Rueda et al., 2020). These results suggest that when there is a high content of inorganic carbon in the medium, glycogen and PHB are produced with higher percentages. Therefore, the best strategy to produce PHB with this strain of *Synechocystis* is to add a high concentration of inorganic carbon (2000 mg/L).

The author Troschl et al. (2018) studied the production of PHB with *Synechocystis* sp. CCALA192, with BG-11 medium, supplemented with 129 mg/L of IC and in nitrogen deprivation conditions. The results showed a maximum of 12.5 %_{dcw}. This result is in accordance with the results obtained in this study, PBR 3, in which the maximum PHB content was 11.4 %_{dcw} and the concentration of IC was between 120-130 mg/L (shown in Figure 17). However, the maximum percentage of PHB obtained in this work was lower than percentages of other authors. For example, Kamravamanesh et al. (2019) obtained 20.4 %_{dcw} employing wild-type strain *Synechocystis* sp. PCC 6714 in BG-11 medium. So, new strategies need to be studied in order to raise PHB productivity.

On the other hand, there are strains of *Synechocystis* (sp. PCC 6714) that reduces the synthesis of PHB when there are high concentrations of CO₂ in the medium (Kamravamanesh et al., 2017).

Moreover, the work of Eberly and Ely (2012) showed a clear reduction of PHB content when the CO₂ concentration was raised from the atmospheric to 20% (in the conditions of the experiment it was calculated that at 20% CO₂, the effective bicarbonate concentration was 120 mM). In this case, the amount of PHB was 2%, certainly quite lower than the amount obtained in this work (Figure 17).

Nitrogen is an essential nutrient needed for the synthesis of important molecules, such as DNA or proteins. Therefore, proteins and aminoacids cannot be synthetized when there is nitrogen limitation. Chlorosis is a clear effect of this, as chlorophyll cannot be longer produced (Markou et al., 2012). The carbon that is fixed trough the photosynthetic Calvin Cycle is then used in the synthesis of lipids or carbohydrates instead of proteins, increasing the NADH pool (Hu, 2013). The accumulation of lipids or carbohydrates seems to be a strain-dependent process (Markou et al., 2012). However, the process is more complex, as it depends on other factors, not only the presence of nitrogen.

Phosphorus is another essential nutrient needed basically for the synthesis of ATP (Adenosin triphosphate). Cells acquire phosphorus and storage it in the form of polyphosphates, that regulate the concentration of the intracellular organophosphate. Phosphorus limitation affects both, carbohydrates and lipids metabolisms (Markou et al., 2012). However, in cyanobacteria the accumulation of carbohydrates under phosphorus limitation conditions seems to be more notable (Lynn et al., 2000). The enzyme ADP-glucose pyrophosphorylase, which controls the carbohydrates metabolism, is inhibited by inorganic phosphorus (Gómez-Casati et al., 2003). All in all, under nitrogen and phosphorus limitation conditions, it is formed an imbalance in the NADH/ATP ratio, which has a direct relation to PHB metabolism (Kamravamanesh et al., 2019; Rueda et al., 2020; Singh et al., 2017).

Cyanobacteria present bicarbonate transporters in the plasma membrane with different affinities for the inorganic carbon, depending on the carbon availability. Once the bicarbonate is accumulated inside the cell, it is used as substrate by an enzyme named carbonic anhydrase (CA), that transforms it into CO₂ (Price et al., 1998). This enzyme is located in the carboxysome, a protein micro-compartment that also contains the enzyme Rubisco. This enzyme is responsible for fixing the CO₂ into an organic compound, which is then used for the Calvin Cycle. These two

enzymes are the components of a mechanism, named photosynthetic CO₂ concentrating mechanism (CCM), that improve the carboxylation in cyanobacteria (Badger and Price, 2003).

What is more, if comparing the content of glycogen and PHB in PBR4 (shown in Figure 16 and Figure 17, respectively), it is shown that the highest content of PHB was acquired when there is the minimum content of glycogen. This result might suggest that there is an interconversion of glycogen to PHB. This is another result that has been previously reported (Rueda et al., 2020). For instance, the author Kamravamanesh et al. (2019) defined the production of PHB in three steps. First, a phase which consists of biomass growth with all nutrients. Then, the glycogen production step, that happens when nitrogen and phosphorus are at very low concentrations and glycogen is produced as storage compound. In this phase, PHB is produced from CO₂. Finally, there is the last step which involves the degradation of glycogen and partially converted into PHB. This is the interconversion phase.

The interconversion of glycogen to PHB studied by Kamravamanesh et al. (2019) showed that when glycogen synthesis is stopped, the cells continued producing PHB under nitrogen and phosphorus deprivation. It was suggested that for the synthesis of glycogen it is necessary to have phosphorus in the medium. So, under the conditions of nitrogen and phosphorus limitation, the cells use intracellular poly-phosphate as energy source to produce acetyl-CoA, which will be used in the glycogen and PHB production. When poly-phosphate is over, glycogen is degraded so as to obtain energy and PHB can be still produced. This energy is delivered in the form of NADPH (Reis et al., 2003).

In previous studies, (Dutt and Srivastava, 2018) revealed that only about 26% of the PHB synthesized is from the carbon fixed, whereas the rest come from recycled carbon. Part of this comes from glycogen, but it is not the main source of carbon. It is suggested that the rest of the carbon comes from the degradation of lipopolysaccharides and non-essential proteins.

On the other hand, glycogen content started to raise during the first days of the accumulation phase whereas PHB started to be accumulated during the last days. This result suggests that cyanobacteria accumulate, in the first place, glycogen as the main carbon reserve when there are stressful conditions. This result was also obtained by Kamravamanesh et al. (2019): glycogen is produced in a greater rate than PHB when nitrogen is limited and if the limitation is persisting, glycogen synthesis is stopped and PHB synthesis begins.

It has been shown that, mutants incapable of synthesising PHB, increased their content of glycogen (Velmurugan and Incharoensakdi, 2018). Moreover, mutants incapable of degrading glycogen did not produce PHB (Koch et al., 2019). On the contrary, the same author showed that mutants incapable of synthesising glycogen, did produce PHB, suggesting that PHB synthesis could bypass the glycogen pool. In this case, the carbon needed for the formation of PHB molecules is derived from CO₂ fixation and the degradation of other metabolites. These results might reinforce the previous hypothesis: glycogen and PHB metabolisms are clearly related to each other.

Nevertheless, Velmurugan and Incharoensakdi (2018) observed that mutants over-producing glycogen did not produce more PHB than the control. Therefore, the authors concluded that glycogen synthesis is not related to PHB synthesis. However, as it has been already explained, it seems clear that both metabolisms are related. It could be thought another explanation to those results: the reactions needed for the synthesis of PHB from the degradation of glycogen can be saturated so, although the strain produces higher content of glycogen, the content of PHB will not be raised. Further studies would be really interesting to confirm this hypothesis because it could reject the idea of raising PHB production by enhancing glycogen synthesis. Finally, this could lead to open new research lines to investigate which substrates, apart from glycogen, are related to PHB metabolism.

5.2 Experiment 2: effect of intermittent additions of N and P on PHB production

Figure 18 shows the evolution of biomass, represented as the volatile suspended solids (VSS) during the whole experiment. Biomass grew during the growth phase (from 0.1 gVSS/L to 0.7 gVSS/L), where there were no nutrients limitation. Then, the maximum of biomass was reached at the start of the accumulation phase and then it decreased as a consequence of the lacking nutrients. The maximum value of biomass reached was 1.6 gVSS/L in PBR3 (high frequency additions of N). Then, PBR4 (low frequency additions) reached a maximum of biomass of 1.5 gVSS/L. PBR1 presented the lowest concentration of biomass, slightly higher than 1 gVSS/L. This suggests that the addition of nutrients enhances the biomass growth, but with a limited extent, since no strong differences were observed.

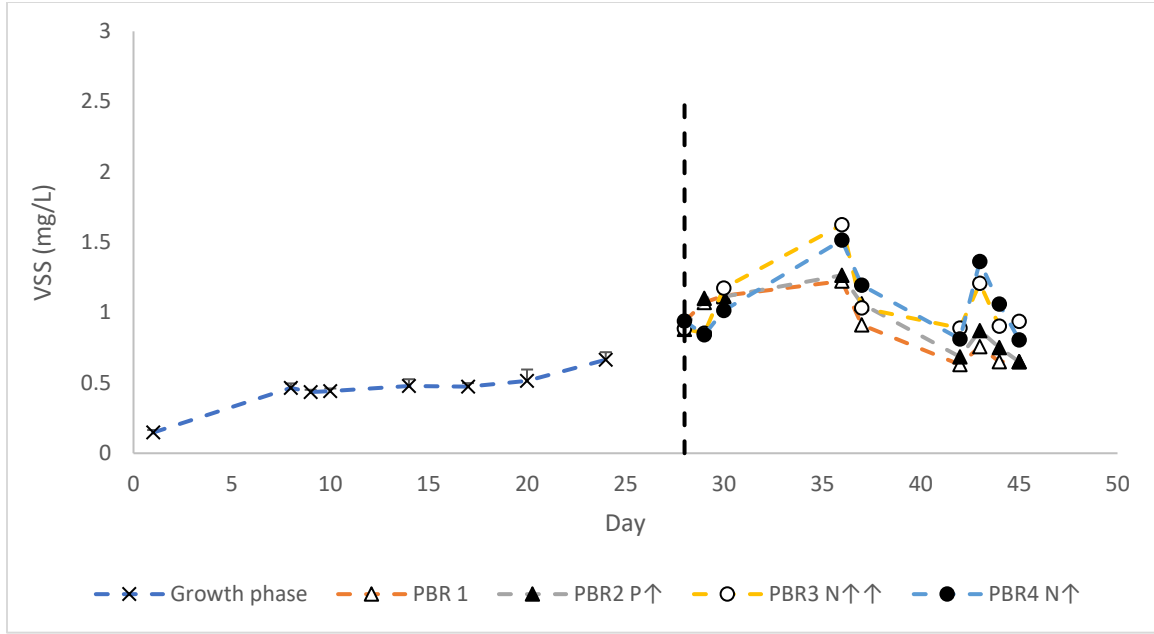


Figure 18. Evolution of volatile suspended solids concentration in experiment 2. The vertical line indicates the start of the accumulation phase (day 28). The growth phase values are calculated as the average of the values of the four PBR replicates and the standard deviation is indicated with error bars. ↑ indicates the different additions: P↑ (additions of phosphorus), N↑↑ (high frequency additions of nitrogen), N↑ (low frequency additions of nitrogen).

Figure 19 shows the evolution of nitrate and phosphate in the whole experiment. The nitrate concentration decreased from the start of the experiment to a final value of zero by day 10, guaranteeing nitrate deprivation in the subsequent accumulation phase, as it was the objective. In PBR3 the concentration of nitrates increased during the accumulation phase as a result of the additions of NaNO_3 . Regarding phosphate concentration, it decreased during the growth phase, as expected, to a final value of zero just before starting the accumulation phase. Then, the concentration of phosphate increased in PBR2 during the accumulation phase as a result of the additions of K_2HPO_4 .

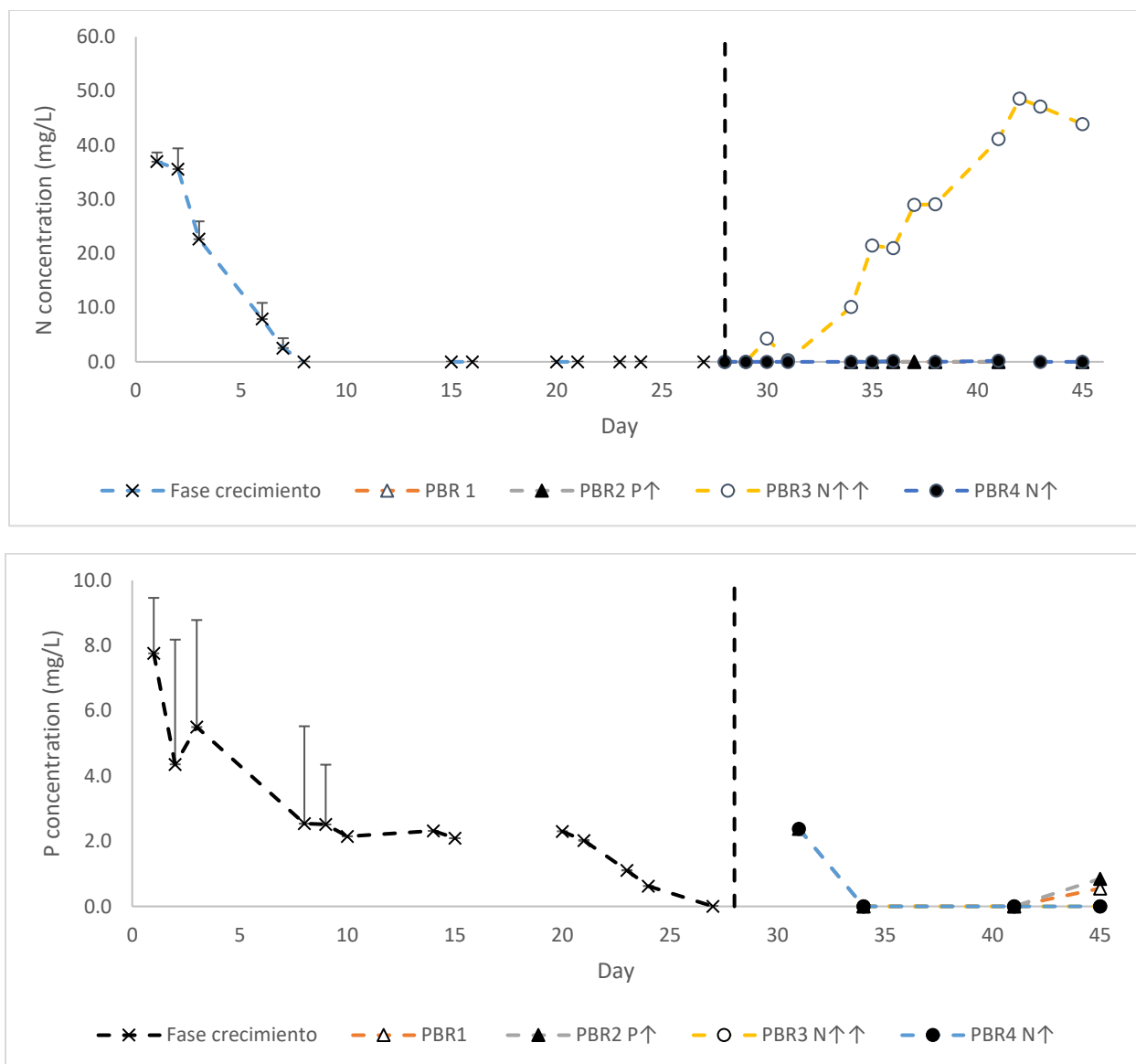


Figure 19. Evolution of nitrogen and phosphorus concentration during experiment 2. The vertical line indicates the start of the accumulation phase (day 28). The growth phase values are calculated as the average of the values of the four PBR replicates and the standard deviation is indicated with error bars. ↑ indicates the different additions: P↑ (additions of phosphorus), N↑↑ (high frequency additions of nitrogen), N↑ (low frequency additions of nitrogen).

Figure 20 shows the evolution of glycogen. First, it is shown the average content of glycogen in the four PBRs. It is clear that there was an increase in the glycogen content during the accumulation phase, mostly in PBR2 (71.0 %). This maximum value was reached in day 29, when there were no concentration of nitrates nor phosphates in the culture. Then, it decreased and increased again until it reached a value of 53.5 % in day 34 and 49.4 % in day 37. PBR4 also presented high values of glycogen, with a maximum value of 49.1 % in day 34 and 38.9 % in day 38. On the other hand,

PBR3 shows low content of glycogen, with a minimum of 12.6 % in day 34. The nitrogen content starts to raise in PBR3 from day 30.

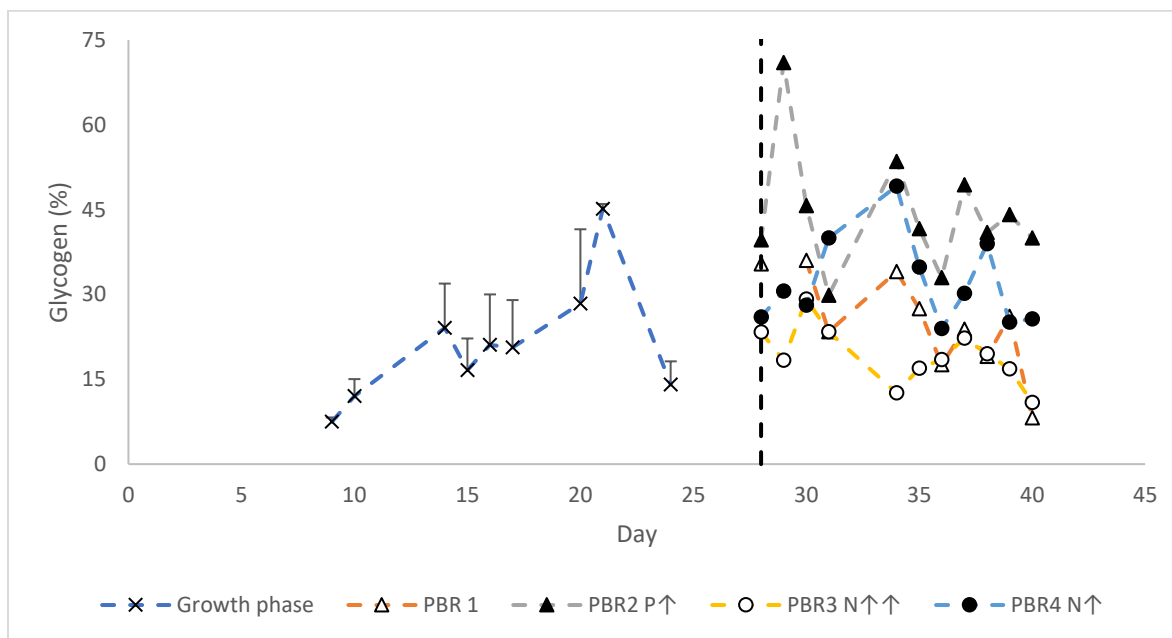


Figure 20. Evolution of glycogen content during experiment 2. The vertical line indicates the start of the accumulation phase. The growth phase values are calculated as the average of the values of the four PBR replicates and the standard deviation is indicated with error bars. ↑ indicates the different additions: P↑ (additions of phosphorus), N↑↑ (high frequency additions of nitrogen), N↑ (low frequency additions of nitrogen).

These results indicate that the studied strain of cyanobacteria does not accumulate glycogen when there is nitrogen in the medium. This result agrees with the fact that carbohydrates, like glycogen, accumulate when there is nitrogen limitation (Markou et al., 2012).

Figure 21 represents the evolution of PHB (%_{dcw}) in the four different conditions. Until day 27, it depicts the growth phase and these values are calculated as the average of the four PBR and they are represented with the standard deviation. The results indicate that the highest content of PHB (14%_{dcw}) was acquired in PBR1, which was the control (no additions of nitrogen or phosphorus). PBR2 presents a maximum value of PHB of 4.3 %_{dcw} after phosphate addition. Finally, PBR4 (with two additions of nitrogen) and PBR3 (with a high concentration of nitrogen) present a very low PHB content. This might indicate that the deprivation of nitrogen is decisive for PHB biosynthesis. In conclusion, nitrogen and phosphorus deprivation, with no addition of nutrients, seems the best approach to enhance the content of PHB.

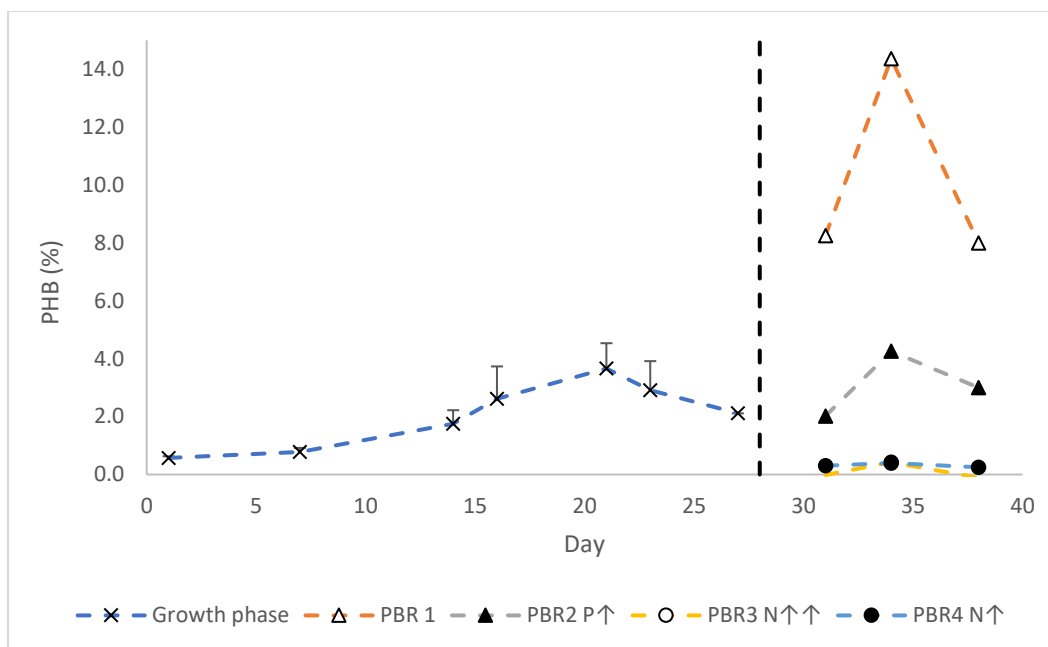


Figure 21. Evolution of PHB content during experiment 2. The vertical line indicates the start of the accumulation phase. The growth phase values are calculated as the average of the values of the four PBR replicates and the standard deviation is indicated with error bars. ↑ indicates the different additions: P↑ (additions of phosphorus), N↑↑ (high frequency additions of nitrogen), N↑ (low frequency additions of nitrogen).

It is worth mentioning that the percentage of PHB obtained in PBR1 is the same (14%_{dcw}) as in the experiment 1 with the same conditions. This result confirms that when growing this strain of *Synechocystis* in BG-11 medium (supplemented with 2000 mg/L bicarbonate), following the approach of nitrogen and phosphorus deprivation, it can be obtained a maximum content of PHB of 14%_{dcw}. As in the previous experiment, glycogen was accumulated during the first days of the accumulation phase, whereas PHB was accumulated later on. However, in this case, the interconversion process is not that obvious.

On the other hand, it is remarkable the fact that in this experiment, 2 g/L bicarbonate were added at the beginning of the accumulation phase, whereas in the first experiment, 2 g/L bicarbonate were added at the beginning of the growth phase. So, adding bicarbonate in the growth phase or in the accumulation phase had no effect over PHB synthesis.

Phosphate is known to alter gene expression and plays an unknown role over bacterial metabolism (Westermarck and Steuer, 2016). Kamravamanesh et al. (2019) revealed that the biomass growth and the PHB content could be raised in the strain PCC 6714 when following a three-step cultivation with high concentrations of phosphorus in the initial phase. Thus, the availability of phosphorus could be related not only with the biomass growth, but also with glycogen and PHB metabolism.

The same author, Kamravamanesh et al. (2019), studied the influence of phosphate pulses during the accumulation phase (deprivation of nitrogen and phosphorus) over the biomass growth, glycogen and PHB content in *Synechocystis* sp. PCC 6714. The results revealed that the pulses only have a positive impact over glycogen production, raising its content. They have no impact over biomass growth. On the contrary, the maximum value of PHB content was lower than the expected value.

The obtained results are therefore in accordance with the previous results of (Kamravamanesh et al., 2019). Figure 18 shows that the volatile suspended solids had a similar behaviour, in both control and phosphorus additions reactor, indicating that the phosphorus addition had no impact over biomass growth. Figure 21 shows that phosphorus pulse reduced the maximum value of PHB in comparison to the control. Nevertheless, Figure 20 does not reveal a clear relationship between the raise in glycogen content and phosphorus pulse.

On the other hand, Wang et al. (2013) revealed that when cyanobacteria consume phosphorus, the intracellular acetyl-CoA pool is raised. The acetyl-CoA produced is then used for PHB and glycogen synthesis under nitrogen and phosphorus limitation. However, Kamravamanesh et al. (2019) hypothesized that, when there are phosphorus additions, cyanobacteria metabolism mainly focus on glycogen production and therefore the maximum value of PHB is lower than the expected value.

5.3 Experiment 3: influence of salinity in the culture media on PHB production

The first experiment showed that, under a high concentration of inorganic carbon (2 g/L), this strain of cyanobacteria, stimulates the production of PHB, reaching the highest value (14 %_{dcw}). However, this change in the metabolism could be due to the extra content of carbon or due to the raise in the electrical conductivity of the medium. In order to analyze this hypothesis and clarify this issue, the third experiment study the effect of the salinity over PHB metabolism.

¡Error! No se encuentra el origen de la referencia. shows the evolution of biomass, represented as the volatile suspended solids (VSS) concentration during the whole experiment. Biomass grew during the growth phase (from 0.1 gVSS/L to 1.0 gVSS/L), where there were all nutrients. Biomass decreased during the first days of the accumulation phase and then, the value increased again. In PBR4, the maximum value of biomass was 1.4 gVSS/L. In PBR3, the maximum value of biomass was 1.3 gVSS/L at day 21. PBR 1 and PBR2 reached the maximum of 1.2 gVSS/L at day 24.

First, **¡Error! No se encuentra el origen de la referencia.** indicates that strain of *Synechocystis* used in this study can tolerate high concentrations of salt, in spite of being a freshwater microorganism. Second, the inorganic carbon might have a positive effect over biomass. This result has already been showed in experiment 1. Third, the behaviour described in **¡Error! No se encuentra el origen de la referencia.** might indicate that the cells could have a period of acclimatation to high salinity. When microorganisms are cultivated in high salinity conditions, it is observed a lag phase in which they perform the corresponding metabolic reactions to cope with that stress (Salgaonkar et al., 2013). The adverse conditions, high salt concentration in this case, make physiologic changes that provoke a longer lag phase (Rodríguez-Contreras et al., 2016).

These results about the salinity effect over biomass growth are in accordance with previous ones (Jantaro et al., 2003), in which the growth rate of *Synechocystis* was not affected by a high concentration of NaCl (29.2 g/L). Miao et al. (2003) reported that *Synechocystis* is a moderately halotolerant cyanobacterium.

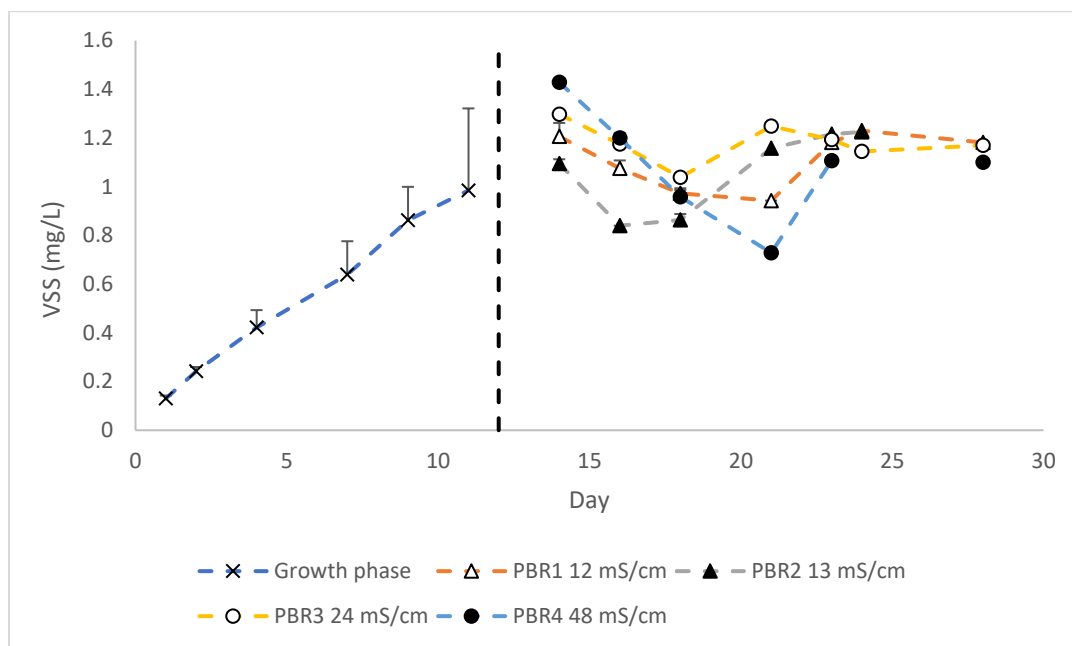


Figure 22. Evolution of volatile suspended solids concentration in experiment 3. The vertical line indicates the start of the accumulation phase (day 12). The growth phase values are calculated as the average of the values of the four PBR replicates and the standard deviation is indicated with error bars.

Halophilic microorganisms (“salt-loving”) can be defined as those that need a certain amount of salt in the medium to survey, including concentrations as sweater (35 g/L of salt) (Oren, 2008). The scientist Donn Kushner made the following classification (

Table 18):

Table 18. Classification of microorganisms according to their relationship to salt.

	NaCl (M)	NaCl (g/L)
Extreme halophiles	2.5 – 5.2	146.1 – 303.89
Borderline extreme halophiles	1.5 – 4.0	87.66 – 233.76
Moderate halophiles	0.5 – 2.5	29.22 – 146.1
Halotolerant	0 – 2.5	0 – 146.1

Halophilic microorganisms are quite common in bacterial kingdom, including the phyla Cyanobacteria (Oren, 2008). These microorganisms can follow two approaches to survive under the osmotic pressure of the environment. First, *high-salt-in strategy* involves the accumulation of molar concentrations of potassium and chloride (Oren, 2008). For this, the microorganisms have adapted their proteins, in order to maintain their structure under conditions of very high concentrations of salt (Lanyi, 1974). As a consequence, these proteins present acidic aminoacids and denature when they grow under low salt conditions (Oren, 2008). Second, *low-salt-in strategy* or haloadaptation involves the biosynthesis and accumulation of organic osmotic solutes, excluding salt from their cytoplasm as much as possible (Oren, 2008). This strategy allows the microorganisms to survive to a wide range of salt concentrations (Ventosa et al., 1998), due to the regulation of the production of this organic osmotic solutes, according to the salt concentration of the environment (Galinski, 1995).

Low-salt-in strategy or haloadaptation is more widespread in halophilic microorganisms than high-salt-in, in spite of the fact that this second strategy demands more expenditure of energy than the first one (Oren, 1999). It is hypothesized that the maximum concentration of salt that microorganisms can tolerate will depend on the balance between the maximum energy they can produce and the energy cost of producing osmotic compounds (Oren, 2008).

Figure 23 shows the evolution of nitrate and phosphate in the whole experiment. Both nutrients, nitrate and phosphate, decreased since the start of the experiment until they reached the final value of 0 mg/L that indicates the start of the accumulation phase. It can be seen that, in this case, phosphorus was consumed faster than nitrogen.

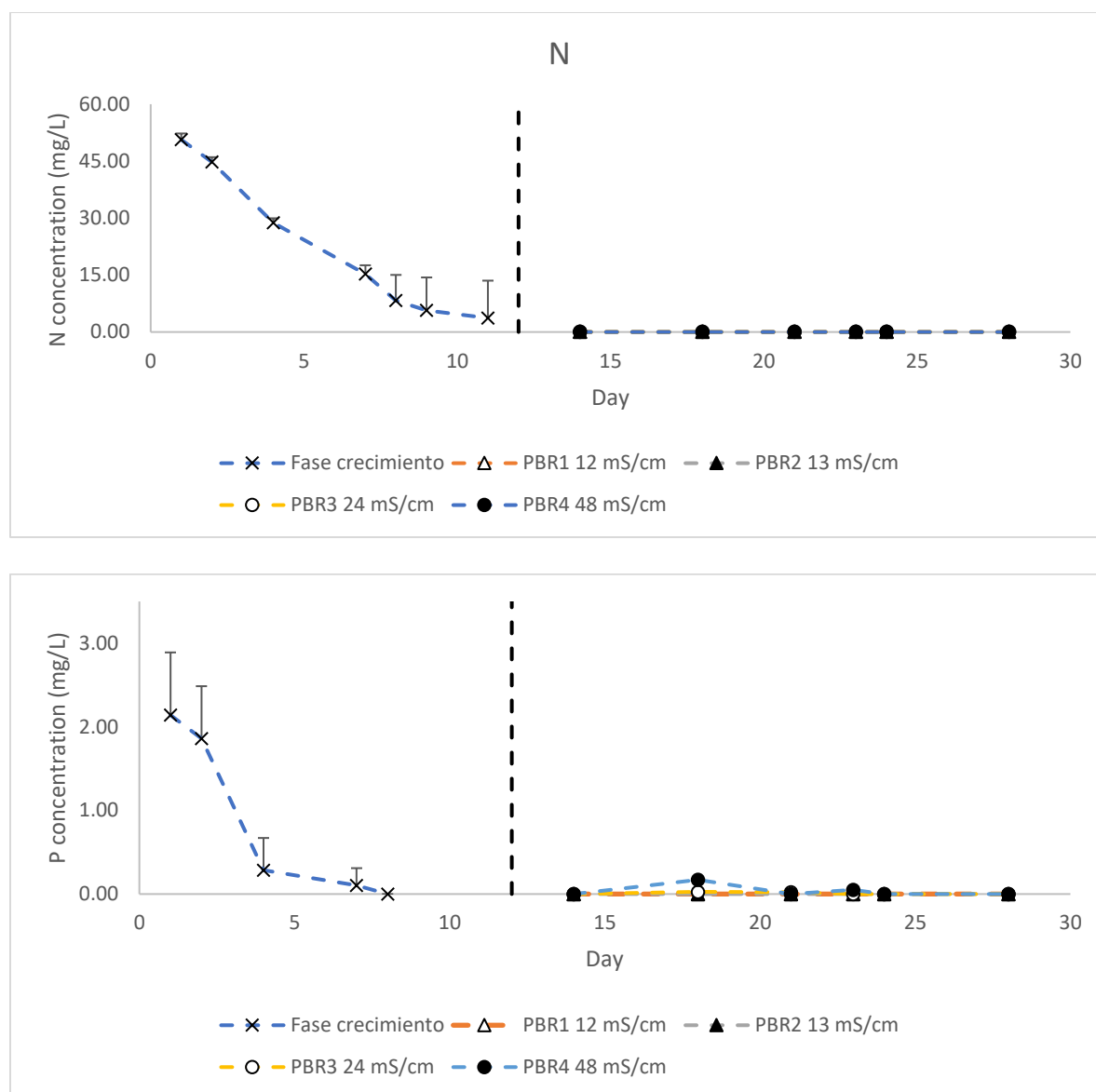


Figure 23. Evolution of nitrogen and phosphorus concentration during experiment 3. The vertical line indicates the start of the accumulation phase (day 12). The growth phase values are calculated as the average of the values of the four PBR replicates and the standard deviation is indicated with error bars.

Figure 24 shows the evolution of glycogen. In this case, glycogen was not measured during the growth phase. The maximum value of glycogen was reached in PBR2 (13 mS/cm), with 48.8 % at day 21. Then, PBR 3 (24 mS/cm) reached a maximum of 36.6 % at day 16. The control, PBR1 (12 mS/cm), reached a maximum value of 32.7 % at day 18.

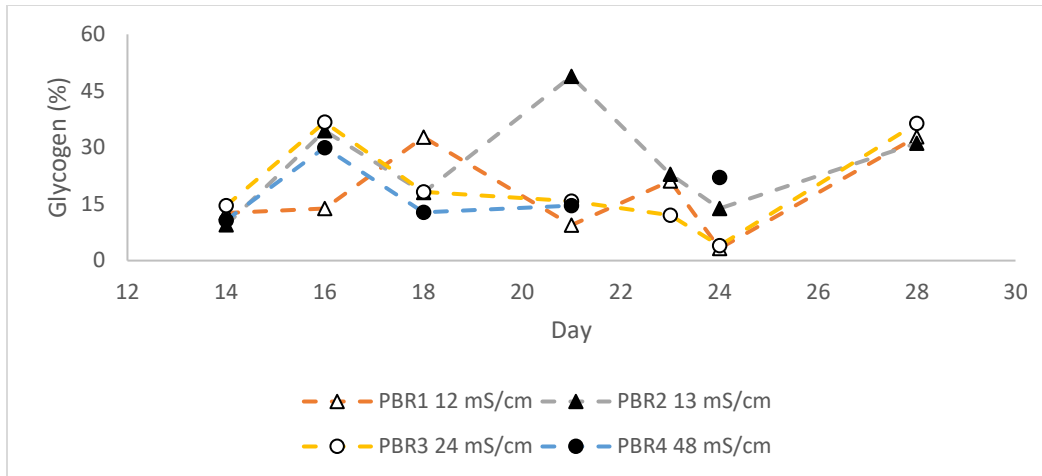


Figure 24. Evolution of glycogen content during experiment 3. The vertical line indicates the start of the accumulation phase. In this case, glycogen was not measured during the growth phase.

Page-Sharp et al. (1998) observed an accumulation of glycogen when the concentration of NaCl was raised in cyanobacterium species. However, Figure 24 indicates that glycogen is accumulated when there is an electrical conductivity around 13 mS/cm, but it decreases when the conductivity is raised. This result will be discussed together with PHB results.

Figure 25 represents the evolution of PHB (%_{dcw}) in the four different conditions. Until day 12, it involves the growth phase and these values are calculated as the average of the four PBR and they are represented with the standard deviation. During the growth phase, PHB was barely produced, with a value of 0.9%_{dcw} at day 10. The maximum content of PHB was 6.2%_{dcw} at day 28 in PBR2 (conductivity of 13 mS/cm). Then, the control PBR1 (conductivity of 12 mS/cm), produced a maximum value of 3.7%_{dcw} at day 24. PBR3 (conductivity of 24 mS/cm) and PBR4 (conductivity of 48 mS/cm) had maximum values of 2.9%_{dcw} and 1.4 %_{dcw}, respectively. This might indicate that high conductivities reduce the PHB content.

Therefore, in the studied conditions, the maximum PHB content is obtained with 5.8 g/L NaCl and 100 mg/L bicarbonate. The results of Shrivastav et al. (2010) showed that the strain of cyanobacteria, *Spirulina subsalsa*, raises its PHB content when it was grew in a medium with high concentration of NaCl.

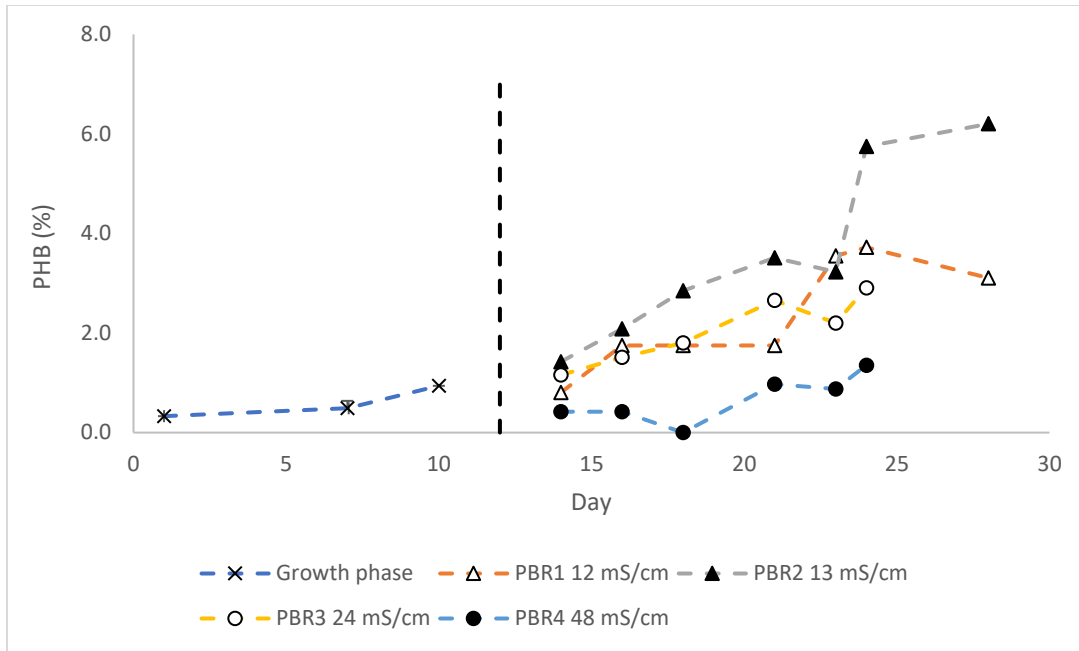


Figure 25. Evolution of PHB content during experiment 3. The vertical line indicates the start of the accumulation phase. The growth phase values are calculated as the average of the values of the four PBR replicates and the standard deviation is indicated with error bars.

In this case, the control (PBR1) did not reach the maximum value of 14%_{dcw} as in the previous experiments. This unexpected result could be due to the fact that the initial concentration of phosphorus was not the same as in the other cases. In this experiment, experiment 3, the initial concentration of phosphate was 2.1 g/L whereas in experiment 1 was 6.61 g/L. This might indicate that the concentration of phosphorus in the growth phase can have a huge impact over PHB synthesis during the accumulation phase. This hypothesis is reinforced by the results of (Kamravamanesh et al., 2019): it was showed that the final PHB content is affected by the concentration of phosphorus in the first step, following a three-step cultivation. The results in Figure 25 would indicate that, if an initial phosphorus concentration of 6 g/L is added, then 5.8 g/L NaCl and 100 mg/L bicarbonate conditions, PHB content higher than 14%_{dcw} is expected. So the raise in PHB content might be related to conductivity instead of to the inorganic carbon content, as it was hypothesized in first experiment.

PBR2 had the conditions that allow the highest content of glycogen and PHB. In this sense, Figure 24 and Figure 25 show the interconversion process of glycogen to PHB, previously observed in experiment 1. In PBR2, glycogen reached the maximum value at day 21 and then, it decreased, reaching a minimum value at day 24. On the contrary, PHB reached the maximum value at day

24. The same behaviour was observed in PBR1. This interconversion process has already been explained by Kamravamanesh et al. (2019).

On the other hand, it is also observed that glycogen was accumulated during the first days of the accumulation phase, whereas PHB accumulated during the last days. This result was previously observed in the others experiment and also by Kamravamanesh et al. (2019), indicating that glycogen is the main carbon reserve when there are stressful conditions due to high salt concentration in cyanobacteria cultivation.

The microorganisms might produce and accumulate PHB as a result of the osmotic stress to balance the osmotic pressure of the environment (Arora et al., 2006). It has been shown that imbalanced conditions, like high concentration of NaCl, present a direct effect over the citrate synthase in the TCA cycle. As a consequence, there is an increase in the Acetyl-CoA pool, which is then used to raise PHB content (Shrivastav et al., 2010). Moreover, as a consequence of this, there is a decrease of the free coenzyme A, which is an inhibitor of PhaA, the enzyme that catalyses the acetoacetyl-CoA formation during PHB synthesis (Ansari and Fatma, 2016). These results might indicate that NaCl could have an effect on the direction of carbon flux (Shrivastav et al., 2010), enhancing the production of PHB under conductivities of 13 mS/cm.

NaCl not only might provoke changes in PHB metabolism, but also in carotenoids production. Salt stress, results in an overproduction of Reactive Oxygen Species (ROS), which can cause oxidative damage to the cells (Wang et al., 2003). As a mechanism of protection, microorganisms as *Chlorella*, raises the content of carotenoids (Li et al., 2009).

In other ways, environmental conditions with high conductivities (higher than 13 mS/cm, due to the presence of both, bicarbonate and sodium chloride) reduce PHB synthesis (Figure 25). This might indicate that the cells inhibit the biosynthetic pathway of polyhydroxybutyrate and activate other metabolic routes to counter the osmotic stress (Rodríguez-Contreras et al., 2016). In this sense, *Synechocystis* has been reported to produce glucosylglycerol, which plays an osmoprotective role under high salt concentrations (Kirsch et al., 2019). Glucosylglycerol is produced in two enzymatic steps: GgpS is a glucosyltransferase that catalyses the synthesis of glucosylglycerol-3-phosphate from ADP-glucose and glycerol-3-phosphate and GgpP catalyses the dephosphorilation of this intermediate into glucosylglycerol (Kirsch et al., 2019). Glucose-1-phosphate is obtained from the phosphorylation of ADP-glucose, catalysed by ADP-glucose

pyrophosphorylase, enzyme which is also involved in the glycogen synthesis (Miao et al., 2003). Glucose-1-phosphate is also an intermediate in the metabolic pathway of polyhydroxybutyrate (Mills et al., 2020). Therefore, it is hypothesized that, under high salt concentrations, carbon flux (a fraction derived from *de novo* CO₂ fixation through the Calvin-Benson cycle) is redirected to glucosylglycerol biosynthesis instead of glycogen or polyhydroxybutyrate synthesis pathways (Figure 26). This can explain why there is no production of PHB when there is a high concentration of NaCl in the medium. Regarding Figure 24, glycogen levels are very low in those PBR with high conductivities (higher than 13 mS/cm). It could be thought the same explanation as for PHB biosynthesis: the carbon flow could be redirected to other metabolites, instead of glycogen (Figure 26).

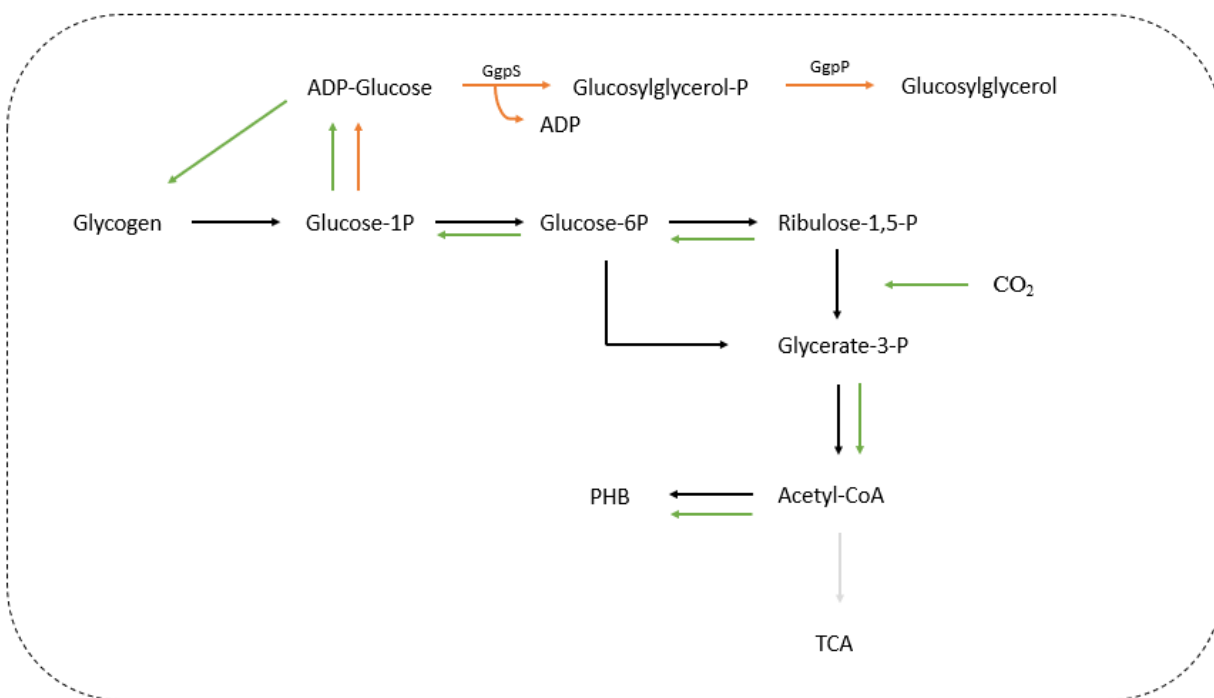


Figure 26. Highly simplified biosynthetic pathways for glycogen conversion to polyhydroxybutyrate (PHB) in cyanobacteria, including the biosynthetic pathway of glucosylglycerol.

All in all, the strain of *Synechocystis* used in this study can recognize the salt stress imposed by the environment and, in consequence, there is a change in their metabolism, probably due to variations in the expression of diverse family of genes, which was also observed by (Kanesaki et al., 2002; Miao et al., 2003). It seems that the regulation that follows as a mechanism of salt acclimation is quite complex. Further studies are needed to understand the implications that might have over PHB synthesis.

6. Conclusion

Polyhydroxybutyrate (PHB) is a type of bioplastic which can be produced by a range of microorganisms, like *Synechocystis* which belongs to cyanobacteria. However, the main withdraw of this process is the low PHB productivity, so studies about the optimization of the process are essential to make the process economically feasible. In this study, different environmental factors have been analyzed in order to increase the PHB content and production in *Synechocystis* cultures. Moreover, different protocols have been designed and implemented as molecular tool (by employing RT-q-PCR technology) to study gene expression related to PHB metabolism.

First, it is known that *Synechocystis* produces PHB when there is a deprivation of nitrogen and phosphorus in the culture. Therefore, the experiments were carried out in two different phases: the growth phase, in which the microorganisms grow in the presence of all nutrients and then, the accumulation phase, that starts when nitrogen and phosphorus are depleted. It is in this last phase when PHB is produced. A high concentration of inorganic carbon in the culture media (2000 mg/L bicarbonate) provided the highest content of biomass (0.89 gVSS/L), of glycogen (82%) and of PHB (14.3 %_{dcw}). The PHB value is 2.8 times higher than the one obtained in previous works with the same strain of *Synechocystis*. This amount of PHB was obtained either when adding the inorganic carbon in the growth phase and in the accumulation phase. Moreover, the final content of PHB might be related to the initial concentration of nitrogen and phosphorus. On the other hand, intermittent additions of nitrogen and phosphorus during the accumulation phase provided higher biomass production, but the amount of glycogen and PHB were significantly decreased.

Second, an electrical conductivity of 13 mS/cm (based on 5.80 g/L NaCl and 100 mg/L bicarbonate) provided a higher PHB value than the control (with 2000 mg/L bicarbonate), suggesting that the increase of PHB content might be related to salinity and not to inorganic carbon. Finally, higher conductivities than 13 mS/cm decreased both PHB and glycogen content.

The results obtained in this work allow to better understand the behavior of *Synechocystis* in relation to the production of PHB. Gaining further insights will allow to know and understand the regulatory mechanisms that determines the production of PHB and, therefore, can be used for industrial scaling.

7. Future perspectives

This section aims to propose and describe ideas for continuing this line of investigation. It is not clear how the environmental conditions affect the metabolism of cyanobacteria, in particular this strain of *Synechocystis*. Therefore, further experiments are needed to clarify this biological process. It could help to understand a little better how *Synechocystis* produces this compound and lastly to determine which are the conditions that make this microorganism produces the highest content of bioplastic.

This work shows the capacity of a strain of *Synechocystis* to produce PHB and raise the productivity when there are stressful conditions, like a high concentration of bicarbonate or sodium chloride. However, only the central metabolism was studied, involving products like glycogen or PHB. In the above discussion about the effect of salinity over PHB production, it was mentioned the possibility of redirecting the carbon flow to the production of other metabolites, like glucosylglycerol, decreasing the content of PHB. It could be really interesting to study that hypothesis, by measuring the content of that metabolite.

Similarly, lipids metabolism is related to PHB biosynthesis, as they have substrates in common, as Acetyl-CoA (Mills et al., 2020). So, it could be interesting to measure the lipid content and see whether they have a positive, neutral or negative effect over PHB biosynthesis. The lipid metabolism also depends on the environmental conditions. For instance, Xia et al. (2014) observed that NaCl stimulates the production of lipids.

On the other hand, if these hypothesis about redirecting the carbon flow to other metabolites are contrasted, it could open the door to mutagenesis: develop mutants which are knock-outs in these other metabolic pathways. Knock-out refers to an organism that presents a modified gene, making it unfunctional. Knock-out can also refer to the molecular technique that modifies a particular gene so as to make it unfunctional. With this strategy, carbon flow could not be redirected to other metabolites, such as glucosylglycerol or lipid molecules, therefore a raise in PHB content would be expected.

Another unforeseen result was the differences in PHB content regarding the controls of each experiment. The controls in experiment 1 and 2 presented the same maximum value (14 %). First, it was surprising as they are biological replicates and these can present variations. However, the

control in the experiment 3 was far from this value. The first hypothesis is the possible effect of the nitrogen and phosphorus concentration at the beginning of the experiment, as this is the main difference regarding both experiments. So, the initial concentration of nutrients in the growing phase could be decisive to the final content of PHB. It is suggested to grow the strain with different concentration of nutrients in the growing phase and measure the PHB content in the accumulation phase.

Once this hypothesis is clarified, it is suggested to repeat the experiment 3, in such conditions that make the control to produce 14% of PHB. The results observed in experiment 3 show that an increase in PHB content could be obtained beyond the 14% previously obtained when there is a minimum amount of bicarbonate (100 mg/L) and NaCl (5.80 g/L) is added.

The concentration of nutrients in the third experiment was intentionally reduced in order to decrease the duration of the growing phase. In experiment 2, the growing phase lasted 28 days whereas in experiment 1 it lasted 11 days. It is not clear why there are this difference regarding the nutrients consuming rate, but it could be thought about differences between the initial state of the inoculum. For instance, the amount of intracellular nitrogen and phosphorus that the cells could have at the moment of starting the experiments. In this sense, it is proposed to analyse the growing phase using inoculums with different nutrients concentrations. It is also proposed to measure the final PHB content and see if the content of nutrients of the inoculum have any effect over PHB production. Other authors make the process with a two-step strategy that involves centrifuging the biomass and changing the photobioreactors in order to start the accumulation phase lacking nitrogen and phosphorus. However, this strategy is avoided to make the process more feasible from the industrial point of view.

Concerning the RT-q-PCR protocol, there are more strategies that could be studied. First, to reduce the cost, it is proposed to extract the RNA without using commercial kits. Zhang (2012) proposed a novel method to extract RNA from *Synechocystis* based on CTAB extraction buffer. This reagent is usually used to extract RNA from plants due to the complications associated to their polysaccharides. In this, work Zhang (2012) obtained high quality RNA and with a higher quantity.

Second, regarding the reverse transcription, there is one strategy to isolate the mRNA that was not studied. It consists of using oligo-dT that anneals with the polyadenylated (polyA) region of the

mRNA. However, this is a widely used strategy with eukaryotic, but not with prokaryotic because they generally lack that region (Bhaya et al., 2000). However, it seems that cyanobacteria, despite being prokaryotic, could have also that region and the strategy of using oligo-dT could work. Some authors, like (Kamravamanesh et al., 2019) used that strategy and obtained the consequent gene expression analysis. Moreover, *Synechocystis* was found to present heterogeneous poly(A) tails in the mRNA through a process similar to the one in chloroplast (Rott et al., 2003). This result also reinforces the proposal of using the oligo-dT strategy in the reverse transcription step.

Third, if the reverse transcription will be performed following the target-specific approach, it is advisable to do one-step RT-q-PCR. This method consists in using a single tube for both, RT step and q-PCR: the transcribed cDNA will be used as template in the subsequent q-PCR (Smith and Osborn, 2009). This method reduces the contamination risk (Smith and Osborn, 2009), but also time and effort.

Once the RT-q-PCR are optimized and implemented for this strain, the following step consists in analysing the gene expression of the main genes involved in the PHB synthesis. Previous studies have shown that the genes encoding the enzymes of the PHA biosynthetic pathway presented lower expression levels in a strain producing higher amount of PHB (Lau et al., 2014). This means that these enzymes are not the limiting step in the production. The same authors, Lau et al., (2014), showed that the photosynthetic activity, which provides the PHB precursors, was higher in the strain producing higher amount of PHB, suggesting that the carbon flux might be the determining factor in PHB biosynthesis. This is an example about the variation of the gene expression regarding PHB activity, so it is expected to see as well that variation in the applied conditions in this project.

Finally, the analytical method to measure glycogen can be criticized since is not specific for glycogen. It measures the total carbohydrates content. However, the used of this method is justify due to the fact that *Synechocystis* used most of the carbon source for the production of glycogen (Velmurugan and Incharoensakdi, 2018). There are other authors that also measured glycogen as total carbohydrates (Kamravamanesh et al., 2019). On the other hand, Koch et al. (2019) carried out a specific-glycogen method which consists in using the enzyme amyloglucosidase. The protocol used in (Koch et al., 2019) is the following:

1. 2 mL of cyanobacterial culture are centrifuged and washed twice with 1 mL of distilled water.

2. The cellular pellets are resuspended in 400 uL KOH (30% w/v) and incubated for 2h at 95°C.
3. Then, 1200 uL ice cold ethanol (final concentration of 70%) are added. The mixture is incubated at -20°C for 2-24 h.
4. The solution is centrifuged at 4°C for 10 min at 10,000x g. The pellet is washed twice with 70% and 96% ethanol and dried in speed-vac for 20 minutes at 60°C.
5. The pellet is resuspended in 1 mL of 100mM sodium acetate (pH 4.5) and 8 uL of aminoglucosidade solution (4.4 U/uL) are added. For the digestion, the mixture is incubated at 60°C for 2h.
6. To 200 uL of the digested solution, 1 mL of O-toluidine-reagent (6% O-toluidine in 100% acetic acid). The tubes are incubated for 10 min at 100°C.
7. The samples are then cooled down on ice for 3 min and OD₆₃₅ is measured.

8. References

- Abed, R.M.M., Köster, J., 2005. The direct role of aerobic heterotrophic bacteria associated with cyanobacteria in the degradation of oil compounds. *Int. Biodeterior. Biodegrad.* 55, 29–37.
- Abed, R.M.M., Dobretsov, S., Sudesh, K., 2009. Applications of cyanobacteria in biotechnology. *J. Appl. Microbiol.* 106, 1–12.
- APHA, AWWA, WEF. *Standard Methods for the Examination of Water and Wastewater*, 22nd ed.; Rice, E.W., Baird, R.B., Eaton, A.D., Clesceri, L.S., Eds.; The American Water Works Association; The American Public Health Association; The Water Environment Federation: Washington, DC, USA, 2012; ISBN 9780875530130.
- Allen, M.M., Smith, A.J., 1969. Nitrogen chlorosis in blue-green algae. *Arch. Für Mikrobiol.* 69, 114–120.
- Ansari, S., Fatma, T., 2016. Cyanobacterial Polyhydroxybutyrate (PHB): Screening, Optimization and Characterization. *PLOS ONE* 11(6).
- Arias, D.M., García, J., Uggetti, E., 2020. Production of polymers by cyanobacteria grown in wastewater: Current status, challenges and future perspectives. *New Biotechnol.* 55, 46–57.
- Arias, D.M., Uggetti, E., García-Galán, M.J., García, J., 2018. Production of polyhydroxybutyrates and carbohydrates in a mixed cyanobacterial culture: Effect of nutrients limitation and photoperiods. *New Biotechnol.* 42, 1–11.
- Arora, N.K., Singhal, V., Maheshwari, D.K., 2006. Salinity-induced accumulation of poly- β -hydroxybutyrate in rhizobia indicating its role in cell protection. *World J. Microbiol. Biotechnol.* 22, 603–606.
- Badger, M.R., Price, G.D., 2003. CO₂ concentrating mechanisms in cyanobacteria: molecular components, their diversity and evolution. *J. Exp. Bot.* 54, 609–622.
- Balaji, S., Gopi, K., Muthuvelan, B., 2013. A review on production of poly β hydroxybutyrates from cyanobacteria for the production of bio plastics. *Algal Res.* 2, 278–285.
- Ball, S.G., Morell, M.K., 2003. From bacterial glycogen to starch: understanding the biogenesis of the plant starch granule. *Annu. Rev. Plant Biol.* 54, 207–233.

- Bhaya, D., Vaultot, D., Amin, P., Takahashi, A.W., Grossman, A.R., 2000. Isolation of Regulated Genes of the Cyanobacterium *Synechocystis* sp. Strain PCC 6803 by Differential Display. *J. Bacteriol.* 182, 5692–5699.
- Bustin, S.A., Benes, V., Nolan, T., Pfaffl, M.W., 2005. Quantitative real-time RT-PCR – a perspective. *J. Mol. Endocrinol.* 34, 597–601.
- Bustin, S.A., Nolan, T., 2004. Pitfalls of Quantitative Real-Time Reverse-Transcription Polymerase Chain Reaction. *J. Biomol. Tech. JBT* 15, 155–166.
- Byrom, D., 1987. Polymer synthesis by microorganisms: technology and economics. *Trends Biotechnol.* 5, 246–250.
- Chae, Y., An, Y.-J., 2018. Current research trends on plastic pollution and ecological impacts on the soil ecosystem: A review. *Environ. Pollut.* 240, 387–395.
- Chorus, I., 1999. Toxic Cyanobacteria in Water - A guide to their public health consequences, monitoring and management.
- Costa, J.A.V., Moreira, J.B., Lucas, B.F., Braga, V. da S., Cassuriaga, A.P.A., Morais, M.G. de, 2018. Recent Advances and Future Perspectives of PHB Production by Cyanobacteria. *Ind. Biotechnol.* 14, 249–256.
- Doi, Y., 1995. Microbial synthesis, physical properties, and biodegradability of polyhydroxyalkanoates. *Macromol. Symp.* 98, 585–599.
- DuBois, Michel., Gilles, K.A., Hamilton, J.K., Rebers, P.A., Smith, Fred., 1956. Colorimetric Method for Determination of Sugars and Related Substances. *Anal. Chem.* 28, 350–356.
- Dutt, V., Srivastava, S., 2018. Novel quantitative insights into carbon sources for synthesis of poly hydroxybutyrate in *Synechocystis* PCC 6803. *Photosynth. Res.* 136, 303–314.
- Eberly, J.O., Ely, R.L., 2012. Photosynthetic accumulation of carbon storage compounds under CO₂ enrichment by the thermophilic cyanobacterium *Thermosynechococcus elongatus*. *J. Ind. Microbiol. Biotechnol.* 39, 843–850.
- Farrel R., 2010. RNA isolation strategies. In: *RNA methodologies*. Elsevier Inc, United States of America, pp 45-79.

- Fasaei, F., Bitter, J.H., Slegers, P.M., van Boxtel, A.J.B., 2018. Techno-economic evaluation of microalgae harvesting and dewatering systems. *Algal Res.* 31, 347–362.
- Fuller, S., Gautam, A., 2016. A Procedure for Measuring Microplastics using Pressurized Fluid Extraction. *Environ. Sci. Technol.* 50, 5774–5780.
- Galinski, E.A., 1995. Osmoadaptation in bacteria. *Adv. Microb. Physiol.* 37, 272–328.
- Geyer, R., Jambeck, J.R., Law, K.L., 2017. Production, use, and fate of all plastics ever made. *Sci. Adv.* 3 (7).
- Gómez-Casati, D.F., Cortassa, S., Aon, M.A., Iglesias, A.A., 2003. Ultrasensitive behavior in the synthesis of storage polysaccharides in cyanobacteria. *Planta* 216, 969–975.
- Griebel, R., Smith, Z., Merrick, J.M., 1968. Metabolism of poly(β -hydroxybutyrate). I. Purification, composition, and properties of native poly(β -hydroxybutyrate) granules from *Bacillus megaterium*. *Biochemistry* 7, 3676–3681.
- Grunberg-Manago, M., 1999. Messenger RNA stability and its role in control of gene expression in bacteria and phages. *Annu. Rev. Genet.* 33, 193–227.
- Gründel, M., Scheunemann, R., Lockau, W., Zilliges, Y., 2012. Impaired glycogen synthesis causes metabolic overflow reactions and affects stress responses in the cyanobacterium *Synechocystis* sp. PCC 6803. *Microbiol. Read. Engl.* 158, 3032–3043.
- Haywood, G.W., Anderson, A.J., Chu, L., Dawes, E.A., 1988. The role of NADH- and NADPH-linked acetoacetyl-CoA reductases in the poly-3-hydroxybutyrate synthesizing organism *Alcaligenes eutrophus*. *FEMS Microbiol. Lett.* 52, 259–264.
- Hein, S., Tran, H., Steinbüchel, A., 1998. *Synechocystis* sp. PCC6803 possesses a two-component polyhydroxyalkanoic acid synthase similar to that of anoxygenic purple sulfur bacteria. *Arch. Microbiol.* 170, 162–170.
- Hu Q., 2013. Environmental effects on cell composition. In: Richmond A, Hu Q (Ed.), *Handbook of microalgal culture: biotechnology and applied phycology*. Blackwell Publishing Ltd, Oxford, pp 114-123.

- Jahn, C.E., Charkowski, A.O., Willis, D.K., 2008. Evaluation of isolation methods and RNA integrity for bacterial RNA quantitation. *J. Microbiol. Methods* 75, 318–324.
- Jambeck, J.R., Geyer, R., Wilcox, C., Siegler, T.R., Perryman, M., Andrady, A., Narayan, R., Law, K.L., 2015. Plastic waste inputs from land into the ocean. *Science* 347, 768–771.
- Jantaro, S., Mäenpää, P., Mulo, P., Incharoensakdi, A., 2003. Content and biosynthesis of polyamines in salt and osmotically stressed cells of *Synechocystis* sp. PCC 6803. *FEMS Microbiol. Lett.* 228, 129–135.
- Jendrossek, D., Schirmer, A., Schlegel, H.G., 1996. Biodegradation of polyhydroxyalkanoic acids. *Appl. Microbiol. Biotechnol.* 46, 451–463.
- Kaewbai-ngam, A., Incharoensakdi, A., Monshupanee, T., 2016. Increased accumulation of polyhydroxybutyrate in divergent cyanobacteria under nutrient-deprived photoautotrophy: An efficient conversion of solar energy and carbon dioxide to polyhydroxybutyrate by *Calothrix scytonemicola* TISTR 8095. *Bioresour. Technol.* 212, 342–347.
- Kamravamanesh, D., Kovacs, T., Pflügl, S., Druzhinina, I., Kroll, P., Lackner, M., Herwig, C., 2018. Increased poly- β -hydroxybutyrate production from carbon dioxide in randomly mutated cells of cyanobacterial strain *Synechocystis* sp. PCC 6714: Mutant generation and characterization. *Bioresour. Technol.* 266, 34–44.
- Kamravamanesh, D., Pflügl, S., Nischkauer, W., Limbeck, A., Lackner, M., Herwig, C., 2017. Photosynthetic poly- β -hydroxybutyrate accumulation in unicellular cyanobacterium *Synechocystis* sp. PCC 6714. *AMB Express* 7, 143.
- Kamravamanesh, D., Slouka, C., Limbeck, A., Lackner, M., Herwig, C., 2019. Increased carbohydrate production from carbon dioxide in randomly mutated cells of cyanobacterial strain *Synechocystis* sp. PCC 6714: Bioprocess understanding and evaluation of productivities. *Bioresour. Technol.* 273, 277–287.
- Kanesaki, Y., Suzuki, I., Allakhverdiev, S.I., Mikami, K., Murata, N., 2002. Salt Stress and Hyperosmotic Stress Regulate the Expression of Different Sets of Genes in *Synechocystis* sp. PCC 6803. *Biochem. Biophys. Res. Commun.* 290, 339–348.

- Karpusas, M., Branchaud, B., Remington, S.J., 1990. Proposed mechanism for the condensation reaction of citrate synthase: 1.9-A structure of the ternary complex with oxaloacetate and carboxymethyl coenzyme A. *Biochemistry* 29, 2213–2219.
- Kavitha, G., Rengasamy, R., Inbakandan, D., 2018. Polyhydroxybutyrate production from marine source and its application. *Int. J. Biol. Macromol.* 111, 102–108.
- Keshavarz, T., Roy, I., 2010. Polyhydroxyalkanoates: bioplastics with a green agenda. *Curr. Opin. Microbiol.* 13, 321–326.
- Kirsch, F., Klähn, S., Hagemann, M., 2019. Salt-Regulated Accumulation of the Compatible Solutes Sucrose and Glucosylglycerol in Cyanobacteria and Its Biotechnological Potential. *Front. Microbiol.* 10.
- Koch, M., Berendzen, K.W., Forchhammer, K., 2020. On the Role and Production of Polyhydroxybutyrate (PHB) in the Cyanobacterium *Synechocystis* sp. PCC 6803. *Life* 10, 47.
- Koch, M., Doello, S., Gutekunst, K., Forchhammer, K., 2019. PHB is Produced from Glycogen Turn-over during Nitrogen Starvation in *Synechocystis* sp. PCC 6803. *Int. J. Mol. Sci.* 20.
- Lanyi, J.K., 1974. Salt-dependent properties of proteins from extremely halophilic bacteria. *Bacteriol. Rev.* 38, 272–290.
- Lau, N.-S., Foong, C.P., Kurihara, Y., Sudesh, K., Matsui, M., 2014. RNA-Seq Analysis Provides Insights for Understanding Photoautotrophic Polyhydroxyalkanoate Production in Recombinant *Synechocystis* Sp. *PLOS ONE* 9.
- Lebreton, L., Andrady, A., 2019. Future scenarios of global plastic waste generation and disposal. *Palgrave Commun.* 5, 1–11.
- Lee, C.S., Lee, S.-A., Ko, S.-R., Oh, H.-M., Ahn, C.-Y., 2015. Effects of photoperiod on nutrient removal, biomass production, and algal-bacterial population dynamics in lab-scale photobioreactors treating municipal wastewater. *Water Res.* 68, 680–691.
- Lekanne Deprez, R.H., Fijnvandraat, A.C., Ruijter, J.M., Moorman, A.F.M., 2002. Sensitivity and accuracy of quantitative real-time polymerase chain reaction using SYBR green I depends on cDNA synthesis conditions. *Anal. Biochem.* 307, 63–69.

- Li, Y., Huang, J., Sandmann, G., Chen, F., 2009. High-Light and Sodium Chloride Stress Differentially Regulate the Biosynthesis of Astaxanthin in *Chlorella Zofingiensis* (chlorophyceae)1. *J. Phycol.* 45, 635–641.
- Lynn, S.G., Kilham, S.S., Kreeger, D.A., Interlandi, S.J., 2000. Effect of Nutrient Availability on the Biochemical and Elemental Stoichiometry in the Freshwater Diatom *Stephanodiscus Minutulus* (bacillariophyceae)*. *J. Phycol.* 36, 510–522.
- Ma, M., Yuan, D., He, Y., Park, M., Gong, Y., Hu, Q., 2017. Effective control of *Poterioochromonas malhamensis* in pilot-scale culture of *Chlorella sorokiniana* GT-1 by maintaining CO₂-mediated low culture pH. *Algal Res.* 26, 436–444.
- Madison, L.L., Huisman, G.W., 1999. Metabolic Engineering of Poly(3-Hydroxyalkanoates): From DNA to Plastic. *Microbiol. Mol. Biol. Rev.* 63, 21–53.
- Markou, G., Angelidaki, I., Georgakakis, D., 2012. Microalgal carbohydrates: an overview of the factors influencing carbohydrates production, and of main bioconversion technologies for production of biofuels. *Appl. Microbiol. Biotechnol.* 96, 631–645.
- Mathews C.K., Van Holde K.E., Appling D.R., Anthony-Cahill S.J., 2013. Fotosíntesis, in: Martín-Romo .(Ed.), *Bioquímica*. Pearson Educación S.A., Madrid, pp. 672-707.
- Miao, X., Wu, Q., Wu, G., Zhao, N., 2003. Sucrose accumulation in salt-stressed cells of *agp* gene deletion-mutant in cyanobacterium *Synechocystis* sp. PCC 6803. *FEMS Microbiol. Lett.* 218, 71–77.
- Mills, L.A., McCormick, A.J., Lea-Smith, D.J., 2020. Current knowledge and recent advances in understanding metabolism of the model cyanobacterium *Synechocystis* sp. PCC 6803. *Biosci. Rep.* 40.
- Miranda, J.A., Steward, G.F., 2017. Variables influencing the efficiency and interpretation of reverse transcription quantitative PCR (RT-qPCR): An empirical study using Bacteriophage MS2. *J. Virol. Methods* 241, 1–10.
- Mohammad Najafi, Z.S., 2014. RNA Preservation and Stabilization. *Biochem Physiol.* 3(1).

- Mokrasch, L.C., R.W. McGilvery R.W., 1956. Purification and properties of fructose-1,6-diphosphatase. *Journal of Biological Chemistry*. 221 (2), 909-917.
- Nelson D.L., Cox M.M., 2015. Capítulo 26: Metabolismo del RNA. In: *Lehninger Principios de Bioquímica*. Ediciones Omega, S.L, Barcelona, pp 1085-1096.
- Oren, A., 2008. Microbial life at high salt concentrations: phylogenetic and metabolic diversity. *Saline Syst.* 4, 2.
- Oren, A., 1999. Bioenergetic Aspects of Halophilism. *Microbiol. Mol. Biol. Rev.* 63, 334–348.
- Padovani, G., Carlozzi, P., Seggiani, M., Cinelli, P., Vitolo, S., Lazzeri, A., 2016. PHB-rich biomass and BioH₂ production by means of photosynthetic microorganisms 49, 55–60.
- Page-Sharp, M., Behm, C.A., Smith, G.D., 1998. Cyanophycin and glycogen synthesis in a cyanobacterial *Scytonema* species in response to salt stress. *FEMS Microbiol. Lett.* 160, 11–15.
- Pascual, A., Vioque, A., 1999. Substrate binding and catalysis by ribonuclease P from cyanobacteria and *Escherichia coli* are affected differently by the 3' terminal CCA in tRNA precursors. *Proc. Natl. Acad. Sci. U. S. A.* 96, 6672–6677.
- Pinto, F.L., Thapper, A., Sontheim, W., Lindblad, P., 2009. Analysis of current and alternative phenol based RNA extraction methodologies for cyanobacteria. *BMC Mol. Biol.* 10, 79.
- Preiss, J., 1984. Bacterial glycogen synthesis and its regulation. *Annu. Rev. Microbiol.* 38, 419–458.
- Preiss, J., Romeo, T., 1994. Molecular biology and regulatory aspects of glycogen biosynthesis in bacteria. *Prog. Nucleic Acid Res. Mol. Biol.* 47, 299–329.
- Price G.D., Sültemeyer D., Klughammer B., Ludwig M., Badger M.R., 1998. The functioning of the CO₂ concentrating mechanism in several cyanobacterial strains: a review of general physiological characteristics, genes, proteins, and recent advances. *Canadian Journal of Botany*. 76(6).
- Price, S., Kuzhiumparambil, U., Pernice, M., Ralph, P.J., 2020. Cyanobacterial polyhydroxybutyrate for sustainable bioplastic production: Critical review and perspectives. *J. Environ. Chem. Eng.* 8.

- Rehm, B.H.A., Steinbüchel, A., 1999. Biochemical and genetic analysis of PHA synthases and other proteins required for PHA synthesis. *Int. J. Biol. Macromol.* 25, 3–19.
- Reis, M. a. M., Serafim, L.S., Lemos, P.C., Ramos, A.M., Aguiar, F.R., Van Loosdrecht, M.C.M., 2003. Production of polyhydroxyalkanoates by mixed microbial cultures. *Bioprocess Biosyst. Eng.* 25, 377–385.
- Rhodes, C.J., 2018. Plastic Pollution and Potential Solutions. *Sci. Prog.* 101, 207–260.
- Rodríguez-Contreras, A., Koller, M., Braunegg, G., Marqués-Calvo, M.S., 2016. Poly[(R)-3-hydroxybutyrate] production under different salinity conditions by a novel *Bacillus megaterium* strain. *New Biotechnol.* 33, 73–77.
- Rott, R., Zipor, G., Portnoy, V., Liveanu, V., Schuster, G., 2003. RNA Polyadenylation and Degradation in Cyanobacteria Are Similar to the Chloroplast but Different from *Escherichia coli*. *J. Biol. Chem.* 278, 15771–15777.
- Rueda, E., García-Galán, M.J., Díez-Montero, R., Vila, J., Grifoll, M., García, J., 2020. Polyhydroxybutyrate and glycogen production in photobioreactors inoculated with wastewater borne cyanobacteria monocultures. *Bioresour. Technol.* 295.
- Salgaonkar, B.B., Mani, K., Braganca, J.M., 2013. Characterization of polyhydroxyalkanoates accumulated by a moderately halophilic salt pan isolate *Bacillus megaterium* strain H16. *J. Appl. Microbiol.* 114, 1347–1356.
- Sauer, J., Schreiber, U., Schmid, R., Völker, U., Forchhammer, K., 2001. Nitrogen Starvation-Induced Chlorosis in *Synechococcus* PCC 7942. Low-Level Photosynthesis as a Mechanism of Long-Term Survival. *Plant Physiol.* 126, 233–243.
- Shanaza Khazir and Sneha Shetty, 2014. Bio-Based Polymers in the World. *International Journal of Life Sciences Biotechnology and Pharma Research.* 3(2), 35-43.
- Shehadul Islam, M., Aryasomayajula, A., Selvaganapathy, P.R., 2017. A Review on Macroscale and Microscale Cell Lysis Methods. *Micromachines* 8, 83.

- Shinde, S., Zhang, X., Singapuri, S.P., Kalra, I., Liu, X., Morgan-Kiss, R.M., Wang, X., 2020. Glycogen Metabolism Supports Photosynthesis Start through the Oxidative Pentose Phosphate Pathway in Cyanobacteria. *Plant Physiol.* 182, 507–517.
- Shrivastav, A., Mishra, S.K., Mishra, S., 2010. Polyhydroxyalkanoate (PHA) synthesis by *Spirulina subsalsa* from Gujarat coast of India. *Int. J. Biol. Macromol.* 46, 255–260.
- Singh, A.K., Sharma, L., Mallick, N., Mala, J., 2017. Progress and challenges in producing polyhydroxyalkanoate biopolymers from cyanobacteria. *J. Appl. Phycol.* 29, 1213–1232.
- Smith, C.J., Osborn, A.M., 2009. Advantages and limitations of quantitative PCR (Q-PCR)-based approaches in microbial ecology. *FEMS Microbiol. Ecol.* 67, 6–20.
- Sreedevi, S., Unni, D., Sreedharan, S., Prakasan, P., Moolakkariyil, S., Benjamin, Prof.S., 2014. Bioplastics: Advances in Polyhydroxybutyrate Research. *Adv. Polym. Sci.*
- Stal, L.J., 1992. Poly(hydroxyalkanoate) in cyanobacteria: an overview. *FEMS Microbiol. Lett.* 103, 169–180.
- Stal L.J., 2012. Cyanobacterial Mats and Stromatolites, in: Whitton, B.A. (Ed.), *Ecology of Cyanobacteria II: Their Diversity in Space and Time*. Springer Netherlands, Dordrecht, pp. 65–127.
- Steinbüchel, A., Aerts, K., Liebergesell, M., Wieczorek, R., Babel, W., Föllner, C., Madkour, M.H., Mayer, F., Pieper-Fürst, U., Pries, A., Valentin, H.E., 2011. Considerations on the structure and biochemistry of bacterial polyhydroxyalkanoic acid inclusions. *Can. J. Microbiol.*
- Steinbüchel, A., Hustede, E., Liebergesell, M., Pieper, U., Timm, A., Valentin, H., 1992. Molecular basis for biosynthesis and accumulation of polyhydroxyalkanoic acids in bacteria. *FEMS Microbiol. Rev.* 9, 217–230.
- Steinbüchel, A., Schlegel, H.G., 1991. Physiology and molecular genetics of poly(β -hydroxyalkanoic acid) synthesis in *Alcaligenes eutrophus*. *Mol. Microbiol.* 5, 535–542.
- Stults, J.R., Snoeyenbos-West, O., Methe, B., Lovley, D.R., Chandler, D.P., 2001. Application of the 5' Fluorogenic Exonuclease Assay (TaqMan) for Quantitative Ribosomal DNA and rRNA Analysis in Sediments. *Appl. Environ. Microbiol.* 67, 2781–2789.

- Sudesh, K., Abe, H., Doi, Y., 2000. Synthesis, structure and properties of polyhydroxyalkanoates: biological polyesters. *Prog. Polym. Sci.* 25, 1503–1555.
- Taiz, L. and Zeiger, E., 2010. *Plant Physiology*. 5th Edition, Sinauer Associates Inc., Sunderland, 782 p.
- Taroncher-Oldenburg, G., Stephanopoulos, G., 2000. Targeted, PCR-based gene disruption in cyanobacteria: inactivation of the polyhydroxyalkanoic acid synthase genes in *Synechocystis* sp. PCC6803. *Appl. Microbiol. Biotechnol.* 54, 677–680.
- Tillett, D., Neilan, B.A., 2000. Xanthogenate nucleic acid isolation from cultured and environmental cyanobacteria. *J. Phycol.* 36, 251–258.
- Troschl, C., Meixner, K., Drosch, B., 2017. Cyanobacterial PHA Production—Review of Recent Advances and a Summary of Three Years’ Working Experience Running a Pilot Plant. *Bioengineering* 4.
- Troschl, C., Meixner, K., Fritz, I., Leitner, K., Romero, A.P., Kovalcik, A., Sedlacek, P., Drosch, B., 2018. Pilot-scale production of poly- β -hydroxybutyrate with the cyanobacterium *Synechocystis* sp. CCALA192 in a non-sterile tubular photobioreactor. *Algal Res.* 34, 116–125.
- Velmurugan, R., Incharoensakdi, A., 2018. Disruption of Polyhydroxybutyrate Synthesis Redirects Carbon Flow towards Glycogen Synthesis in *Synechocystis* sp. PCC 6803 Overexpressing *glgC*/*glgA*. *Plant Cell Physiol.* 59, 2020–2029.
- Ventosa, A., Nieto, J.J., Oren, A., 1998. Biology of Moderately Halophilic Aerobic Bacteria. *Microbiol. Mol. Biol. Rev.* 62, 504–544.
- Wang, B., Pugh, S., Nielsen, D.R., Zhang, W., Meldrum, D.R., 2013. Engineering cyanobacteria for photosynthetic production of 3-hydroxybutyrate directly from CO₂. *Metab. Eng.* 16, 68–77.
- Wang, W., Vinocur, B., Altman, A., 2003. Plant responses to drought, salinity and extreme temperatures: towards genetic engineering for stress tolerance. *Planta* 218, 1–14.
- Westermarck, S., Steuer, R., 2016. Toward Multiscale Models of Cyanobacterial Growth: A Modular Approach. *Front. Bioeng. Biotechnol.* 4.

Whitton, B.A., Potts, M., 2012. Introduction to the Cyanobacteria, in: Whitton, B.A. (Ed.), Ecology of Cyanobacteria II: Their Diversity in Space and Time. Springer Netherlands, Dordrecht, pp. 1–13.

Xia, L., Rong, J., Yang, H., He, Q., Zhang, D., Hu, C., 2014. NaCl as an effective inducer for lipid accumulation in freshwater microalgae *Desmodesmus abundans*. *Bioresour. Technol.* 161, 402–409.

Zhang, Z., 2012. A novel RNA extraction method for cyanobacteria. LSU Masters Theses.

Annex I

This annex contains the protocols according to manufacture's instructions of RNA extraction, RNA purification, reverse transcription and q-PCR.

A. RNA extraction from Bacterial Cells

You will need to prepare the following dissolutions:

- **Fresh Lysis buffer:** add 10 μL 2-mercaptoethanol for each 1 mL Lysis buffer. Use 350 μL of fresh Lysis buffer for each bacterial pellets.
- **Lysoenzyme solution** (100 μL): 77 μL of water, 20 μL of lysoenzyme, 1 μL 10 mM Tris-Hcl (pH 8.0), 2 μL 5mM EDTA.

1. Add 100 μL of prepared lysozyme solution to the cell pellet and resuspend by vortexing.
2. Add 0.5 μL 10% SDS solution. Vortex to mix well.
3. Incubate the cells in the tube for 5 minutes at room temperature.
4. Add 350 μL lysis buffer prepared with 2-mercaptoethanol. Vortex to mix well.
5. Transfer the liquid phase to a Homogenizer. Inserted in a RNase-free tube, and centrifuge at 12,000 x g for 2 minutes at room temperature.
6. Add 250 μL 100% ethanol to each volume of bacterial cell homogenate.
7. Mix thoroughly by vortexing to disperse any visible precipitate that may form by adding ethanol.
8. Transfer the sample (including any remaining precipitate) to a Spin Cartridge (with a collection tube).
9. Centrifuge both spin Cartridge and Collection tube at 12,000 x g for 15 seconds at room temperature. Discard the flow-through, and reinsert the Spin Cartridge in the same collection tube.

B. DNase on-column treatment

You will need to prepare:

- PureLink DNase for on-column treatment (80 UI): 8 μL 10X DNase I reaction buffer, 10 μL Resuspended DNase (3U/ μL), 62 μL RNase free water.

1. Add 350 μ L Wash Buffer I to the spin Cartridge (from step 9A). Centrifuge at 12,000 x g for 15 seconds at room temperature. Discard the flow-through and the collection tube. Place the Spin Cartridge into a new collection tube.
2. Add 80 μ L PureLink DNase mixture directly onto the surface of the Spin Cartridge membrane.
3. Incubate at room temperature for 15 minutes.
4. Add 350 μ L Wash Buffer I to the spin Cartridge. Centrifuge at 12,000 x g for 15 seconds at room temperature. Discard the flow-through and the collection tube. Place the Spin Cartridge into a new collection tube.
5. Add 500 μ L Wash buffer II with ethanol to the Spin Cartridge.
6. Centrifuge at 12,000 x g for 15 seconds at room temperature. Discard the flow-through, and reinsert the Spin Cartridge into the same Collection tube.
7. Repeat Steps 5-6 once.
8. Centrifuge the Spin Cartridge and Collection tube at 12,000 x g 1 minute at room temperature to dry the membrane with attached RNA. Discard the Collection Tube and insert the Spin Cartridge into a Recovery Tube.
9. Add 30 μ L -100 μ L RNase-free water to the centre of the Spin Cartridge.
10. Incubate at room temperature for 1 minute.
11. Centrifuge the Spin Cartridge and recovery tube for 2 minutes at 12,000 x g at room temperature.
12. Store your purified RNA at -80°C.

C. Reverse transcription

The components of the kit must be stored on ice. RNA must be on ice all the time.

1. Mix: 1 μ L RNA, 1 μ L Random Primer and 10 μ L RNase-free water.
2. Add: 4 μ L 5x Reaction buffer, 1 μ L Ribolock RNase Inhibitor, 2 μ L 10 mM Dntp Mix, 1 μ L RevertAid RT.
3. Mix gently and centrifuge.
4. For random primer, incubate for 5 minutes at 25 °C followed by 60 min at 42°C.
5. Terminate the reaction by heating at 70°C for 15 minutes.

D. q-PCR

1. Mix: 5 μ L PowerUp™ SYBR™ GreenMaster Mix (2X), 1.5 μ L 300 nM forward primer, 1.5 μ L 300 nM reverse primer, 1 μ L DNA sample (1-10 ng cDNA) and 1 μ L water.

The following tables (Table 19, Table 20) describe the conditions of the thermal cycles:

Table 19. Standard cycling mode.

Step	Temperature	Duration	Cycles
UDG activation	50°C	2 minutes	Hold
Dual-Lock DNA polymerase	95°C	2 minutes	Hold
Denature	95°C	15 seconds	40
Anneal	55-60 °C	15 seconds	
Extend	72°C	15 seconds	

Table 20. Dissociation curve conditions (melt curve stage).

Step	Ramp rate	Temperature	Time
1	1.6°C/second	95°C	15 seconds
2	1.6°C/second	60°C	1 minute
3	0.15°C/second	95°C	15 seconds

Annex II

This annex contains the protocols for the RNA extraction, RNA purification and reverse transcription with the modifications that allows the best results.

A. RNA extraction

You Will need to prepare the following dissolutions:

- **Fresh Lysis buffer:** add 10 μL 2-mercaptoethanol for each 1 mL Lysis buffer. Use 350 μL of fresh Lysis buffer for each bacterial pellets.
 - **Lysoenzyme solution** (100 μL): 77 μL of water, 20 μL of lysoenzyme, 1 μL 10 mM Tris-Hcl (pH 8.0), 2 μL 5mM EDTA.
1. Add 100 μL of prepared lysozyme solution to the cell pellet and resuspend by vortexing.
 2. Add 0.5 μL 10% SDS solution. Vortex to mix well.
 3. Incubate the cells in the tube for 5 minutes at room temperature.
 4. Add 350 μL lysis buffer prepared with 2-mercaptoethanol. Vortex to mix well.

If you want to use **TRIzol reagent**, follow TRIzol protocol.

5. Bead beating: the final mixture after step 4 is transfer into tubes containing crystal beads. These beads must be RNase-free. Then, the tubes containing the samples and the beads are vortex for 1 minute and then, the tubes are cooled down on ice for 1 minute. These steps are repeated three times.
6. Centrifuge for 2 min.
7. Transfer the liquid phase to a Homogenizer. Inserted in a RNase-free tube, and centrifuge at 12,000 x g for 2 minutes at room temperature.
8. Add 250 μL 100% ethanol to each volume of bacterial cell homogenate.
9. Mix thoroughly by vortexing to disperse any visible precipitate that may form by adding ethanol.
10. Transfer the sample (including any remaining precipitate) to a Spin Cartridge (with a collection tube).

11. Centrifuge both spin Cartridge and Collection tube at 12,000 x g for 15 seconds at room temperature. Discard the flow-through, and reinsert the Spin Cartridge in the same collection tube.
12. Add 700 μ L Wash Buffer I to the spin Cartridge. Centrifuge at 12,000 x g for 15 seconds at room temperature. Discard the flow-through and the collection tube. Place the Spin Cartridge into a new collection tube.
13. Add 500 μ L Wash buffer II with ethanol to the Spin Cartridge.
14. Centrifuge at 12,000 x g for 15 seconds at room temperature. Discard the flow-through, and reinsert the Spin Cartridge into the same Collection tube.
15. Repeat Steps 13-14 once.
16. Centrifuge the Spin Cartridge and Collection tube at 12,000 x g 1 minute at room temperature to dry the membrane with attached RNA. Discard the Collection Tube and insert the Spin Cartridge into a Recovery Tube.
17. Add 30 μ L -100 μ L RNase-free water to the centre of the Spin Cartridge.
18. Incubate at room temperature for 1 minute. Centrifuge the Spin Cartridge and recovery tube for 2 minutes at 12,000 x g at room temperature.
19. Store your purified RNA at -80°C or procedure with the **DNase I treatment**.
20. Mix 8 μ L of RNA sample, 1 μ L 10 x Reaction Buffer, 1 μ L (1U) DNase I.
21. Incubate at 37 °C for 30 minutes.
22. Add 1 μ L 50 mM EDTA and incubate at 65 °C for 10 minutes.
23. Store your purified RNA at -80°C.

TRIzol Protocol in combination with bead beating

1. Incubate the lysate (from step 4A) with TRIzol reagent at room temperature for 5 minutes to allow complex dissociation of nucleotides complexes.
2. Bead beating: the final mixture after step 4 is transfer into tubes containing crystal beads. These beads must be RNase-free. Then, the tubes containing the samples and the beads are

vortex for 1 minute and then, the tubes are cooled down on ice for 1 minute. These steps are repeated three times.

3. Add 0.2 mL of chloroform per 1 mL of TRIzol Reagent used. Shake the tube vigorously by hand for 15 seconds.
4. Incubate at room temperature for 2-3 minutes.
5. Centrifuge the samples at 12,000 x g for 15 minutes at 4°C.
6. Transfer 400 µL (approx.) of the colorless, upper phase containing the RNA to a fresh RNase-free tube.
7. Add an equal volume of 70% ethanol to obtain a final ethanol concentration of 35%. Vortex to mix well.
8. Invert the tube to disperse any visible precipitates that may form after adding the ethanol.
9. Transfer the sample (including any remaining precipitate) to a Spin Cartridge (with a collection tube).
10. Centrifuge both spin Cartridge and Collection tube at 12,000 x g for 15 seconds at room temperature. Discard the flow-through, and reinsert the Spin Cartridge in the same collection tube.

B. Reverse transcription protocol for specific-target

The components of the kit must be stored in ice. RNA must be in ice all the time.

1. Mix: 1 µL RNA, 1 µL Random Primer and 10 µL RNase-free water.
2. Add: 4 µL 5x Reaction buffer, 1 µL Ribolock RNase Inhibitor, 2 µL 10 mM Dntp Mix, 1 µL RevertAid RT.
3. Mix gently and centrifuge.
4. For specific-target, incubate for 60 min at 42°C.
5. Terminate the reaction by heating at 70°C for 10 minutes.

Annex III

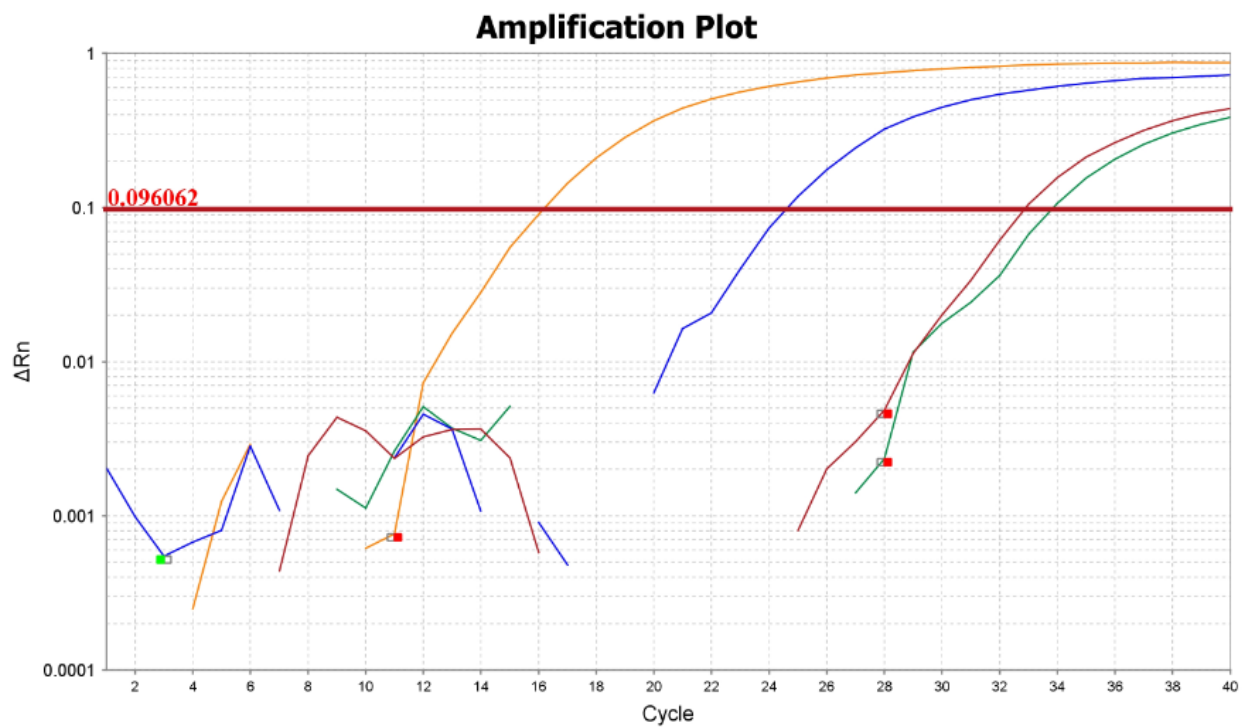


Figure 27. Results of q-PCR (using primers of bacterial general 16S). Orange curve represents the positive control. Blue curve represents the sample using the on-column modified treatment. Red curve represents the negative control. Green curve represents the sample using the treatment in dissolution.

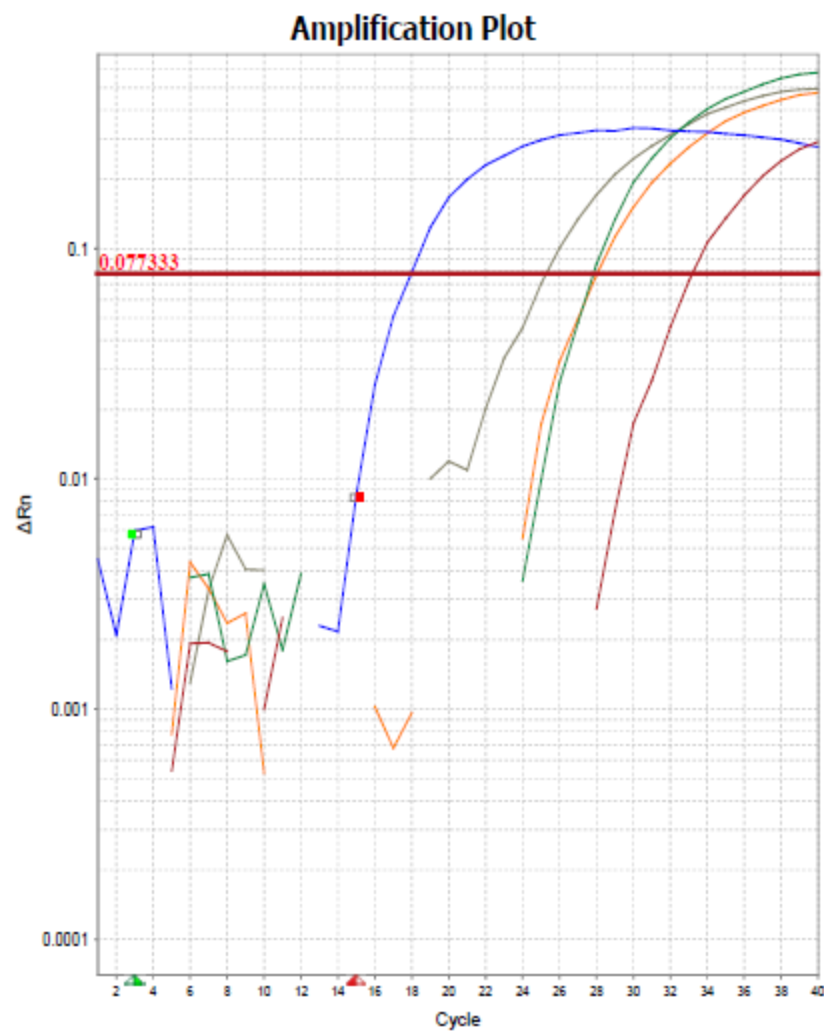


Figure 28. Results of q-PCR (using primers of general 16S specific of *Synechocystis*). Results of RT-q-PCR using primers from 16S rRNA from *Synechocystis*. Blue curve represents the positive control. Red curve represents the negative control. Grey, orange and green represent the samples.

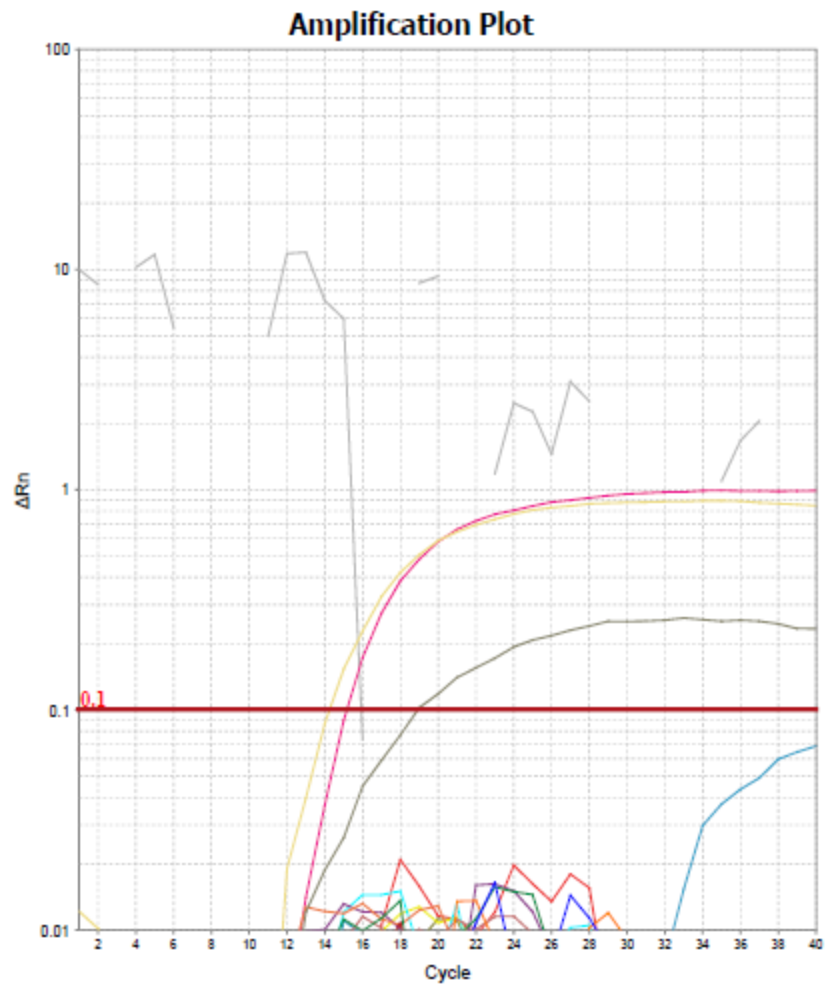


Figure 29. Results of q-PCR targeting different genes. RT was performed using random primers. First, *fbp* gene: grey curve represents the positive control. Second, *glgX* gene: light yellow curve represents the positive curve. Third, *rnpA* gene: pink curve represents the positive curve. Blue curve represents sample 1 when targeted with *glgX* gene. The rest of samples and the negative control are not detected.

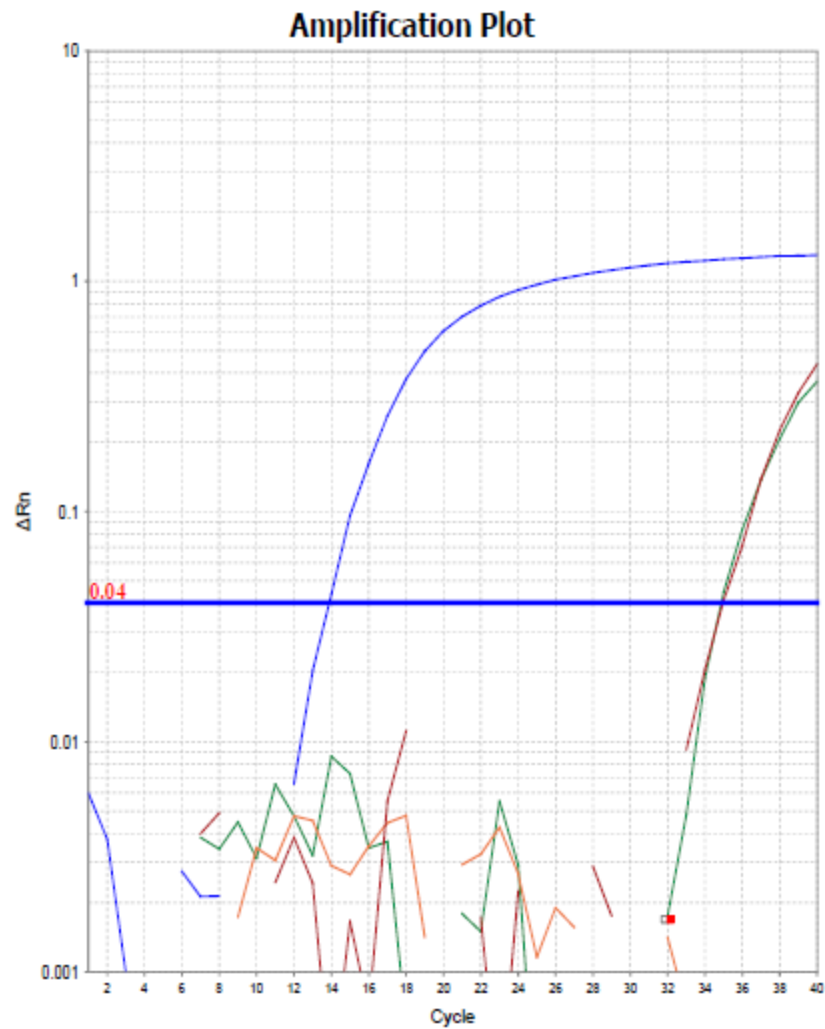


Figure 30. Results of RT-q-PCR using primers from *rnpA* gene *Synechocystis*, after the second extraction. Blue curve represents de positive control. Red curve represents the negative control. Green curve represents the frozen sample. The inoculum sample is not detected.

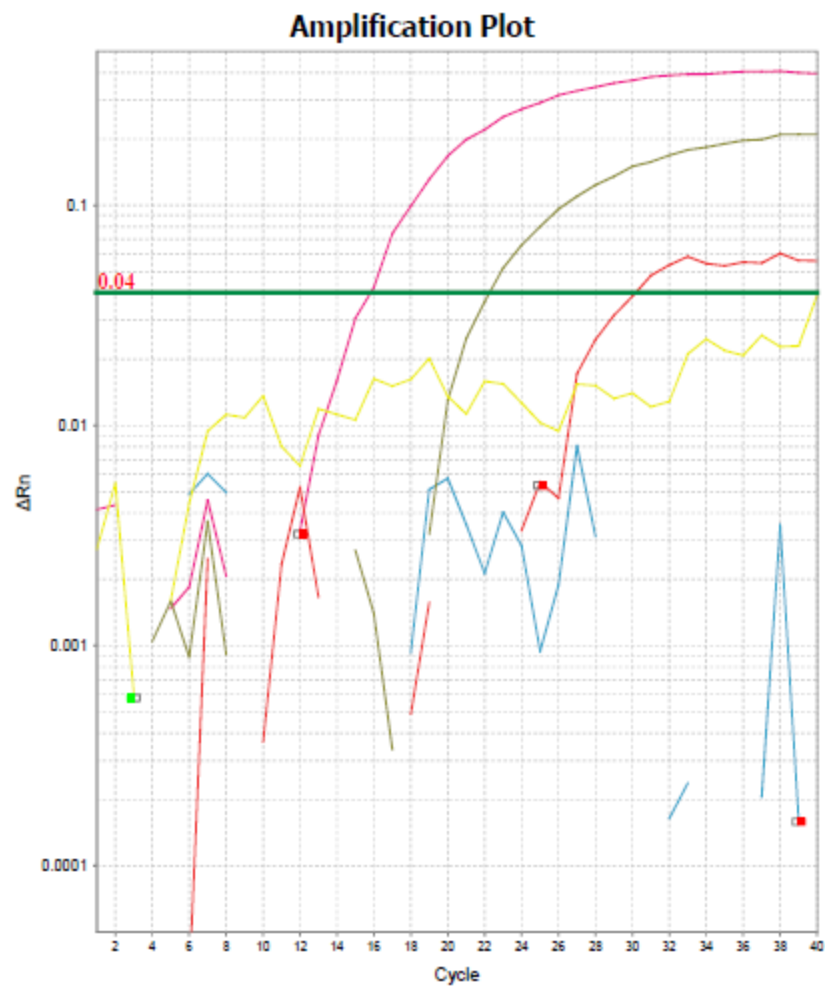


Figure 31. Results of q-PCR (using primers of bacterial general 16S), after the second extraction. Pink curve represents the positive control. Yellow curve represents the negative control. Grey curve represents the sample from the inoculum. The red curve represents the frozen sample.

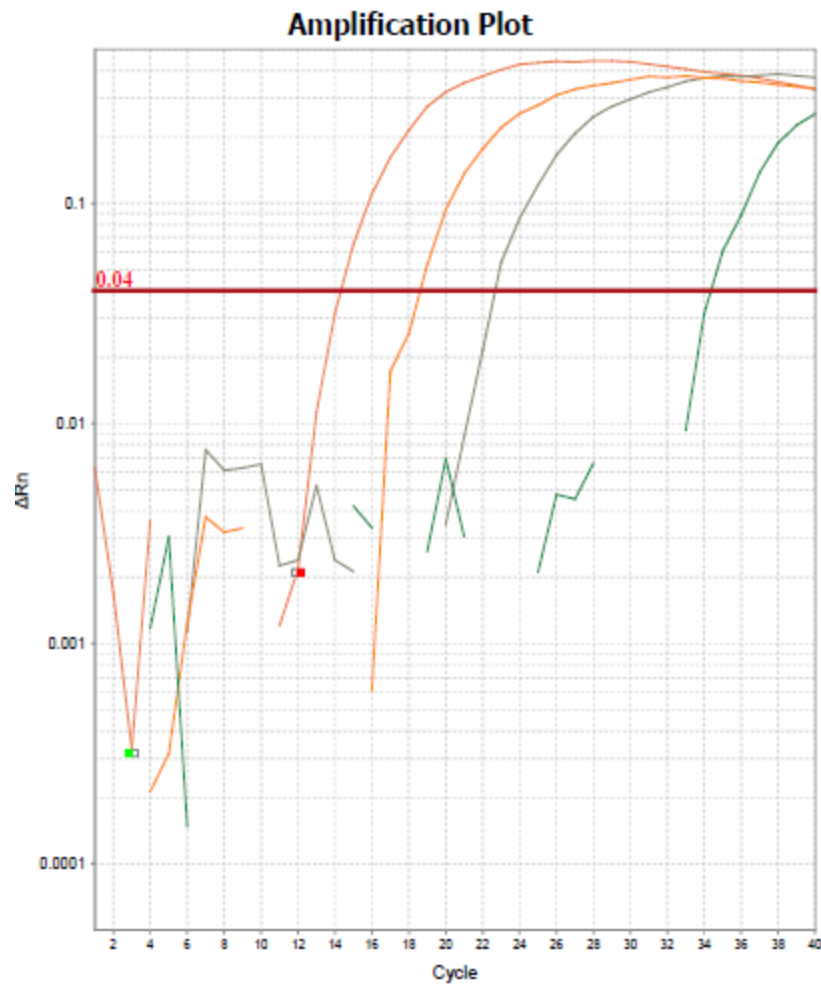


Figure 32. Results of q-PCR (using primers of 16S rRNA from *Synechocystis*), after the second extraction. Brown curve represents the positive control. Green curve represents the negative control. Orange curve represents the sample from the inoculum. The grey curve represents the frozen sample.

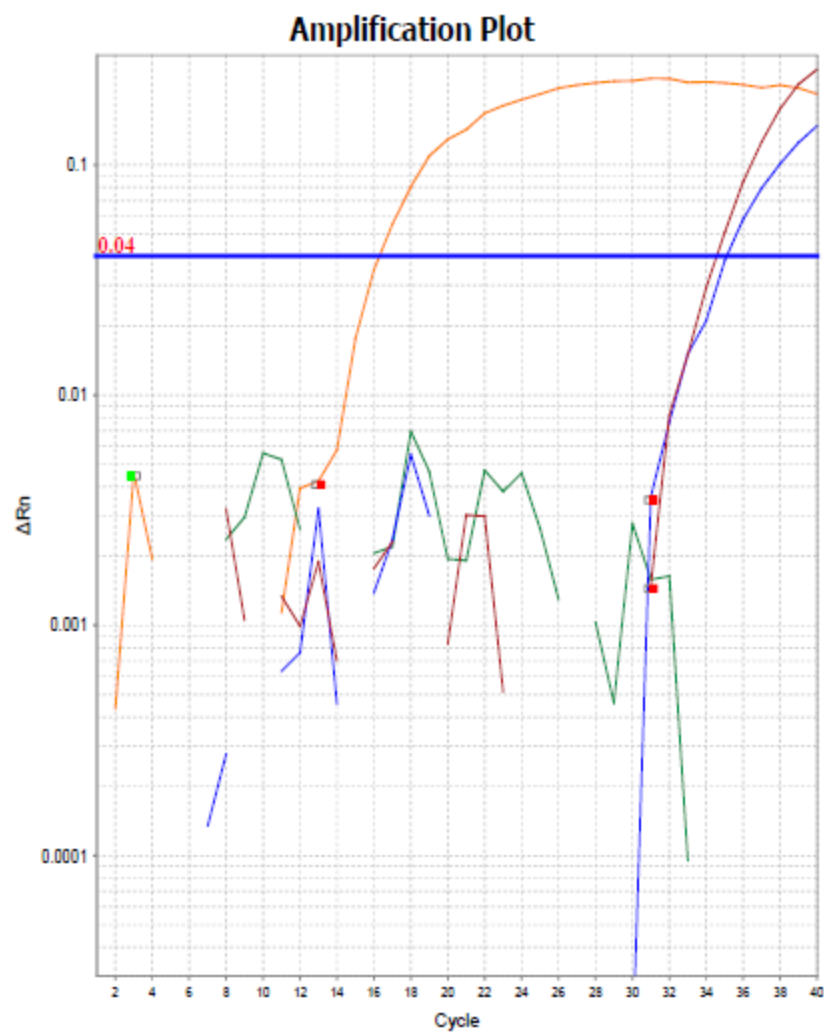


Figure 33. Results of RT-q-PCR using primers from *rnpA* gene *Synechocystis*. Orange curve represents de positive control. Blue curve represents the negative control. Maroon curve represents de inoculum sample. Green curve represents the frozen sample. 2 μ L of sample were added instead of 1 μ L.

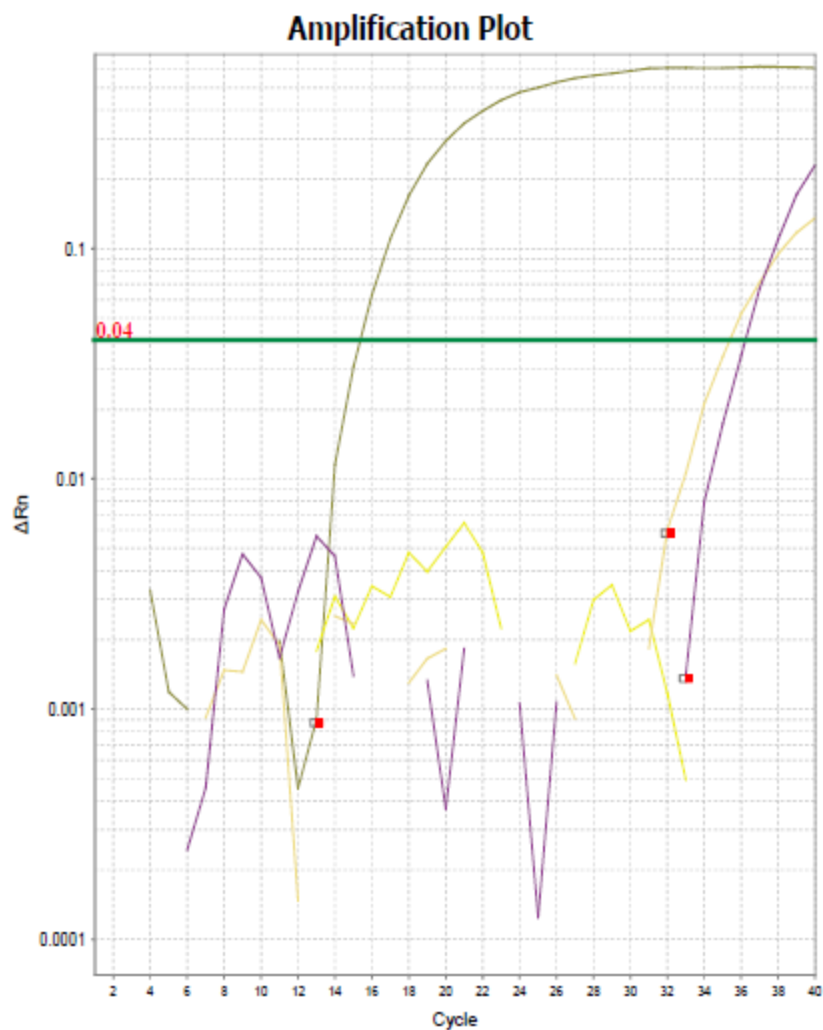


Figure 34. Results of RT-q-PCR using primers from *rnpA* gene *Synechocystis*. Grey curve represents de positive control. Purple curve represents the negative control. Yellow curve represents de inoculum sample. Yellow curve represents the frozen sample. 3 μ L of sample were added instead of 1 μ L. 500 nM primers were used instead of 300 nM.

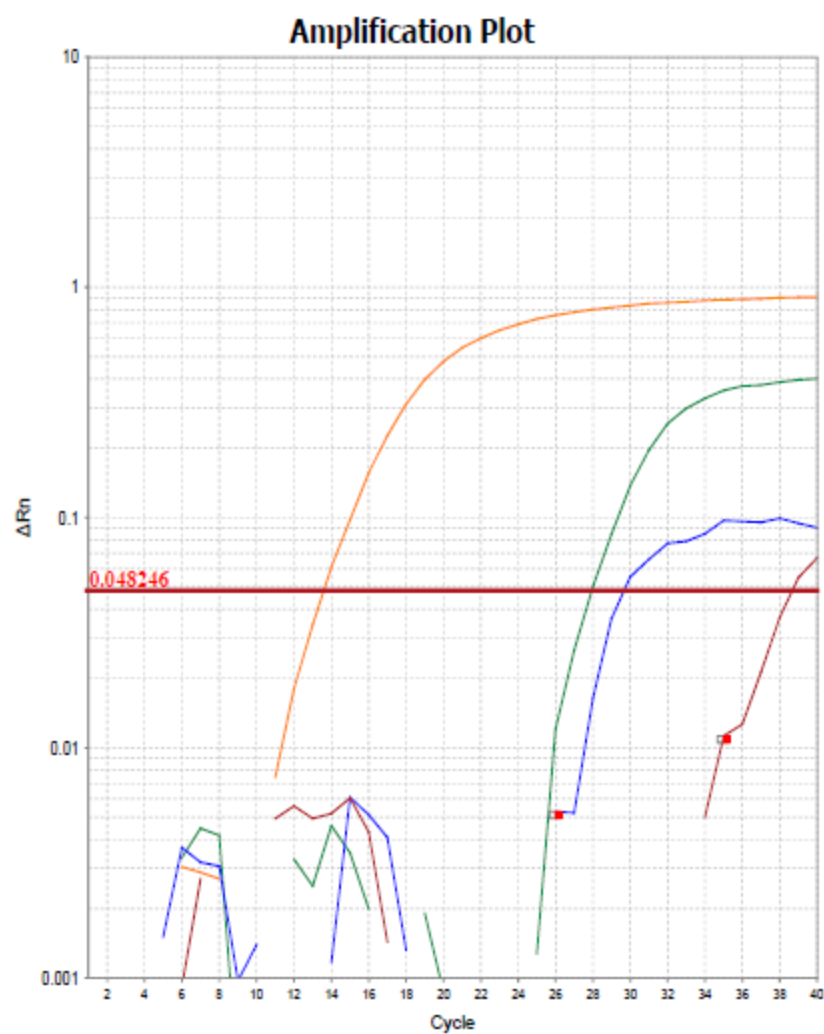


Figure 35. Results of RT-q-PCR using primers from *fbp* gene *Synechocystis*. Orange curve represents de positive control. Red curve represents the negative control. Green curve represents de inoculum sample. Blue curve represents the frozen sample

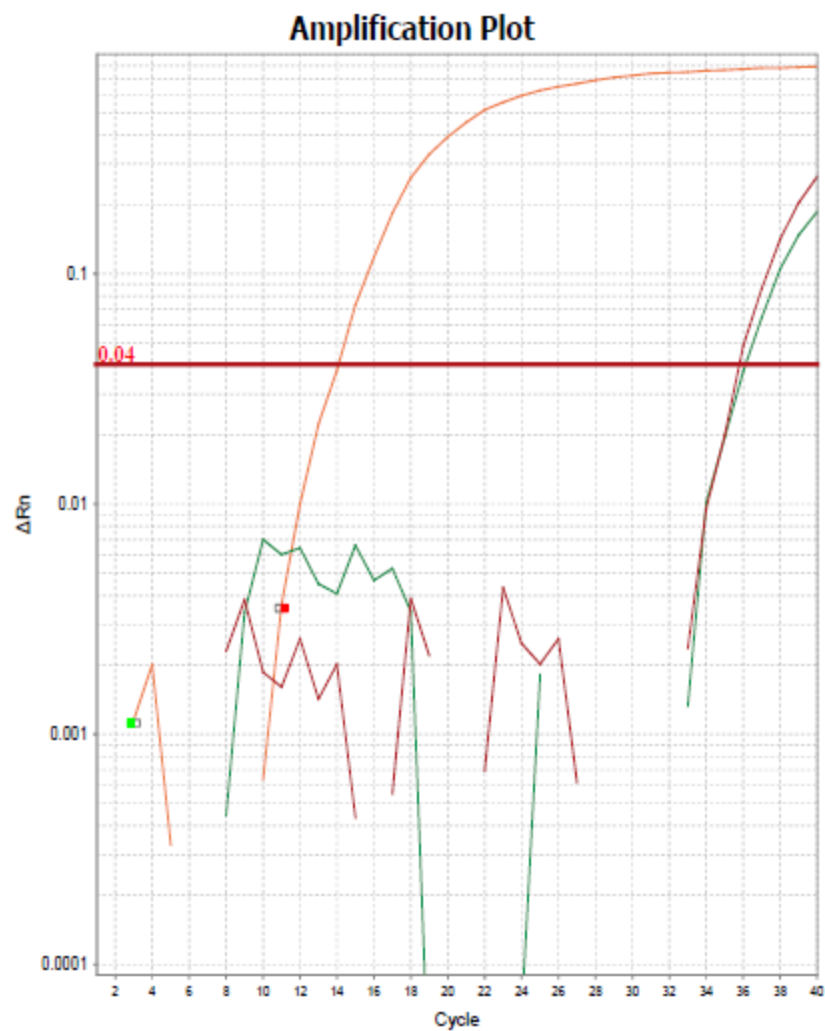


Figure 36. RT-q-PCR results, targeting *fbp* gene from *Synechocystis*, using the gene-specific RT approach. Orange curve represents the positive control. Red curve represents the negative control. Green curve represents N1, (negative control from RT, including the mixture of primers and the enzyme, without RNA sample).

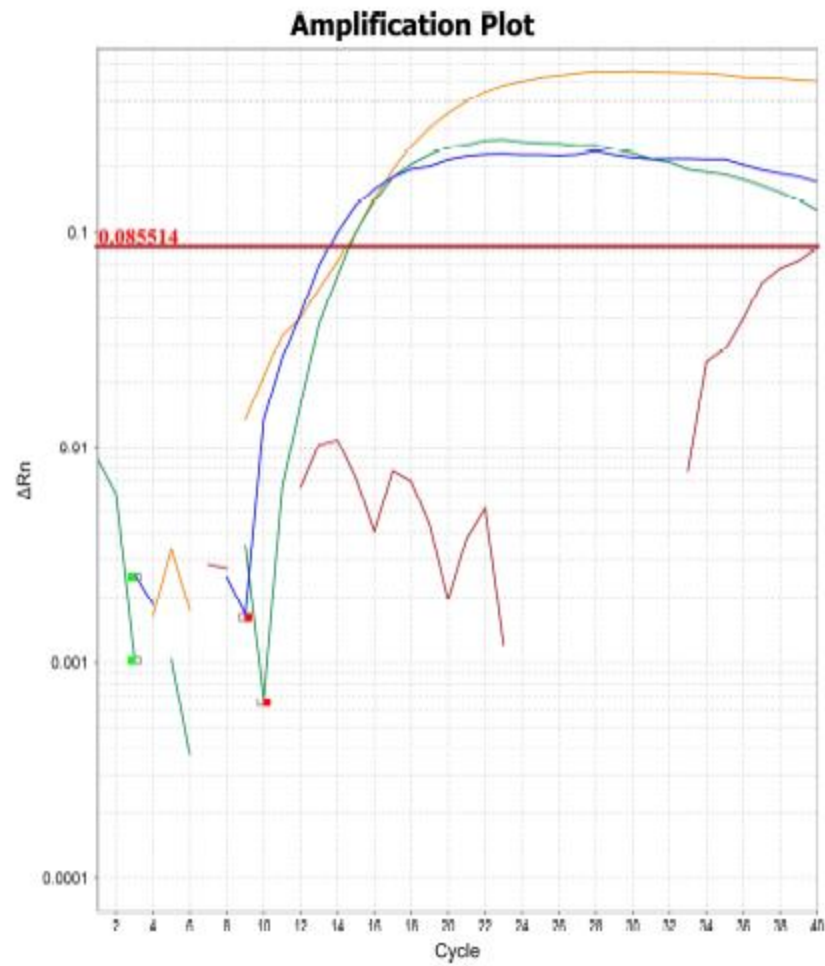


Figure 37. Results of RT-q-PCR using a mixture of primers during the RT. q-PCR has targeted 16S rRNA gene. Orange curve represents de positive control. Red curve represents the negative control. Blue curve represents de inoculum sample. Gren curve represents the frozen sample.

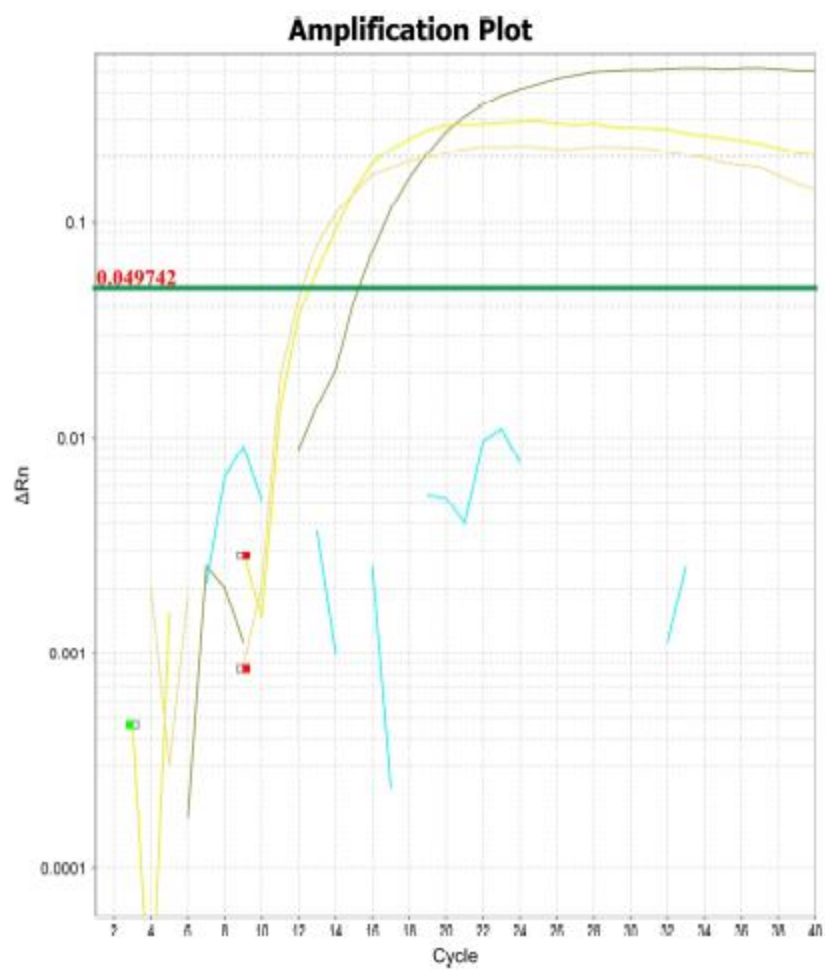


Figure 38. Results of RT-q-PCR using a mixture of primers during the RT. q-PCR has targeted *fbp* gene. Grey curve represents de positive control. Blue curve represents the negative control. Yellow curve represents de inoculum sample. Light yellow curve represents the frozen sample.

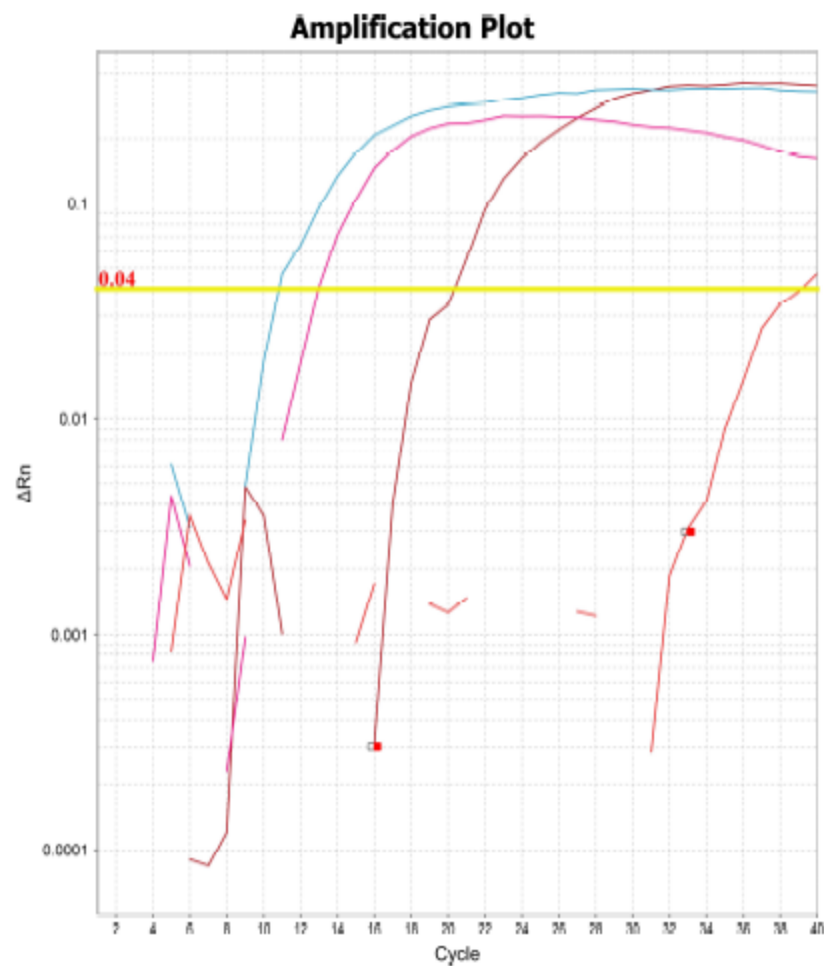


Figure 39. Results of RT-q-PCR using a mixture of primers during the RT. q-PCR has targeted *gltA*. Maroon curve represents de positive control. Red curve represents the negative control. Blue curve represents de inoculum sample. Purple curve represents the frozen sample.

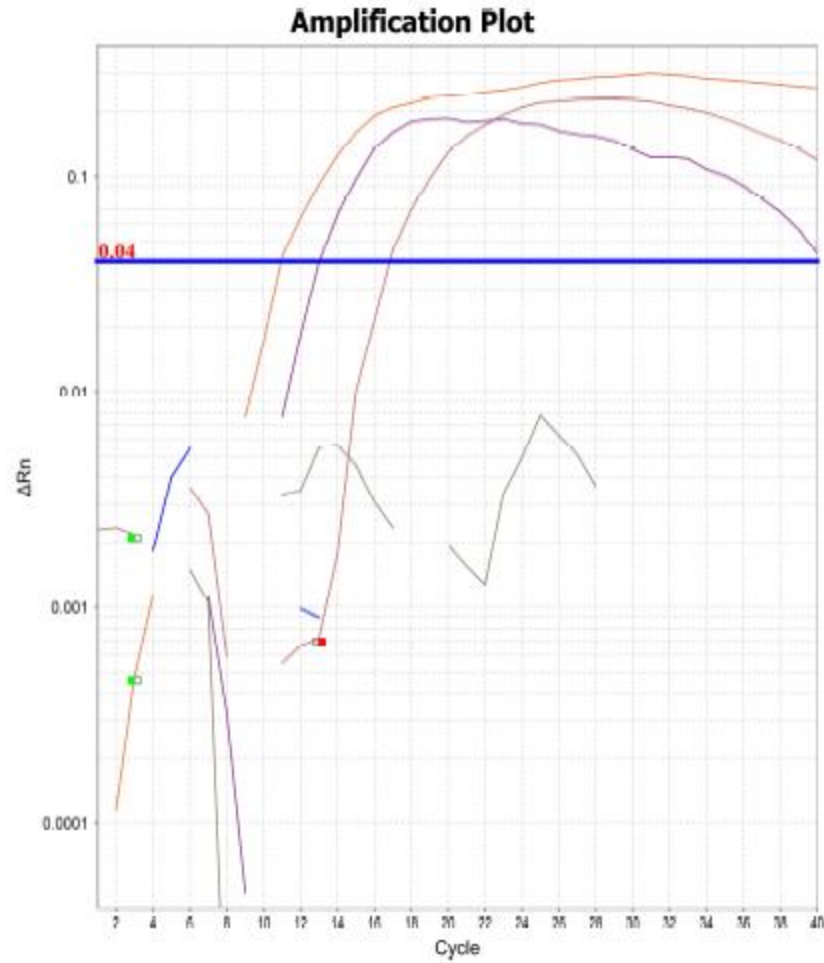


Figure 40. Results of RT-q-PCR using a mixture of primers during the RT. q-PCR has targeted *rnpA*. Maroon curve represents de positive control. Grey curve represents the negative control. Orange curve represents de inoculum sample. Purple curve represents the frozen sample.

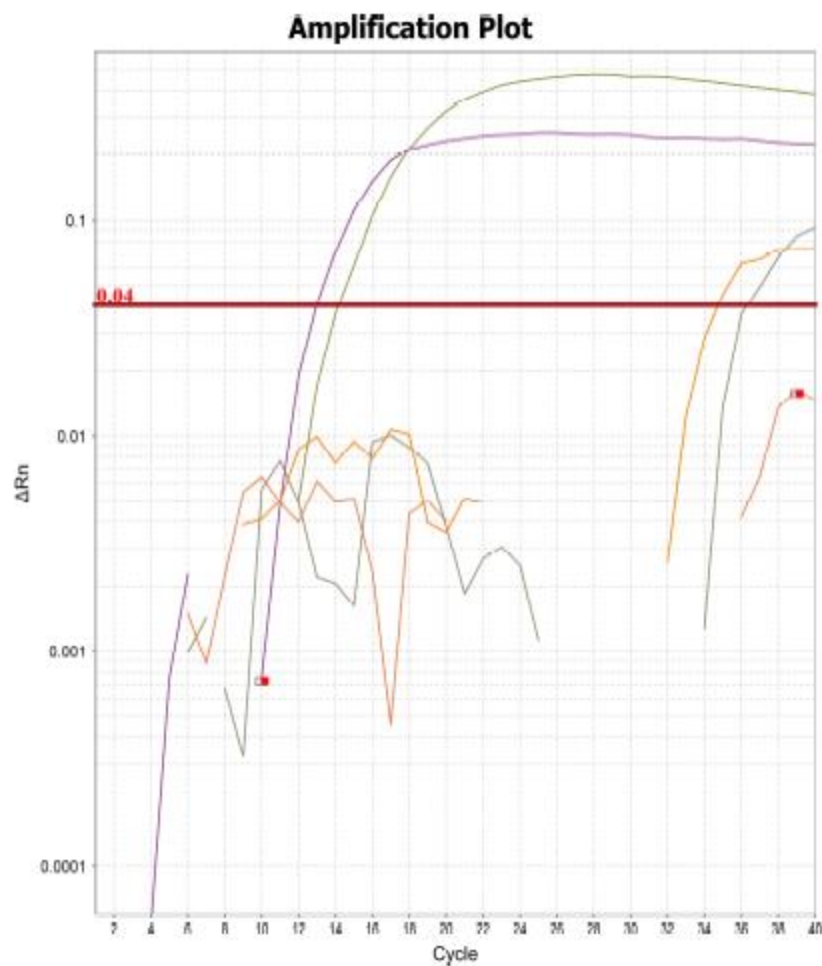


Figure 41. RT-q-PCR results, targeting 16S rRNA from *Synechocystis*, using the mixture of primers. Green curve represents the positive control. Orange curve represents the negative control. Purple curve represents N1, (negative control from RT, including the mixture of primers and the enzyme, without RNA sample). Grey curve represents N2 (negative control from RT, including the mixture of primers and RNA sample, without the enzyme).

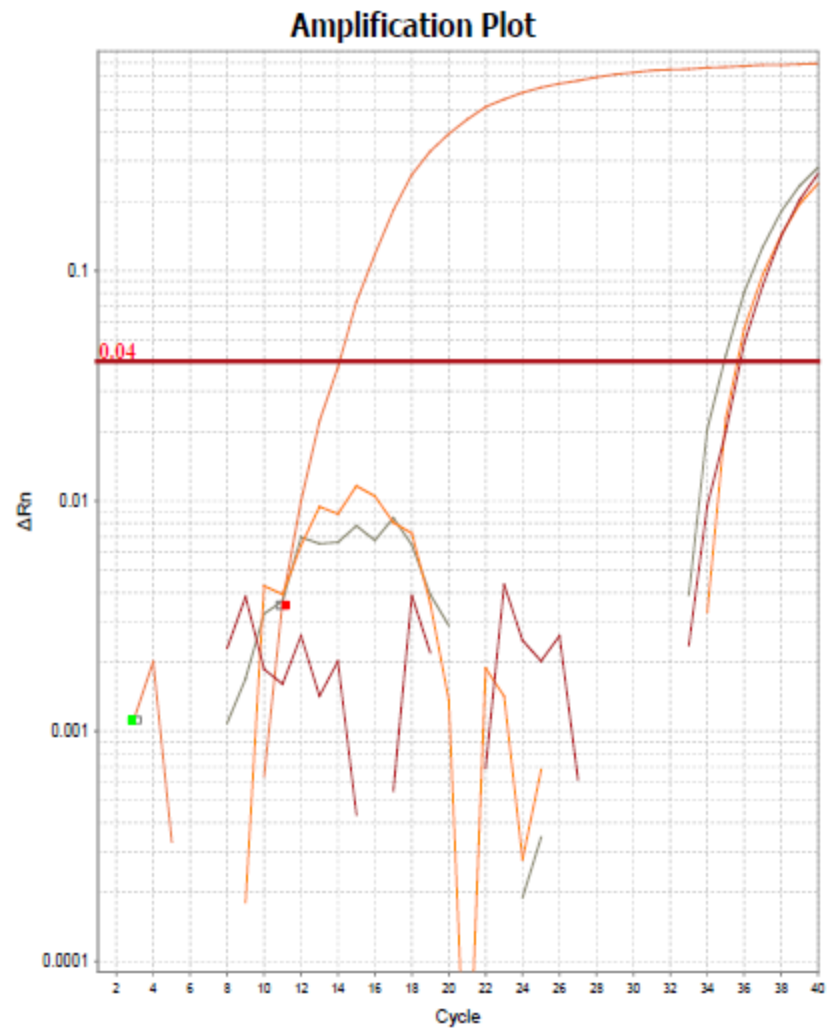


Figure 42. q-PCR results, targeting *fbp* gene, after applying 10 mM random primers in the RT. Orange curve represents the positive. Red curve represents the negative. Light orange represents the sample from the inoculum. Grey curve represents the frozen sample.